

# **ADVANCED SIMULATION OF AN ADAPTIVE LOWER LIMB PROSTHESIS**

Vom Fachbereich Maschinenbau  
an der Technischen Universität Darmstadt  
zur  
Erlangung des Grades eines Doktor-Ingenieurs (Dr.-Ing.)  
genehmigte

D i s s e r t a t i o n

vorgelegt von  
**M.Sc. Nasim Alnu'man**  
aus Amman, Jordanien

Berichterstatter: Prof. Dr.-Ing. Holger Hanselka

Mitberichterstatter: Prof. Dr. rer. nat. Michael Schäfer

Tag der Einreichung: 21.01.2010

Tag der mündlichen Prüfung: 04.05.2010

Darmstadt 2010

D17



## Abstract

The normal daily human activities include different levels of energy and strength needs, and this applies also for walking such that walking at high speeds needs more stiff muscles compared with walking slowly, and walking during carrying heavy loads or on inclined surfaces needs more energy than during doing the light housekeeping activities. For a healthy individual the human foot has already the ability to change its stiffness and to store and return a part of the elastic energy in a compliant structure of muscle fibres and series elastic elements. In the case of amputations in the lower limbs the amputated limbs are replaced with artificial limbs. A problem appears by this replacement that the new artificial limbs are designed to satisfy some described tasks and any change in these tasks or in the boundary conditions leads to an incompliance and unsatisfactory motion of the amputees. For example, the use of soft foot for walking at high speeds leads to a larger motion of the body centre of mass compared with walking at the preferred walking speed. In order to overcome these problems or reduce their effects, the need arises to design adaptive prostheses that have the ability to change their properties according to the surrounding conditions.

This work has the goal to evaluate the usefulness of using adaptive elastic foot prosthesis, through the numerical modelling and simulation of the human gait of an above-knee amputee with an adaptive elastic foot. The body of the amputee is divided into a limited number of rigid bodies (segments) connected together by hinge joints. A two dimensional model of the human body is built from these segments using a commercial multibody simulation program. The initial conditions of the system, some of the body segments relative motions and forces are given as inputs in the model. In order to integrate the adaptive elastic foot in the rigid bodies system a numerical model of the foot is built using the finite element method and then reduced by static condensation. The reduced elastic model is then integrated in the rigid bodies' model of the human gait. This model is used to simulate the stance period of the human gait.

Four parameters, the vertical ground reaction force (GRF), the body centre of mass (BCoM), the ankle joint moment and the hip joint rotation are considered as defining characteristics of the human gait. These characteristics are used in the evaluation of the model results and latterly in the evaluation of the adaptive foot usefulness. The simulation model is validated through comparison with experimental results of the human gait. The model shows good consistency with experimental results and can be further used in simulating the human gait using prosthetic feet with different mechanical properties and positions.

Different prosthetic foot properties and walking conditions are studied for the adaptive elastic prosthetic foot. The stiffness of the foot sole is changed for normal walking on level and inclined surfaces and for fast walking on level surfaces. The changes in stiffness show changes in the vertical BCoM motion which improve the gait form for walking faster than the normal walking speed but show no significant changes on the other parameters. The ankle joint inclination is also changed for walking on uphill inclined surfaces; the results show that increasing the inclination angle reduces the vertical GRF and increases the horizontal motion of the BCoM and relatively the step size, which improves the uphill motion on inclined surfaces.

Also designs of beam elements with changeable stiffness that could be used in an adaptive prosthetic foot's sole are considered. In this part two concepts are developed and studied theoretically then two models are manufactured and proved experimentally. The results show good changes in the stiffness of the models, then the first model consisting of two plates sliding one in the other shows experimentally a change of  $\pm 8.5\%$  in the stiffness and the second model consisting of two plates screwed together gives experimentally an average change of  $\pm 18\%$  in the stiffness. Since these models are designed to be used as replacements for human limbs (where the available external energy sources are limited) attention was given to model a light weight system with minimum energy consumption for controlling and driving it. Also attention was given to design a system that could be used with the different commercially available prosthetic feet without the need to make large changes in the original models designs and sizes.

## Zusammenfassung

Die Alltagsaktivitäten eines Menschen unterscheiden sich in ihrem Energie- und Kraftaufwand. Beispielsweise versteifen sich die Muskeln beim Rennen im Vergleich zum langsamen Gehen. Es wird ein höherer Energiebedarf beim Tragen schwerer Gegenstände und beim Gehen auf steilen Anstiegen benötigt als bei leichten Haushaltstätigkeiten. Gesunde Menschen verfügen über einen Fußapparat, der die Fähigkeit verfügt, seine Steifigkeit zu verändern, elastische Energie zum Teil zu speichern und bei Bedarf wieder abzugeben. Im Falle amputierter unterer Extremitäten wird dieser durch künstliche Gliedmaßen ersetzt. Verändern sich die Anforderungen an die Prothese und damit die korrespondierenden Randbedingungen des mechanischen Systems, so kann dies für den Amputierten zu unbefriedigenden und gestörten Bewegungsabläufen führen. Beispielsweise führt die Verwendung eines weichen Fußes bei hohen Bewegungsgeschwindigkeiten zu einer erhöhten Auslenkung des Körperschwerpunkts. Um solche Auswirkungen zu reduzieren werden adaptive Prothesen erforscht, die ihre Systemeigenschaften den Umgebungsbedingungen entsprechend anzupassen.

Diese Arbeit hat das Ziel, den Nutzwert einer adaptiven elastischen Fußprothese mit Hilfe der numerischen Modellierung und Simulation des menschlichen Gangs eines Oberschenkelamputierten zu ermitteln. Der Körper wird in eine begrenzte Anzahl von Starrkörperelementen (Segmenten) unterteilt, die über Drehgelenke miteinander verbunden sind. Daraus wird ein zweidimensionales Modell des menschlichen Körpers mit einem kommerziellen Mehrkörpersimulationsprogramm entwickelt. Die Anfangsbedingungen des Systems, Relativbewegungen der Segmente und Kräfte gehen als Eingangsgrößen in das Modell ein. Zur Integration des adaptiven elastischen Fußes in das Starrkörpermodell wird der Fuß numerisch mit der FEM abgebildet und die resultierenden Bewegungsgleichungen mittels statischer Kondensation reduziert. Das reduzierte Modell des Fußes wird in das Starrkörpermodell des menschlichen Körpers eingefügt, um mit dem Gesamtmodell die Standphase des menschlichen Gangs zu simulieren. Vier Parameter, die vertikale Bodenreaktionskraft, der Körperschwerpunkt, das Moment am Fußgelenk und die Rotation des Hüftgelenks, werden als Ausgangsgrößen des Simulationsmodells berechnet und in der Bewertung des adaptiven Fußes betrachtet. Durch einen Vergleich mit experimentellen Messungen des menschlichen Gangs wurde das Modell validiert und bestätigt, dass es den Gang für verschiedene Fußprothesen adäquat abbildet.

Zur Untersuchung der adaptiven elastischen Fußprothese werden unterschiedliche Systemeigenschaften bei verschiedenen Umgebungsbedingungen berücksichtigt. Die Steifigkeit der Fußsohle wird für den normalen Gang auf ebenen und steigungsbehafteten Oberflächen und für einen schnellen Gang auf ebenen Oberflächen variiert. Die Veränderung der Steifigkeit wirkt sich auf die vertikale Bewegung des Körperschwerpunktes aus und verbessert den Gang bei erhöhter Geschwindigkeit. Eine signifikante Beeinflussung anderer Parameter wurde nicht festgestellt. Die Neigung des Sprunggelenks wurde für den Gehvorgang bei positiver Steigung verändert. Hier zeigen die Simulationsergebnisse, dass eine Vergrößerung der Sprunggelenkneigung die vertikalen Bodenreaktionskräfte reduziert sowie die horizontale Auslenkung des Körperschwerpunkts und die relative Schrittlänge vergrößert.

Weiterhin entstanden zwei Entwürfe zur Konstruktion einer Fußsohle bestehend aus Balkenelementen zur Beschreibung der Steifigkeitsveränderung. Hierbei wurde beim ersten Konzept, bestehend aus zwei ineinander verschiebbaren Platten, eine Steifigkeitsveränderung von  $\pm 8.5\%$  und bei dem zweiten Konzept, deren zwei Plattenelemente zusätzlich miteinander verschraubt wurden, eine Steifigkeitsveränderung von  $\pm 18\%$  erzielt. Da die Verfügbarkeit externer Energiequellen eingeschränkt ist, wurde bei der Auslegung des Systems auf ein möglichst geringes Gewicht und einen minimalen Energiebedarf im aktiven Betrieb geachtet. Desweiteren wurde auf die Kompatibilität mit verschiedenen kommerziell verfügbaren Fußprothesen Wert gelegt.

## Acknowledgment

The work presented in this dissertation was done over a period of four years as I was a Ph. D. Student in the institute system reliability and machine acoustics SzM at Technische Universität Darmstadt. Here I wish to express my grateful appreciation to Professor Dr.-Ing. Holger Hanselka, who gave me the opportunity to undertake my research at the institute. My thanks go also at Professor Dr. rer. nat. Michael Schäfer, chair of the institute numerical methods in mechanical engineering FNB, who agreed to be my co-advisor.

My sincere and great appreciation goes to Professor Dr.-Ing. Thilo Bein and Dr.-Ing. Valerio Carli for their scientific advices during my research time and for their comments that helped me to reach my goals. Thanks are also due to the company Otto Bock for providing the data used in this research.

I would like to thank Professor Dr.-Ing. Kai Wolf our former manager by deputy for his friendly support and encouragement during his work time in the institute. Also my thank goes to Dr.-Ing. Joachim Bös our present manager by deputy for proof reading my dissertation and for his helpful suggestions and comments.

I also want to show my gratitude to my colleges Soong-Oh Han, Dr.-Ing. Lothar Kurtze, and our secretaries Suzanne Kritzer and Katrin Jordan for their immeasurable motivating words during my work at the institute and for their help in the administrative issues. A big “Thank” goes also to all my former and present colleges for their cooperativeness, good working atmosphere, and for the pleasant time we spent together.

I would like to acknowledge the KAAD (Katholischer Akademischer Ausländer-Dienst) for the financial support of my living expenses throughout my study in Germany and for the intensive varicoloured cultural program they have offered along this period.

For all my Friends in Darmstadt and all over the world, who have brought joy into my life and who have made my residence time in Germany as being in my homeland thankful I say: “Behold, how good and pleasant it is when brothers dwell together in unity! ... For there the Lord has commanded the blessing, even life for evermore.” (Psalms, 133).

Finally, I would like to thank my family, my father George, my mother Antoinette, my brother Haitham and my sister Fardous, they have been my strongest supporters during my study and without their love, encouragement, patience, and understanding, it was for me not possible to complete this research.

Hiermit erkläre ich an Eides statt, dass ich die vorliegende Arbeit selbständig und nur unter Verwendung der angegebenen Hilfen angefertigt habe.

Nasim Alnu'man

Darmstadt, May 5, 2010



# Contents

<b>LIST OF FIGURES</b>	<b>IX</b>
<b>LIST OF SYMBOLS AND ABBREVIATIONS</b>	<b>XIII</b>
<b>1 INTRODUCTION</b>	<b>1</b>
1.1 BACKGROUND AND MOTIVATION	1
1.2 SCOPE AND OBJECTIVES OF THIS WORK	3
1.3 WHAT IS DIFFERENT IN THIS WORK?	4
1.4 OUTLINE	5
<b>2 LITERATURE REVIEW</b>	<b>7</b>
2.1 HUMAN GAIT	7
2.2 PROSTHESIS	9
2.3 MODELLING OF HUMAN GAIT	12
2.4 MULTIBODY DYNAMICS AND FEM	15
<b>3 THEORETICAL BACKGROUND</b>	<b>17</b>
3.1 HUMAN GAIT	17
3.2 BASICS OF PROSTHETIC LIMBS	21
3.3 DYNAMICS OF FLEXIBLE MULTIBODY SYSTEMS	25
<b>4 EVALUATION CRITERIA FOR THE FUNCTIONALITY OF PROSTHESES:</b>	<b>32</b>
4.1 THE DISPLACEMENT OF THE BCOM	32
4.2 GROUND REACTION FORCES	33
4.3 ANKLE JOINT MOMENT	34
4.4 HIP JOINT ROTATION	35
<b>5 NUMERICAL MODELLING OF THE HUMAN GAIT</b>	<b>36</b>
5.1 BUILDING THE RIGID BODIES MODEL	37
5.2 GROUND CONTACT MODEL	39
5.3 PRE-EVALUATION OF THE RIGID BODIES MODEL	41
5.4 INTEGRATION OF THE ELASTIC ELEMENTS IN THE MODEL	45
5.4.1 <i>Building the finite element model</i>	46
5.4.2 <i>Reducing the FE model</i>	49
5.4.3 <i>Integration of FE model in the multibody system</i>	50
5.4.4 <i>Some problems faced in the simulation of the human gait</i>	51
5.5 SIMULATION RESULTS FOR WALKING ON LEVEL SURFACE	54
<b>6 ADAPTATION OF FOOT PROPERTIES WITH DIFFERENT GAIT CONDITIONS</b>	<b>59</b>
6.1 WALKING ON LEVEL SURFACES	59
6.1.1 <i>Changing the stiffness of the foot sole</i>	59
6.1.2 <i>Changing the inclination angle of the ankle joint</i>	61
6.2 ENTERING INCLINED SURFACES (UPHILL) FROM A LEVEL SURFACE	64
6.2.1 <i>The effect of changing the stiffness</i>	65
6.2.2 <i>The effect of changing the inclination angle of the ankle joint</i>	68
6.2.3 <i>The effect of changing the C-spring deformation form</i>	71

6.3 WALKING AT DIFFERENT VELOCITIES	74
<b>7 DESIGN OF A FOOT SOLE WITH CHANGEABLE STIFFNESS</b>	<b>77</b>
7.1 ANALYTICAL MODELS OF THE TWO CONCEPTS	78
7.1.1 <i>Sliding perforated plate</i>	78
7.1.2 <i>Two screwed beams</i>	81
7.2 THE FABRICATION OF THE PROTOTYPE	85
7.3 THE ANALYTICAL AND EXPERIMENTAL RESULTS	86
7.3.1 <i>Results of the sliding perforated plate concept</i>	86
7.3.2 <i>Results of the two screwed beams concept</i>	89
7.4 AN OPERATING SYSTEM FOR THE ADAPTIVE SOLE	92
7.5 COMMENTS	93
<b>8 DISCUSSION AND CONCLUSIONS</b>	<b>95</b>
<b>9 FUTURE WORK</b>	<b>96</b>
<b>REFERENCES</b>	<b>97</b>
<b>APPENDIX</b>	<b>103</b>
<b>RESUME OF THE AUTHOR</b>	<b>106</b>



## List of Figures

Figure 1.1: O <sub>2</sub> cost in unilateral amputees walking with prostheses at different amputation levels.....	1
Figure 1.2: Speed in unilateral amputees walking with a prosthesis at different amputation levels.....	2
Figure 1.3: Vertical component of the GRF of an able-bodied female walking at three different velocities.....	2
Figure 2.1: Typical intersecting metabolic cost curves for walking and running.....	8
Figure 2.2: Lateral view of the foot model consisting of eight segments, eight joints and seven spring-damper elements modelling the contact with the ground .....	14
Figure 3.1: A step verses a stride and the track width.....	17
Figure 3.2: The divisions of the gait cycle.....	18
Figure 3.3: The five phases of the stance period of the gait cycle with the line of action of the GRFs on the ipsilateral leg.....	19
Figure 3.4: The three phases of the swing period of the gait cycle with the swinging ipsilateral leg .....	19
Figure 3.5: BCoM motion .....	20
Figure 3.6: The sequence of foot support area during stance.....	21
Figure 3.7: A modular lower limb above knee prosthesis.....	22
Figure 3.8: Open-chain and closed-chain systems .....	25
Figure 3.9: The position vector of a deformed point $P$ on a flexible body relative to the body fixed local reference frame $B$ and the global coordinate system $G$ .....	27
Figure 4.1: BCoM motion in sagittal plane. ....	33
Figure 4.2: Vertical GRFs .....	34
Figure 4.3: Ankle joint moment .....	34
Figure 4.4: Hip joint rotation.....	35
Figure 5.1: Flow chart of pre-processor module of the multibody simulation program SIMPACK.....	37
Figure 5.2: The human gait model with the different parts assembled together .....	38
Figure 5.3: Modelling of the vertical GRFs as spring-damper elements at two points.....	39
Figure 5.4: Vertical and horizontal GRFs at the foot's heel.....	40
Figure 5.5: The prosthetic foot Flex-Walk .....	41
Figure 5.6: The foot Flex-Walk modelled as a complex of four rigid bodies and three hinge joints. ....	42
Figure 5.7: Experimentally measured and simulated GRFs acting on the foot Flex-Walk.....	43
Figure 5.8: Experimentally measured and simulated torque at the ankle of the foot Flex-Walk .....	44
Figure 5.9: Experimental and simulated rotation of the thigh at the hip joint .....	44
Figure 5.10: Simulated BCoM vertical motion .....	45
Figure 5.11: The C-Walk foot from Otto Bock .....	46
Figure 5.12: The deflection of the C-spring for the real and the numerical model .....	47
Figure 5.13: The C-spring .....	48
Figure 5.14: The deflection of the base spring for the real and the numerical model .....	49
Figure 5.15: The base spring .....	49
Figure 5.16: The foot C-Walk modelled as a complex of two elastic elements, heel element, and titan ring.....	50
Figure 5.17: The foot C-Walk modelled as a complex of two elastic elements, heel element, and titan ring in the multibody dynamic model .....	51
Figure 5.18: The moment of the hip joint at the prosthetic side for two Flex-Walk and C-Walk prosthetic feet users.....	52

Figure 5.19: The experimentally measured and the simulated GRFs acting on the prosthetic foot.....	55
Figure 5.20: The experimentally measured and the simulated moment at the ankle of the prosthetic foot.....	56
Figure 5.21: The experimental and numerical rotation of the thigh at the hip joint.....	57
Figure 5.22: The experimentally measured and the simulated sacral BCoM vertical motion with respect to its horizontal motion .....	58
Figure 6.1: The simulated vertical GRFs acting on the prosthetic foot for the different stiffness values of the prosthetic foot sole.....	59
Figure 6.2: The simulated moment at the ankle of the prosthetic foot for different stiffness values of the prosthetic foot sole .....	60
Figure 6.3: The simulated rotation of the thigh at the hip joint for the different stiffness values of the prosthetic foot sole .....	60
Figure 6.4: The simulated BCoM motion for four different stiffness values of the foot sole.....	61
Figure 6.5: The simulated vertical GRFs acting on the prosthetic foot for four different ankle joint inclinations.....	62
Figure 6.6: The simulated moment at the ankle joint of the prosthetic foot for four different ankle joint inclinations.....	63
Figure 6.7: The simulated rotation of the thigh at the hip joint for four different ankle joint inclinations .....	63
Figure 6.8: The simulated BCoM vertical and horizontal motion for four different ankle joint inclinations .....	64
Figure 6.9: The simulated vertical GRFs acting on the prosthetic foot for different stiffness values of the prosthetic foot sole and different ground inclinations.....	65
Figure 6.10: The simulated moment at the ankle of the prosthetic foot for different stiffness values of the prosthetic foot sole and different inclinations .....	66
Figure 6.11: The simulated rotations of the thigh at the hip joint for the different stiffness values of the prosthetic foot sole and different ground inclinations.....	67
Figure 6.12: The simulated BCoM motion for the different stiffness values of the prosthetic foot sole and different ground inclinations.....	68
Figure 6.13: The simulated vertical GRFs acting on the prosthetic foot for four different ankle joint inclinations.....	69
Figure 6.14: The simulated moment at the ankle joint of the prosthetic foot for four different ankle joint inclinations.....	69
Figure 6.15: The simulated rotation of the thigh at the hip joint for four different ankle joint inclinations .....	70
Figure 6.16: The simulated BCoM vertical and horizontal motion for four different ankle joint inclinations.....	71
Figure 6.17: The simulated vertical GRFs acting on the prosthetic foot for different ring diameters on a 6 degrees inclined surface.....	71
Figure 6.18: The simulated moment at the ankle of the prosthetic foot for different ring diameters on 6 a degrees inclined surface.....	72
Figure 6.19: The simulated rotations of the thigh at the hip joint for the different ring diameters on a 6 degrees inclined surface.....	73
Figure 6.20: The simulated BCoM motion for different ring diameters on a 6 degrees inclined surface .....	73
Figure 6.21: The simulated BCoM motion for the two walking speeds.....	74
Figure 6.22: The simulated vertical GRFs acting on the prosthetic foot for two walking speeds .....	75
Figure 6.23: The simulated moment at the ankle of the prosthetic foot for two different walking speeds .....	75

Figure 6.24: The simulated rotations of the thigh at the hip joint for the two walking speeds ...	76
Figure 7.1: The first model consisting of two beams one sliding into the other.....	78
Figure 7.2: A cross section of the beam at the slotted region.....	79
Figure 7.3: A cross section in the beam at the stiff region .....	79
Figure 7.4: The model as a simple cantilever beam with the force acting upward .....	80
Figure 7.5: The model consisting of two beams connected together with screws .....	81
Figure 7.6: The deformation of the first lower beam.....	82
Figure 7.7: A simply supported beam representing the deformation of the upper beam .....	83
Figure 7.8: The two beams with spring element fixed at the screws .....	85
Figure 7.9: The results of the analytical model describing the system with one beam sliding through a hollow beam .....	87
Figure 7.10: Experimental results of the model with one beam sliding through a hollow beam	88
Figure 7.11: The difference in the measured force between loading and unloading of the system measured for the beam at the position of 7 mm.....	89
Figure 7.12: The results of the analytical model describing the two beams screwed together with different clearance values between them .....	89
Figure 7.13: Analytical force deflection relation result of the model describing the two beams screwed together with different spring preloads .....	90
Figure 7.14: The results of the analytical model describing the two beams screwed together with springs with different spring constants at the screws .....	91
Figure 7.15: Experimental Results of the model with two beams screwed together with different clearance in between.....	92
Figure 7.16: The difference in the measured force between loading and unloading of the system measured for the beams with 0.65 mm clearance.....	92
Figure 7.17: Configuration of an adaptive foot system.....	93



## List of Symbols and Abbreviations

### Latin Symbols

${}^G A^B$	transformation matrix from the local body reference frame $B$ to the ground
$b$	beam width [m]
$c_g$	damping coefficient of ground model [Ns/m]
$c_{gmax}$	maximum value of damping coefficient [Ns/m]
$D$	modal damping matrix
$E$	Young's modulus, modulus of elasticity [N/m <sup>2</sup> ]
$e_{lsm}$	components of the permutation symbol
$F_r$	generalized active force [N]
$F_r^*$	generalized inertia force [N]
$F_{hor}$	horizontal reaction force [N]
$F_{ver}$	vertical reaction force [N]
$f_g$	gravitational force [N]
$h$	beam thickness [m]
$I$	identity matrix
$I_{kmn}$	mass inertia dyadic
$I_y$	moment of inertia
$K$	mass matrix
$\hat{K}$	generalized stiffness matrix
$K$	system kinetic energy [J]
$k_g$	stiffness of the ground contact model [N/m]
$k_s$	spring constant [N/m]
$M$	mass matrix
$\hat{M}$	generalized mass matrix
$M$	number of mode shapes
$M_y(x)$	equation of moment
$M$	number of mode shapes
$m_i$	mass of particle $i$ [kg]
$N$	the number of particles in the multibody system
$n$	number of degrees of freedom
$P_i$	particle $i$
$Q$	generalized applied forces
$q$	vector of the modal coordinates
$q_C$	modal coordinates of the constraint modes
$q_N$	modal coordinates of the fixed-boundary normal modes
$q$	modal coordinates
$q_i$	generalized coordinates
$s_P$	vector of position of point $P$ before the deformation
$T$	kinetic energy [J]
$u$	vector of deformation of the nodes of the FE model
$u_P$	vector of deformation of the node $P$ of the FE model
$u_B$	boundary DOF
$u_I$	interior DOF
$V$	potential energy [J]
$V_g$	gravitational energy [J]
${}^R \mathbf{v}^{P_i}$	velocity of particle $P_i$ in the inertial reference frame $R$ [m/s]
$\mathbf{v}_P$	velocity of particle $P_i$ [m/s]

$v_k$	velocity of the particle $k$ [m/s]
$w(x)$	equation of beam deflection
$x_r$	generalized coordinates
$z$	vertical penetration of the contact point in the ground
$\mathbf{0}$	zero matrix

## Greek Symbols

$\Delta$	slot length in the beam element [m]
$\delta$	clearance between the beams [m]
$\lambda$	Lagrange multipliers
$\xi$	generalized coordinate vector
$\Phi$	modal matrix
$\Phi_P$	slice from the modal matrix that corresponds to the translational DOF of node $P$
$\Phi^*$	slice from the modal matrix that corresponds to the rotational DOF of node $P$ .
$\Phi_{IC}$	physical displacement of the interior DOF in the constraint modes
$\Phi_{IN}$	physical displacement of the interior DOF in the normal modes
$\varphi$	shape vector
$\Psi$	algebraic constraint equations
${}^G\omega^B_B$	angular velocity of the flexible body relative to the global coordinate system [rad/s]
$\omega_k$	angular velocity of the particle $k$ [rad/s]

## Subscripts and Other Symbols

$\langle \rangle_I$	internal DOF
$\langle \rangle_B$	boundary DOF
$\langle \rangle_N$	normal modes
$\langle \rangle_C$	constraint modes
$\langle \rangle_t$	translational DOF
$\langle \rangle_r$	rotational DOF
$\langle \rangle_m$	modal DOF
$\langle \dot{\phantom{x}} \rangle$	first time derivative
$\langle \ddot{\phantom{x}} \rangle$	second time derivative

## Abbreviations

BCoM	Body Centre of Mass
CFRP	Carbon Fibre Reinforced Plastic
CWS	Chosen Walking Speed
DOF	Degrees of Freedom
FE	Finite Element
FEM	Finite Element Method
GRF	Ground Reaction Force
MBS	Multibody System
PTS	Preferred Transition Speed
WHO	World Health Organization

# 1 Introduction

## 1.1 Background and Motivation

The loss of part or all of an extremity can be a dramatic interruption to a person's life. According to the estimations of the World Health Organization (WHO) in the year 2000, 0.8% of people of the total population have some physical disability that needs prostheses or orthoses. In the amputation cases the main causes are trauma, tumour, peripheral vascular diseases, congenital diseases and diabetes. Also another important factor increasing the number of amputees is the increasing age of people in almost all societies. This is combined in many cases with diseases like diabetic mellitus, which is the leading cause of non-traumatic lower extremity amputations. About 15% of diabetic patients develop foot ulcer and diabetic foot problems and 15-25% of them will undergo different levels of amputations in the lower limbs.

For these reasons yearly more and more technological innovations are trying to make artificial limbs more comfortable, efficient, and lifelike. These innovations enable the individuals to continue their life as an active member in the society with minimum dependency on the others.

Many studies have ascertained that energy conservation and expenditure is a defining characteristic in human gait. A patient with a prosthesis needs more energy for the same activities compared with a healthy person. Figure 1.1 shows the energy expenditure in form of  $O_2$  cost (ml/kgm) for lower limb unilateral amputees with different levels of amputation. All patients were tested at their chosen walking speeds (CWS). The figure shows that patients with higher amputation levels have higher  $O_2$  costs compared with those having lower amputation levels. The energy cost in transpelvic amputees is almost twice as much as the energy cost in normal persons. Figure 1.2 shows that the CWS depends also on the amputation level and declines as the amputation level gets higher. The CWS in transpelvic amputees is almost 50% of healthy persons' speed.

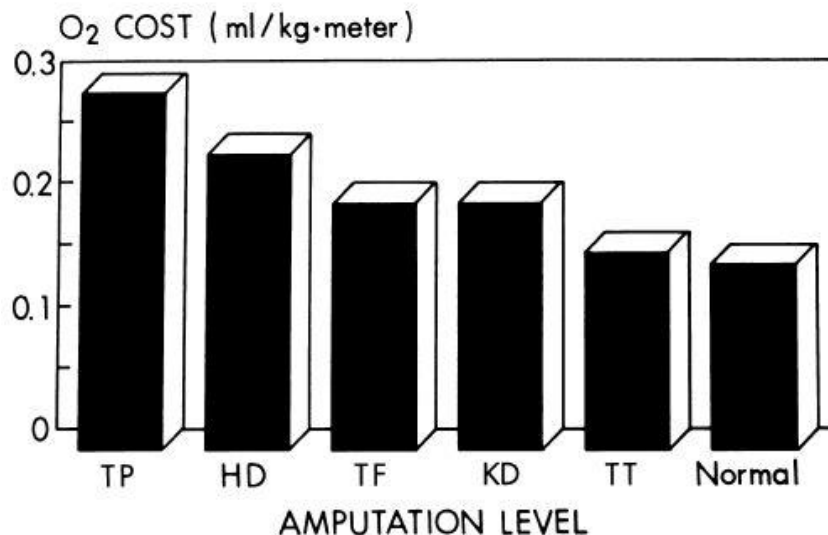


Figure 1.1:  $O_2$  cost in unilateral amputees walking with prostheses at different amputation levels. TP = transpelvic; HD = hip disarticulation; TF = transfemoral; KD = knee disarticulation; TT = transtibial [Waters 1992]

During normal human gait, the storage of elastic energy in compliant structures of muscles and muscle fibres and the return of this energy is an important energy saving mechanism that may

reduce the muscle fibre work, and be an important determinant in the preferred gait mode and the preferred transition speed (PTS) [Sasaki 2006]. Figure 1.3 shows that the vertical component of the ground reaction force (GRF) acting on one of the lower limbs during one stance period changes according to the walking speed. This means when an amputee using an elastic prosthetic foot increases his walking speed, the elastic prosthetic foot will react to the increasing forces by larger deformation and this in turn influences the gait form.

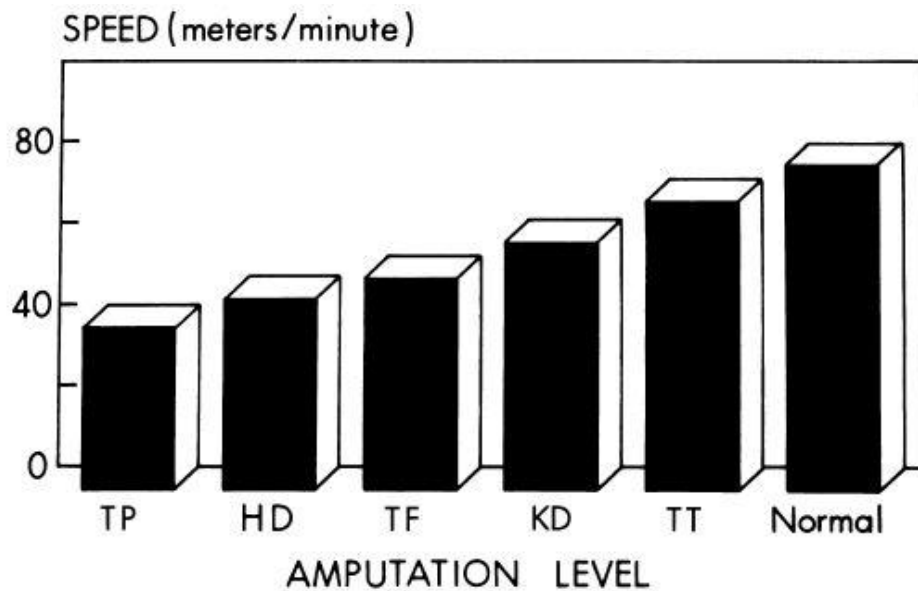


Figure 1.2: Speed in unilateral amputees walking with a prosthesis at different amputation levels. TP = transpelvic; HD = hip disarticulation; TF = transfemoral; KD = knee disarticulation; TT = transtibial [Waters 1992]

In uphill walking on inclined surfaces, the ankle-foot system of healthy individual adapts to the inclination level by creating a roll-over shape that changes in orientation with different levels of inclination [Hansen 2004].

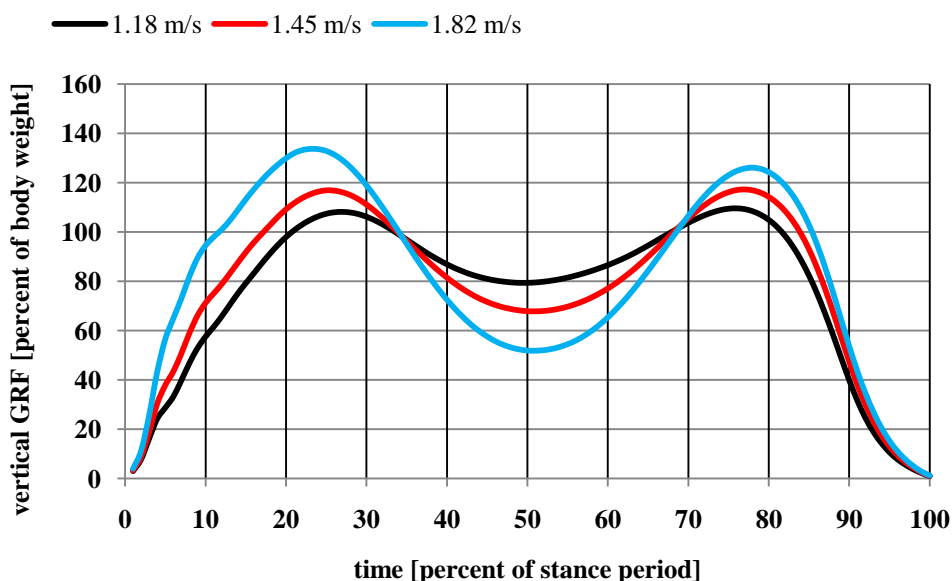


Figure 1.3: Vertical component of the GRF of an able-bodied female walking at three different velocities. Source: Otto Bock GmbH



From these facts it is clear that a sound human foot is an adaptive system that adjusts itself according to the surrounding conditions. In the design of non-adaptive prosthetic feet an optimization process is done to reach feet that suit the average values of walking speed and weight on level surfaces. This leads to limitations in the mobility of the amputees and limits the comfort and the ability of walking at different speeds or on different inclined surfaces.

From statistics based on 15 lower limb amputees wearing an electronic knee recording their activities over a period of 30 days, it was found that the need to change walking speed occurs in average 437 times daily. This was the second most important activity after stop and stand which occurs 1450 times in average, and walking on inclined surfaces occurs 38 times daily [Zahedi 2004]. These statistics show that a normal optimized lower limb prosthetic is still not sufficient to fulfil the typical amputees' daily activities, and that various improvements are possible and could be of great value.

In order to overcome these problems and difficulties, reducing the energy expenditure and improving the comfort of walking, the need arises to develop an adaptive prosthetic foot that changes its properties according to the walking conditions. Such an adaptive foot can achieve its goals when it is designed, optimized and constructed with special suitable adaptive properties that suit the needs of the individual amputees.

The numerical modelling of the human gait qualifies itself as one of the most suitable methods for the optimization processes of the properties of adaptive prosthetic feet. Numerical models can evaluate different properties of the feet minimizing the complexity, costs and time of design process. Therefore fewer prototypes should be latterly constructed to be further evaluated on amputees.

Also, according to many experimental tests, the amputees react differently to the different prosthetic limbs according to their individual needs and abilities. Some amputees find a prosthetic limb acceptable and comfortable, others find it painful and unpleasant. Accordingly the numerical simulation of human gait with adaptive artificial limbs offers the possibility to understand quantitative and qualitative how the changes in the prosthetic feet properties will influence the gait cycle of the amputees. The use of numerical simulation can answer many design questions in short time, thus reducing the reliance on prototypes, involving test subjects whose individual needs have an effect on the overall design.

## **1.2 Scope and Objectives of this Work**

The purpose of this work is to evaluate, by means of numerical simulation, the effects and usefulness of changing the properties of adaptive prosthetic feet and to estimate if these changes will improve the patient's comfort and mobility. Many parameters are considered in this work for the adaptive foot (the foot stiffness, the ankle joint deformation, and the ankle joint inclination angle) and different walking conditions (CWS, fast speed, and uphill walking on inclined surfaces).

In order to fulfil these goals many mile stones are planned, and many limitations are taken in consideration. They are summarized here:

- A numerical model of the human gait for an above-knee amputee using a multi-body system (MBS) simulation program is to be built.
- The multi-body model simulates the stance period of the gait, which is the period representing the contact of two-feet with the ground followed with a one foot contact with the ground and ending with a new two-feet contact. The swing period of the prosthetic limb is not to be simulated since the changes in the adaptive foot do not influence this period.

- The human gait during walking is three-dimensional. In this work just a two-dimensional model is built. The reason is that the forces acting on the body in the third dimension (frontal plane) are small, and the motions in this plane are also small compared with the sagittal plane. Besides that, the changes in the properties of the adaptive foot will be just in the vertical and horizontal directions.
- A reasonable model for the contact between the foot and the ground should be developed based on the models found in literature and depending on the purposes of this project.
- The prosthetic foot is to be modelled numerically as an elastic element, since the modern prosthetic feet are elastic and undergo large deformations, which influences the entire gait. Also they are the elements of the prosthetic limb that make the contact with the ground. From this appears the importance of simulating them as elastic elements in the multibody model. This simulation of elastic bodies in rigid bodies' numerical models is potentially a powerful tool in designing prosthetic feet. For this purpose a FE model of the foot should be built and then integrated in the rigid bodies' MBS model. The finite element model of the elastic foot is simplified by static condensation enabling it to be integrated in the MBS model. This also reduces the MBS simulation time and improves its results which are closer to the reality. The use of elastic elements makes it easier and more accurate to evaluate the effects of contact points and elasticity changes.
- The numerical model should estimate a reasonable kinematic pattern for gait including both single and double support phases. This is done by comparing the results of the model with both the experimental results and the results of other models found from other researchers.
- The parameters that can be used in evaluating the motion of amputees in the numerical model are to be determined. The reasons for the selection of these parameters are to be given, since the purpose of this work is numerical evaluation and estimation of the usefulness of adaptive feet before they are manufactured and further experimentally verified by amputees, (which is out of the scope of this work).
- Here the study is limited by the numerical evaluation of three parameters of the adaptive foot, and at three conditions, that are already mentioned above. These parameters are not evaluated experimentally in this study which is out of the scope of this dissertation.
- Also a second goal in this dissertation is the design of a beam element to be used as an adaptive foot with changeable stiffness. This design is verified analytically and experimentally.

### **1.3 What is Different in this Work?**

The importance of this work, and the differences between this work and other works, which can be derived from the objectives explained in the previous section and from the literature review in chapter 2, are described in the following points:

- Many researchers have suggested the development of adaptive prosthetic feet as an important step in improving the gait of amputees (for example [Zahedi 2005]) but there are no works found that evaluate the effectiveness and validity of such adaptive feet on the whole body motion under different walking conditions before manufacturing these feet and trying them on amputees. Also no study has a suggestion of the definite required amount and type of change in the adaptive properties of the feet to improve the gait. Then the studies depend in their estimations on comparison between the sound leg and the prosthetic leg, which can be inaccurate. In this work the study of the different adaptive properties using a numerical model of the whole gait reduces such problems and improves the quality of the evaluation of the adaptive properties.

- Many models that simulate the gait of healthy individuals were built [Gilchrist 1996 and Wojtyra 2000] but just one model was found that simulates the gait of amputees with limb prostheses [Pflanz 2001]. In the work of Pflanz, the properties of the foot were not measured and used in the simulation but estimated and modified in order to get a gait pattern similar to the experimental results. In this study the prostheses properties are experimentally measured and then used in the simulation which limits the latitude of modelling and makes the design closer to reality.
- The multibody models used in the simulation of human gait were all consisting of rigid bodies and there are no models found that deal with elastic elements. In this work the foot is to be modelled as an elastic element. Also this elastic element undergoes relatively large deformation which already influences the whole gait.
- The use of elastic elements in multibody simulation of different mechanical systems was usually done for elements connecting two rigid bodies or more at a limited number of contact points and the connection stay continuous along the simulation time. In this study the elastic element is modelled in the MBS to make contact with the ground and lately leave the ground, which include a non continuous contact starting at some point in time and ending lately. This modelling form can lead to numerical problems that should be solved and in the literature there were no references or systematic solutions found that can be considered in the modelling.
- In this study two simple concepts for beams with changeable stiffness are developed and the two concepts have lead to large changes in the stiffness. In the literature there are limited models and concepts of beams with changeable stiffness and the changes of stiffness in them are very small, for example [Carli 2006].

## 1.4 Outline

The organization of the text in this dissertation is as follows:

This dissertation is dealing with two subjects combined; one is in the medical field and the other is in the mechanical engineering field. Therefore the literature review in chapter 2 is divided into two main parts. The first is about the human gait and the prosthesis, and the second part is about multibody dynamics and finite element methods. Chapter 3 gives the necessary theoretical background in three fields entitled human gait, basics of prosthesis and multibody dynamics of elastic elements. Chapter 4 shows the parameters selected to be used in evaluating the human gait and the functionality of prostheses. The reasons for this selection are also explained in this chapter.

Chapter 5 displays the numerical modelling process of the human gait, which is built in order to achieve the goals of the whole work. In this chapter the concepts that are adopted and developed in the design of the model are shown. The modelling and integration of the elastic foot in the rigid bodies' dynamical model and the model of foot-ground contact are explained.

An evaluation of the model and a comparison with experimental results is also shown in this chapter, and the results are discussed before using the model further in chapter 6.

Chapter 6 represents the effect of using an adaptive foot on the human gait in different conditions. Three parameters are selected as potential adaptive properties, and the simulation is run for them followed by the results. In this chapter the results of simulating a human gait of a lower limb amputee using a prosthetic foot called C-Walk are represented. The results show the effects of changing the stiffness of the foot sole, the ankle inclination angle and the ankle deformation on the human gait. These effects are shown at three different conditions, namely, walking on level ground, walking uphill on inclined surfaces, and walking at two different velocities.

Since the stiffness is one of the important properties of the foot that could influence the gait, two models of adaptive beams that could be used as soles for prosthetic feet are studied analytically and experimentally and displayed in chapter 7.

Finally chapters 8 and 9 summarize the results, discuss them and give the conclusions combined with suggested potential future work that could be undertaken.

## 2 Literature Review

The present dissertation deals with a range of topics including human gait, lower limb prosthesis, modelling of human gait, and multibody dynamics and FEM. Many books and research papers dealing with these subjects have been written and published in the past. This literature review gives an overview of some developments and studies done in these topics which helped as a base and start point for this work.

### 2.1 Human Gait

The human locomotion has interested many researchers for a long time. In the past decades many terms and concepts in gait analysis have appeared. In 1905 Marks introduced a qualitative description of the normal human locomotion and classified the walking process in eight phases. His work was the basic tool for many further improvements and studies in human walking [Marks 1905]. One of the pioneer contributions to the research in gait analysis was done by Jacquelin Perry through decades of works, which resulted in finer descriptive terms for the functional tasks and phases of gait. Her work has received wide acceptance, and the terms she has developed are also used in this dissertation [Perry 1992].

Saunders et al. have determined in a study the factors giving the human ambulation its sinusoidal form, these are assumed to be the factors that reduce the energy needs of the body during walking. They called these factors the six determinants of normal gait [Saunders 1953]. These determinants were further studied by many researchers. In 1981 Inman et al. studied them again and modified them slightly [Inman 1981]. Some of the researchers had made a finer review of the determinants of gait and showed that not all factors are really significant. Gard and Childress showed that the pelvic obliquity and knee flexion during the stance phase have no or a very small (at most 2-4 mm) effect on the body vertical excursion during normal walking because of their timing. They showed that these two determinants just provide shock absorption. Otherwise they showed that body vertical displacement during walking is a factor of effective leg length, foot rocker radius and step length [Gard 2001]. Another study done by Croce et al. in 2001 showed that the heel rise (foot/leg combination) has a major role in reducing the vertical displacement of the BCoM. According to their study, the determinants of gait issued by Saunders et al. were generally correct, but they support the findings of Gard and Childress that the pelvic obliquity and knee flexion during stance phase are not the major contributors to the reduction in the vertical BCoM displacement. They consider the heel rise as the most important contributor followed by the pelvis rotation with a 10% contribution [Croce 2001].

The energy cost of human locomotion is studied by many researchers, and the major parameters influencing this energy cost are assumed to be the speed, gait pattern and body size. Raynor et al. estimated in their study of the transition speed in human gait that the loading rate of muscles reflect the ability of the musculo-skeletal system to store and utilize the elastic energy. The capacity to store elastic energy and further utilize it depends on the rate at which the series elastic structures in the muscles are stretched. They estimate that transition from a walking to a running gait will allow the elastic energy to be effectively utilized as a consequence of the flight phase [Raynor 2002]. Usherwood and Bertram studied the gait transition cost in humans and present the assessment of the metabolic cost for the Walk-run/run-walk transition. They estimated that the gait selection for a speed is partly related to metabolic cost. Humans elect to transit from walking to running with increasing speed but do that at speeds where walking is still metabolically more economic [Usherwood 2003]. Figure 2.1 shows the metabolic energy cost for running and walking at different speeds for a typical subject. The intersection represents the speed at which walking and running have the same energy cost.

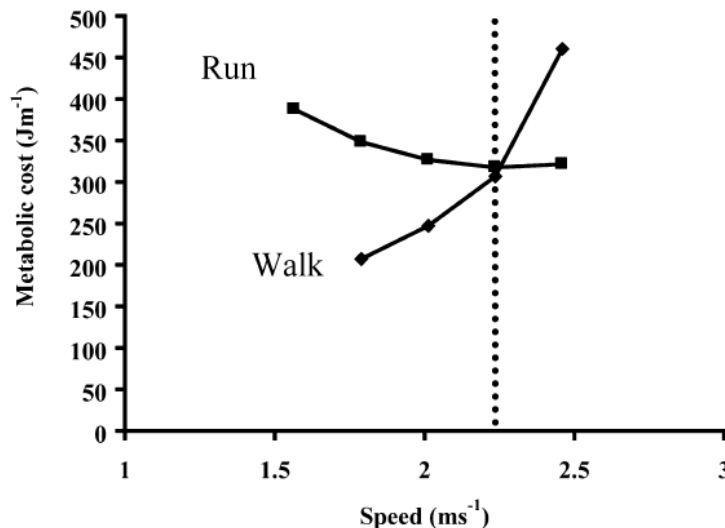


Figure 2.1: Typical intersecting metabolic cost curves for walking and running [Usherwood 2003]

The walking of adult humans owes much of its efficiency in the conservation of energy by transforming between the kinetic and potential energy (In general as the velocity of the BCoM decreases from initial contact to mid-stance, its elevation increases and the inverse occurs in the rest of the step from mid-stance to pre-swing phase). Wang et al. studied this transformation of energy in erect walking at three speeds and in bent-hip, bent-knee walking. The fluctuations of potential energy and kinetic energy of the BCoM were measured. In upright walking the fluctuations in potential energy are out of phase compared with the kinetic energy, which indicates the transfer of energy between the two forms and accordingly the energy is conserved. The highest energy recovery was reported to occur at the comfortable selected walking speed, the next highest was in fast and slow walking, and the lowest is at the bent-hip, bent-knee walking [Wang 2003].

An important study published by Gordon et al. in January 2009 studied the change in the energy cost by changing the vertical centre of mass movement during gait. According to this study they concluded that reducing the vertical BCoM movement is not a successful strategy for improving the metabolic or mechanical energy use during normal walking by able-bodied subjects. This does not support the hypothesis that reducing the centre of mass is energetically optimal. They studied the walking of ten subjects at different walking speeds and two body configurations leading to different BCoM motions. The results show that reducing or increasing the vertical BCoM movement, beyond the movement values at the subjects' preferred walking speed, increases the metabolic and mechanical energy cost. From these results it may be estimated that the BCoM motion is not itself that costs energy and there may be an optimal BCoM form (trajectory) during walking that is combined with minimal metabolic and mechanical energy cost of the body segments [Gordon 2009].

The control of the human gait is done through a central nervous system that activates the different muscle groups to keep the body stable and to adapt the gait to the changes in the lower limb properties or to changes in the boundary conditions. This central nervous system recalibrates the muscles activity according to the altered force environment (For example increased body weight, change in walking direction and speed, path inclination, ...) such that the whole body works as an adaptive system and stays balanced with respect to its centre of mass, and gives a stable and safe ambulation [Noble 2006, Jo 2007].

In order to evaluate the quality of a gait and its deviation from the average normal profile many studies and researches have been done. Schutte et al. have suggested an index for quantifying

deviation from normal gait depending on 16 independent variables derived from 16 selected kinematic gait variables. In their study they have developed one single normalcy index, which can be simply considered as a measure of the distance between a set of discrete variables describing a patient's gait pattern and the average values of those variables in subjects without gait abnormalities. Nevertheless the normal gait is a subjective notion, this index has the potential of being an objective measure of gait deviation from normal gait pattern [Schutte 2000].

## **2.2 Prosthesis**

The beginning of prosthetics and amputation surgery goes back to the very early human medical practice. A 45,000 years old human skull in the Smithsonian institution shows shaped and aligned teeth representing the earliest anthropological evidence of an amputee. Limb prostheses in old ages were designed for many purposes, for example: cosmetic appearance, function, and/or psycho-spiritual sense of wholeness. They have begun as simple crutches or leather and wooden cups depicted in Moche pottery and have developed with time into modified crutches or pegs to free the hands for other functions. A peg leg consists of an open socket with cloth rags to soften the distal fibula and tibia, and increase the range of motion. With the Roman civilization the prostheses have further developed. A roman Prosthesis (about 300 B.C.) constructed from wooden core, bronze shim, and leather straps was unearthed in Italy. During the dark ages the knights had prostheses for use in battles but they were usually heavy, cumbersome, and their function was for aesthetics rather than practicality. For example artificial legs were set to ride in stirrups, and to hide the disgrace and weakness. For everyday life the use of peg legs or crutches was preferred. Some of the artificial limbs developed at the end of this age and the beginning of the Enlightenment age were mechanical masterpieces, for example the iron arm of the German knight Götz von Berlichingen, which have independently moving joints that can be set with the sound hand and relaxed through a release and springs. Another example is the above knee prosthesis of Pare (1510-1590). It had an adjustable harness, knee lock control and fixed forefoot position, which are engineering features existing in many modern limb prostheses. In 1696 Pieter Verduuin introduced the first non-locking, below knee prosthesis which was made of external hinges and leather cuff that bore weight. It had also a wooden foot and a copper shell. The socket was lined with leather. With the time the lower limb prostheses had further developed in function, materials utilized and their shapes. In 1800 James Potts designed a prosthesis consisting of a wooden shank and socket, a steel knee joint, and an articulated foot that was controlled by catgut tendons from the knee to the ankle. In this foot the flexion of the knee caused dorsi flexion of the foot, and the extension of the knee caused plantar flexion of the foot. With the time, after the marvellous development in the material industry, the rubber foot came into use eliminating the complicated articulated ankles (1861). And in 1912 the first aluminium prosthesis was made [Nupoc 2005] [Wilson 1992]. After the Second World War the design of prostheses had rapidly developed, and here is a summary of the developments in the different parts of the prostheses.

### **Sockets**

About 1950 the quadrilateral socket was developed with well defined walls, permitting the use of the remaining muscles and an air space was left between the distal end and the bottom of the socket, according to the German practice, which was used successfully from most of the patients. Then the Patellar tendon-bearing (PTB) prosthetic socket was developed in 1959, which involves total contact between stump and socket including a contact support at the distal end. At the same time the materials used have developed and changed to overcome the deficiencies of wood and leather. For example thermosetting resins were used for laminating tabular stockinette-over-plastic replicas of the stump to form the sockets and structural components of prostheses [Wilson 1992]. In the last decade of the 20<sup>th</sup> century and first years of

the 21<sup>st</sup> rapid technological advances in the lower limb prostheses was developed, based on the increased understanding of human biomechanics of locomotion combined with experimentations. These days the design of a new socket has a distributed weight bearing, instead of localized weight bearing, to reduce peak pressure and increase the amputee comfort. Silicon liners were developed as an alternative for patients who are unable to manage the difficult donning process but could benefit from suction. A silicon locking liner is used with a shuttle and pin lock to develop a suction for suspension of the prosthesis. The silicone elastomeric liner creates a soft and slightly elastic inner liner between the residuum skin and the more rigid weight bearing parts of the prosthetic socket. Also it allows volume fluctuations through the addition of prosthetic socks [Murali 2001] [Marks 2001]. New alternatives appeared to be used instead of the external sockets such as direct skeletal attachment via osseointegration. The osseointegration is seen as an optimized system that combines better control over the prosthesis due to the enhanced sensation from the amputees and increased power transfer from the residuum [Zahedi 2004].

## **Knee**

Locomotion studies show the importance of control of the shank rotation at both stance and swing periods. For earlier prosthetic knees the shank motion was controlled in swing period by introducing friction about the knee bolts. This system was known as constant friction knee and was an optimization that gives smooth gait at only one cadence for a given amount of friction. The development of fluid-controlled prosthetic knees in the 1950s has solved a part of the problem of constant friction. The strong damping forces that can be generated in hydraulic knee controllers are used to assist stance stability and cushion the heel strike [Mak 2003].

Thigh amputees using these earlier systems were forced to hold the prosthetic knee in full extension throughout the stance period of the gait cycle to prevent the leg from collapsing. Since this eliminates the shock absorption offered originally by the bending of the sound knee and causes an unnatural gait, a growing number of prosthetic knees were developed with a stance flexion feature. The first prosthetic knee offering this feature was Bouncy-Knee from Blatchford Company in the 1980s, which contains a friction brake that engages automatically and stabilises the knee when the amputee bears his weight on the limb. This knee joint contains a rubber element that allows a small flexion in the knee during the early stance phase matching the flexion of sound knee partially and therefore absorbs a part of the shock [Marks 2001].

The C-Leg system developed by Otto Bock in the 1990s was the first completely microprocessor controlled prosthetic knee. This knee has hydraulically controlled swing and stance phases. In this foot the hydraulic system function is controlled through a microprocessor enabling the amputees to ambulate closer to their natural gaits. A set of sensors in the C-leg collect data about the position of the leg in the space and use it in adjusting the resistance of a hydraulic damper up to 50 times a second, therefore controlling the stance and swing phases, which in turn fulfils the stability and security needs. This has lead to a smooth and harmonious gait, almost similar to the sound leg. It has made it safer for amputees to walk on uneven ground and reduced the energy needed to prepare the leg for the swing phase [Dietl 1998]. The completely computerized knee joint C-leg was compared with other conventional hydraulic knee joints and it shows advantages during the swing phase control, such that the swing phase comes to a smooth and harmonic end. Also the computerized prosthetic leg offers the shortest running time compared with conventional hydraulic prosthetic knee joints [Kastner 1999]. One of the aims of the completely controlled prosthetic knee and respectively adaptive knee is to be able to adapt to the different modes of locomotion whilst optimizing the use of the power from the amputee. Zahedi et al. reported that the use of adaptive prosthesis by a sample of 10 amputees indicated an enhanced control and an increased comfort and safety during ambulation. Also increased comfort and safety in manoeuvring various terrains was clearly noted [Zahedi 2005]. Wetz et al. compare the C-leg knee joint with conventional artificial knees on 25



amputees. Their study shows that active patients benefit from the new computerized knees in almost all cases. Less physically active amputees show significant functional improvements but less than that of active amputees [Wetz 2005].

## **Feet**

Artificial feet have also developed to provide better functions for the users. The earlier models were single axis models. To enhance the patient's ability to walk the articulated feet were later developed. One of these feet is the Navy ankle foot, which contained a block of rubber with variable stiffness to control motions in three planes. The disadvantage of this foot is that it needs excessive maintenance. The Greissinger foot from Germany is another foot which provides three planes of action and needs less maintenance. In 1956 the SACH (solid ankle cushion heel) foot was introduced. It was an ultimate in simplicity, needs very little maintenance and provides acceptable function for most patients. Many other feet were developed based on the SACH foot. In the late 1970s John Campbell developed a SACH foot with a part of the three way function and called it SAFE (Stationary attachment-flexible endoskeletal) foot. An energy storing foot was produced firstly in the early 1980s in an effort to provide athletics with a lower-limb amputation with more functions. In this system the energy is stored in an elastic keel during stance phase, and released at the pre-swing phase of the gait. Further developments resulted from the market competition, and amputee expectations lead to the design of prosthetic feet with shock absorbing systems [Wilson 1992] [Zahedi 2004].

The appearance of the energy storing prosthetic feet has lead to new series of studies in optimizing their design and form utilizing the numerical methods available. As an example Jang et al. have developed a new effective systematic methodology for the design of a flexible keel. In their study they have considered the energy storing as an optimization factor and developed a dynamic FE model simulation to find out the factors improving the effectiveness and energy storing capacity of the foot. In their study they used data from healthy people as inputs for the dynamic simulation but they have not considered the effects of this optimized foot on the other kinematic parameters of the gait [Jang 2001]. Also Kwan and Hubbard tried to find out the optimal foot shape for passive dynamic biped by changing the foot length and ankle placement. They found a representative foot shape (through changing these two parameters) for short period solution (shorter and quicker steps) but for long period solutions (longer and slower steps) the shape was not any more representative [Kwan 2007].

The C-Walk foot from the company Otto Bock and Flex-Foot from the company Össur are two examples of the modern prosthetic feet with energy saving and return ability that have been developed in the last two decades. These feet take the advantages of using carbon-fibres composites in manufacturing prosthetic feet. The large elasticity and the superior strength-to-weight characteristics of carbon-fibres composites made them a suitable material in prosthesis. In these feet during the load response and mid stance phases of the locomotion energy is stored in the carbon-fibre spring elements of the foot complex and released again later in the rest of the gait cycle pre-swing phase. Such modern prosthetic feet provide a good replacement for active amputees with high activity levels. Another development was done to reduce the lack of shock absorption through introducing a shock absorbing mechanism in the shin of the feet. Gait studies have confirmed that shock absorbers improve the performance of artificial limbs and make them more acceptable for the patients [Otto Bock 2009a] [Össur 2009].

## **CAD/CAM**

To accelerate the fitting and fabrication of prosthesis and reduce the costs and human errors, Computer-Aided Design/Computer-Aided Manufacturing (CAD/CAM) was suggested and used in the design of human prosthetic limbs. The idea was conceived firstly in the 1960s but the first system using this idea appears in the 1980s and was specified for sockets design [Mak 2003].

## 2.3 Modelling of Human Gait

Many attempts in developing an efficient way for obtaining equations of motion for multibody systems have appeared in the recent years. One of the motivations for these developments was the advance in computer hardware and software combined with advances in the numerical methods. Another motivation was the automation in industry and the use of robots in executing various tasks instead of humans in factories.

Multibody analysis has been applied in biodynamic modelling extensively compared with other application areas. The reasons for this were the need to understand the dynamic behaviour of bio systems, specially the human body. The human body dynamic models have been used in many applications for example in crash-victim simulations. In these simulations the human body model is placed in a model of the vehicle and then the vehicle undergoes a crash simulation. With such models the seats in the car and the safety systems are evaluated and improved before real crash tests are done. This saves the high costs of real crash tests and the time of designing. Also the forces acting on the spinal column can be measured by these models and further used in the design of the seats and seat belts in the vehicles [Huston 1976], [Fleck 1994]. Wölfel et al. have built a dynamic FE model of a sitting man to estimate the unknown internal compressive and shear forces in the lumbar vertebral disks of the human body from an arbitrary base excitation input function. The long term whole-body vibration can cause degeneration in the lumbar spine and one of the benefits of this model is its ability to measure the internal forces acting on the lumbar spine. These internal forces cannot be measured experimentally as force transducers cannot be implemented in the force lines because of ethical reasons. A numerical model allows one also to adjust its parameters for different body height, weight, and configuration [Wölfel 1998]. Another application range of dynamic models is in the design of internal body joints replacements. Leardini and Moschella have used dynamic simulation to estimate the art of total ankle prosthesis design. Their model has been demonstrated to be valuable for describing the geometry and kinematics of the intact human ankle joint. Simulation results based on their model are also able to define the performance of current and possible novel designs of ankle replacements [Leardini 2002].

In human locomotion the multibody dynamic is also used in building models of the gait during walking. Onyshko and Winter have built one of the earlier mathematical models for the human locomotion. Their model consists of seven segments, three segments for each leg, and six joints, all moving in the sagittal plane. The approach followed was of the initial value problem, it is to say, starting with initial kinematic conditions (initial positions, angles, and velocities) and system inputs (applied joint moments) in order to find the system responses. The model simulates one step and divided it into four phases. The four phases need four different sets of governing equations of motion to suit the changes in the body contact with the ground which is simulated in form of joints. Dynamically they have used Lagrangian mechanics in obtaining the equations of motion [Onyshko 1980].

Pandy and Berme modelled the single support phase of the gait where the motion is synthesized through using a pre-programmed set of inputs for the joints moments. The purpose of their model was to identify the determinants responsible for the observed variation in the horizontal and vertical GRFs during normal gait. Their model is divided into two phases. The first is to study the stance knee flexion-extension, and the second is to study the foot and knee interaction. From their model they estimated that the stance knee flexion-extension generates the necessary level of the whole-body vertical acceleration in the first region of single support (mid stance), which results in the first peak of vertical GRFs. The second peak is estimated to be a result of an increasing ankle moment during the terminal stance phase [Pandy 1988]. Gilchrist and Winter modelled the normal human walking in a nine-segments three-dimensional model. Their model used the joints moments measured in gait analysis as driving moments. This model has completed one stand phase starting with the foot flat phase and ending with the heel contact of

the opposite foot. After that the deviations between the simulated movements and the measured one become too large to be considered acceptable. At the heel strike of the opposite foot a sharp change in the Anterior/posterior forces and the vertical forces of the facing foot is noted. The benefit of this model was that it does not force the model to fit pre-determined trajectories. Nevertheless it was able to estimate a reasonable kinematics of the model using the direct dynamic approach [Gilchrist 1997]. Similarly many works were done further utilizing the previous concepts and the direct dynamic approach which is able to predict some system behaviours. The measured data is firstly analysed with inverse dynamic approach and then adopted for the numerical model. Also the modelling of the foot contact with ground through spring-damper elements instead of joints makes it possible to simulate the gait as one unit with no need to divide it into shorter phases. Wojtyra has built a three-dimensional model where the body is divided into 8 segments, and this model shows good consistency between measured and calculated results. However, there are some differences, which he refers to the fact that the foot in his model was modelled as a rigid body with a limited number of contact points (five points). The differences observed in Wojtyra's model between measured and simulated data are less than 15% of the maximal values, which are modest differences in biomechanical calculations [Wojtyra 2000].

The inverse dynamic analysis is the most important source of the data used in the direct dynamic models, and therefore has been extensively studied and improved. The goal of these developments is to improve the consistency of the kinematic data, which in term will improve the outcome of the dynamic simulation models and its ability of adapting the data of single person in the gait models without large deviation from normality in the results [Silva 2002]. Inverse dynamics is also used in building multi-segment models of the body instead of using direct dynamics. The inverse dynamic methods are computationally very efficient and do not require numerical integration of the differential equations of the model. One example of these models done by Ren et al. is assumed to predict a complete cycle of the human gait through formulating walking as an optimal motor task. They used the minimization of mechanical energy expenditure as performance criterion combined with multiple constraints. The inputs for the model were three simple gait descriptors namely the walking velocity, cycle period and double stance duration [Ren 2007].

The feet and the contact between feet and ground play large role in the human gait. They are studied by many researchers, and many concepts and assumptions in their modelling were suggested. Here are shown some of these models and studies. Scott and Winter proposed a complex model of the human foot consisting of eight segments and eight monocentric joints. In their model the contact with the ground is modelled as a nonlinear spring and nonlinear damper, at seven independent contact points. The model was used as an objective tool to estimate the kinematics and kinetics of foot during stance period. Figure 2.2 shows the foot model of Scott and Winter with the joints at the bones connection points. The soft tissues are represented through spring-damper elements located under the head of the metatarsals [Scott 1993]. Leardini et al. have proposed a new protocol to track the large number of foot segments during the stance phase of gait with smallest number of markers, the protocol enabled the measuring of three dimensional rotations of five joints and the measurement of planar angles in both transverse plane and sagittal plane. Through this protocol an enhanced understanding of the dynamic of the human foot is obtained which can be used in clinical applications or in designing more complex feet assemblies either for numerical modelling purposes or for improvements of artificial feet [Leardini 2007]

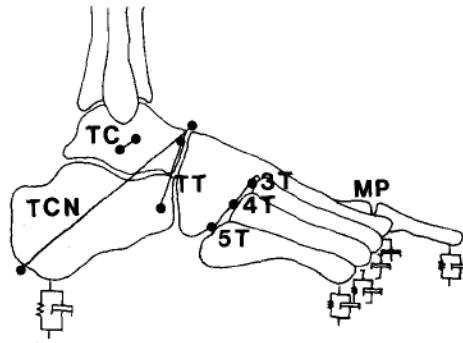


Figure 2.2: Lateral view of the foot model consisting of eight segments, eight joints and seven spring-damper elements modelling the contact with the ground [Scott 1993]

Gerritsen et al. modelled the foot contact with the ground as a non-linear visco-elastic element. They used this model in a four segments model of the body during heel-toe running to investigate the influences of muscle activation, positions and velocities of body segments, and surface properties on impact forces. This study showed that the muscle activation has a small influence at the limited case of initial joint moments. The kinematic condition otherwise has a large impact on the forces. The foot angles have a large influence on the peak impact force and they are inversely related. The vertical velocity of the heel is directly related with the peak force such that an increase in velocity of 0.1 m/s leads to a force increase of 212 N. Some other factors are also considered in this study. One benefit of using simulation in this study was the fact that experimentally it is impossible to change just one parameter and keep the others fixed since subjects in reality may adapt their gait pattern and mask any changes resulting from changing one single parameter [Gerritsen 1995]. Gilchrist and Winter have gone further with the use of visco-elastic elements in modelling the foot contact with ground and developed a three dimensional model of the foot with nine visco-elastic elements. Their model allows more freedom of movement and model the physical system more closely because it needs no joints to simulate the contact with the ground as it was the case in earlier models [Gilchrist 1996]. Chi and Schmitt studied the mechanical energy of feet during impact which occurs in the first 10-20 ms after heel-strike. Through their study they modelled the contact with ground through a spring-damper element and show that the foot has an effective mass of 6.3% of the body weight in walking but this mass goes down to 5.3% in running. According to their study the effective mass is insensitive to heel pad-resilience and effective leg stiffness [Chi 2005].

Some studies have tried to understand and analyse the function of muscles of the human being and to build an approach to determine the muscle forces. Bogey et al. tried to develop a new approach in which the muscle forces are determined from the electromyography data. Electromyography is an approach to study the muscle activities (during different activities including walking). It can measure the timing of single muscle activation, if a muscle is on or off and if its activity is large or small. However this measurement cannot quantifying the force of the muscle. The force of a single muscle cannot be directly measured without invasive methods, such as tendon force transducers, but invasive techniques are not appropriate for clinical use. In walking and generally in locomotion the inverse dynamics approach is the most prevalent method of understanding the role of muscles during movements but this approach quantifies the force of a group of muscles. In the Bogey et al. approach they try to process the electromyography data into force values after evaluation of the forces of a group of muscles through inverse dynamic analysis [Bogey 2005].

Many studies have tried to model the parts of the body near to its anatomical conditions and form, such that modelling the knee joint as bones in contact instead as a simple hinge joint and modelling the muscles through mathematical functions that contain the muscles' different

properties (elasticity, active parts (motors) and the damping). One of the most modern examples of simulation programs for human body motion that utilize these detailed studies is AnyBody program. This program is a three dimensional model of the human being that can be modified according to the exercise under study (for example: cycling, walking, running, ...). In this program the muscle and bones are modelled and can be disconnected or modified to simulate for example the cases of injuries or muscle weakness [AnyBody 2009].

## **2.4 Multibody Dynamics and FEM**

The integration of elastic elements in a multibody system consisting of rigid bodies has interested many researchers in the past. Such a combination is a powerful tool for further development in machine design, robotics, biomechanics and many other fields. The flexible bodies can largely change the dynamics of multibody systems, especially when they are long members in the system. Many studies have been published on methods for the dynamics of flexible multibody systems but there are also large discussions and disagreements about the acceptable and optimal method. The reason of these disagreements is the approximations adopted in these methods which can lead, if they are not properly ordered - according to many researchers - to the neglecting of significant terms and accordingly causing erroneous results.

One of the pioneer works that helped in the development of multibody dynamics of flexible bodies was done by Craig et al. [Craig 1968]. In this work the authors have developed a method for treating a complex structure as an assembly of substructures. For these substructures the mass and stiffness matrices are used together with the geometrical compatibility of the substructures boundaries. The rotations and displacements of substructures boundaries are constrained with those displacements of the adjoining substructures and build together the constraint modes. The compatibility requirements along the substructures boundary in this system lead to the coordinate transformation matrices. These transformation matrices are employed to obtain the whole system mass and stiffness matrices using the matrices of the substructures. This method offers the possibility to reduce the system matrices without causing large changes in the dynamic results of the system.

Huston [Huston 1990] has developed a method for flexible bodies using finite segment modelling. In this method the flexible element is modelled as a system of rigid bodies connected with joints containing springs and dampers. According to the writer the incorporation of the flexibility into the joints of the system avoids the neglect of significant terms due to approximations.

The other methods for the analysis of flexible body motion in a multibody dynamic system can be roughly divided into three groups according to Wallrapp and Schwertassek [Wallrapp 1999]:

- 1- The method of floating frame of reference formulation. In this method the motion of the flexible body is described through superposition of the motion of a reference system fixed on the flexible body and the deformation of the body with respect to this reference system. This method is the most popular in research of dynamics of flexible multibody systems. Also it is the preferred method in MBS simulation programs based on the description of the systems through relative coordinate system. This is because the mass matrix of MBS consisting of rigid bodies is already complex and fully occupied such that the addition of the flexible body mass matrix to the system will not add any disadvantage to the whole mass matrix. An additional advantage of this method is that by small deformations the equation of motion can be easily linearised, and this reduces the calculation time.

- 2- The method of incremental finite element formulation. Here the motion of the finite element structure is described through the coordinates of the nodes. In this method the deformation of the body in case of large forces and large deformations is calculated through dividing the force

into small increments. Then an iteration method is followed in small stepwise form utilizing the linear approximations in the equations of motion of the system for small deformations and this leads to the calculation of the whole deformation.

3- The large rotation vector approach. This method is suggested for beam elements. In this approach the equations of motion are derived in a form containing the deformation of the points of the beam axis and the rotation of the beam cross section with respect to an inertia system as a product of an interpolation function and an undefined function of time. This method allows large deformations in the system.

Shabana has suggested a new method called Absolute nodal coordinate Formulation. This method tries to avoid the disadvantages of the other methods in a simple way. The FEM was developed originally for static analysis of structures and the variables used in FEM programs do not allow large motion of the rigid bodies since such a large motion results in a wrong mass matrix. In using the derivatives of the material nodes coordinates instead of the angles to describe the rotation of the cross sections and lines of beams and plates it is possible to describe the large motion of the rigid bodies of such beams and plate elements. This method gives a simple mass matrix compared with the method of floating frame of reference formulation but a more complex stiffness matrix [Shabana 1997].

These methods and works were the bases of many further developments considering the elastic elements as substructures. Some researchers have tried to develop systems suitable for special forms that are commonly used. For example Ghiringhelli et al. implemented the finite volume beam in multibody dynamics [Ghiringhelli 2000]. According to their work a  $C^0$  beam is discretised based on the finite volume concept. This means only collocated evaluation of the elastic forces is required for the nonlinear formulation, which simplifies the computations of the elastic part contribution in the equilibrium equations of the multibody system. This system is assumed to be a faster analysis approach especially in dynamic problems like nonlinear multibody numerical approximations but its use is limited to the special case of beams.

The MBS simulation programs have also adopted these developments in their structures. In the multibody simulation program ADAMS, the flexible elements are integrated after reduction using Craig-Bampton Method. In this reduction a subset of Eigen modes are selected by the user and displayed in a modal Craig-Bampton space. This allows the simulation of the elastic bodies as a part of the whole system without the need to have any external link with other programs [Adams 2008].

Weule et al. utilized this capability of the program ADAMS in structural optimization of machine tools including the static and dynamic workspace behaviour. Before the development of such programs it was not visible to optimize the static and dynamic behaviour of the workspace. One of the benefits of generating loads on elastic elements within a multibody system is to take a variety of system configurations into considerations without incorporating the time consuming changes using conventional FE models [Weule 2003]. Müller et al. utilized this development in the topology and shape optimization of the flexible mechanical systems. They have developed an automated coupling of MBS and FEM and also with an optimization program based on FEM. This approach enables the automated determination of complex loading-conditions like rotation and acceleration for bodies in mechanical systems and using them in the structural optimization [Müller 1999].

### 3 Theoretical Background

The study of the human body movement as a machine has its foundations in three major areas namely - mechanics, anatomy and physiology, and more specifically, biomechanics, musculoskeletal anatomy and neuromuscular physiology. The knowledge of these three fields forms the foundations for the study of human movement. This theoretical background starts with an introduction to the human gait as base for understanding the functions of prosthetic limbs, followed by a description of the different elements of prostheses and their functions. Since the evaluation of the human gait is to be done through numerical simulation, a brief background of the dynamics of multibody systems is in the last section.

#### 3.1 Human Gait

The first and most important step in the analysis of human movements is the understanding of the primary purpose of these movements. Without this understanding it is impossible to evaluate its effectiveness. The body can move using joints and levers in a large variety of ways. To recognize and analyse this motion it is important to divide it into many steps that have some notable events helping in the understanding of the beginning and end of these steps.

Walking is one of the most important daily human movements and is characterized by the translation of the body's centre of gravity forward in an energy efficient manner as a result of the alternating pattern of the lower extremity joint movements during the stance and swing phase. This manner or style of walking is described by the term "gait". The base for the design, development, and evaluation of prosthesis is the understanding of the normal gait. The term "normal gait" is used to describe the parameters of walking that have been generalized through sex, genetic predisposition, age, and anthropometrical variables [Mak 2003].

A gait cycle is the period of time between two identical events of the walking cycle, however a gait cycle starts generally when the foot contacts the ground and ends when the same foot comes again in contact with the ground. One normal gait cycle consist of two steps, and they build together one stride (see Figure 3.1). Cadence is the number of steps taken per unit of time usually expressed in steps per minutes.

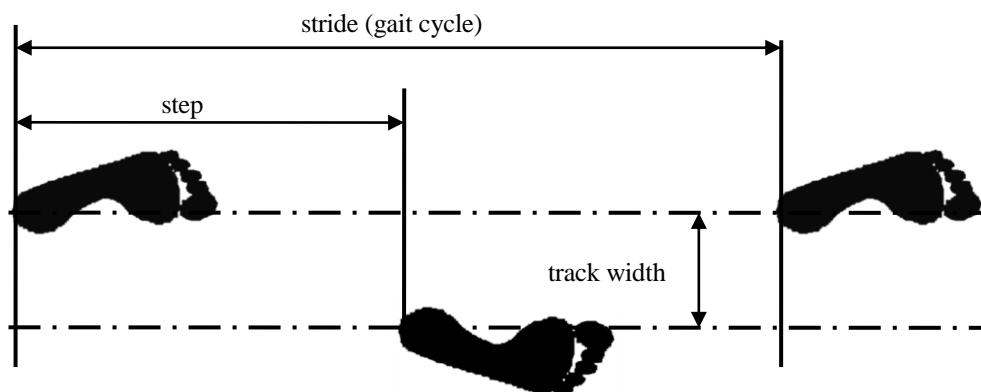


Figure 3.1: A step verses a stride and the track width

Through observing one of the legs along the gait cycle, the gait cycle can be divided in two parts, the stance phase (the phase when the foot is in contact with the ground) and the swing phase (the foot is not in contact with the ground). The stance phase is also divided into two parts, single support, when one leg is in contact with the ground and double support when both feet are in contact with the ground. At the customary 80 m/min rate of walking, the stance phase takes in average 62% of the gait cycle and the swing phase 38% [Perry 1992]. By increasing the walking speed the time of the swing phase increases. Every double-limb support takes about

12% of the gait cycle leaving 38% for the single support. The absence of the period of double support distinguishes running from walking.

Functionally a gait cycle is divided into three tasks, weight acceptance, single limb support, and limb advancement.

Furthermore and in order to make the observation of human gait easier, the stance phase is divided into five discrete events and the swing phase into three discrete events. These steps are all observable and have functional purposes (see Figure 3.2).

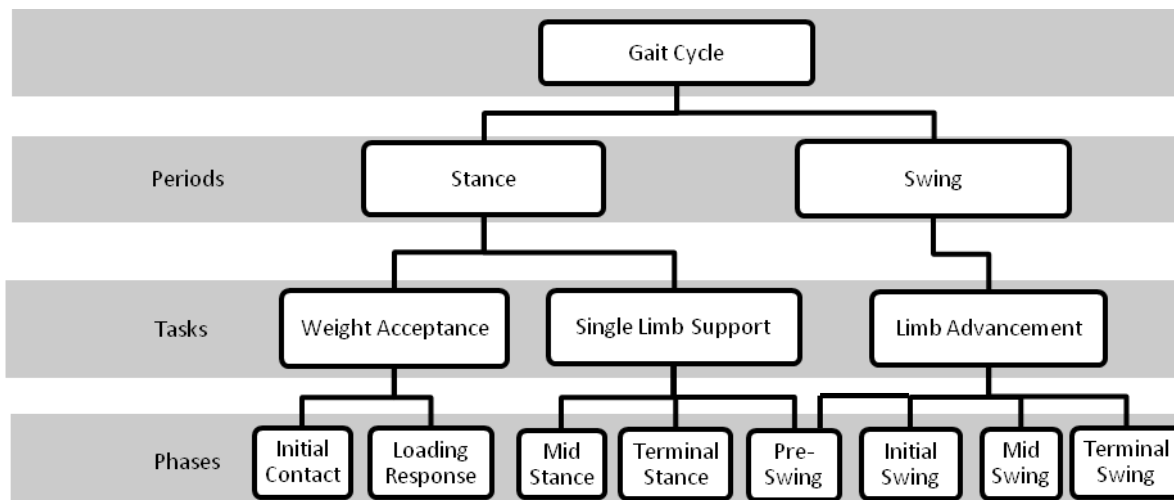


Figure 3.2: The divisions of the gait cycle

The stance phase consists of (Figure 3.3):

a- Initial Contact (IC): This phase occurs in the interval 0-2% of the normal gait cycle at the instant when the foot of the leading leg touches the ground. The objective of this step is to prepare the limb to start the stance phase with a heel rocker.

b- Load Response (LR): The time from the initial contact of the ipsi-lateral foot until the contra-lateral foot is lifted for swing. It takes the interval 0-12% of the normal gait cycle and has the purpose to absorb the shock, to give weight bearing stability and preservation of progression. This period is the first double support period.

The term ipsi-lateral is used to describe the part of the body facing the observer and the term contra-lateral is used to describe the opposite side.

c- Mid Stance (MSt): It occupies the interval 12-31% of the gait cycle and represents the first half of the single support period. It begins when the opposite foot is lifted and continues until the body weight is completely aligned over the forefoot. This period stabilizes the limb and trunk and allows progression over the stance foot.

d- Terminal Stance (TSt): It is the second half of the single support occurs in the interval 31-50% of the gait cycle. Starts with heel rise and ends when the contra-lateral foot contacts the floor. In this period the body moves forward beyond the supporting limb.

e- Pre-Swing (PSw): Averagely this occurs in the interval 50-62% of the gait cycle. It is the last phase of stance and the second double support. It starts with the initial contact of the contra-lateral limb and ends with toe-off of the ipsi-lateral limb. Through this phase the limb is positioned for swinging.



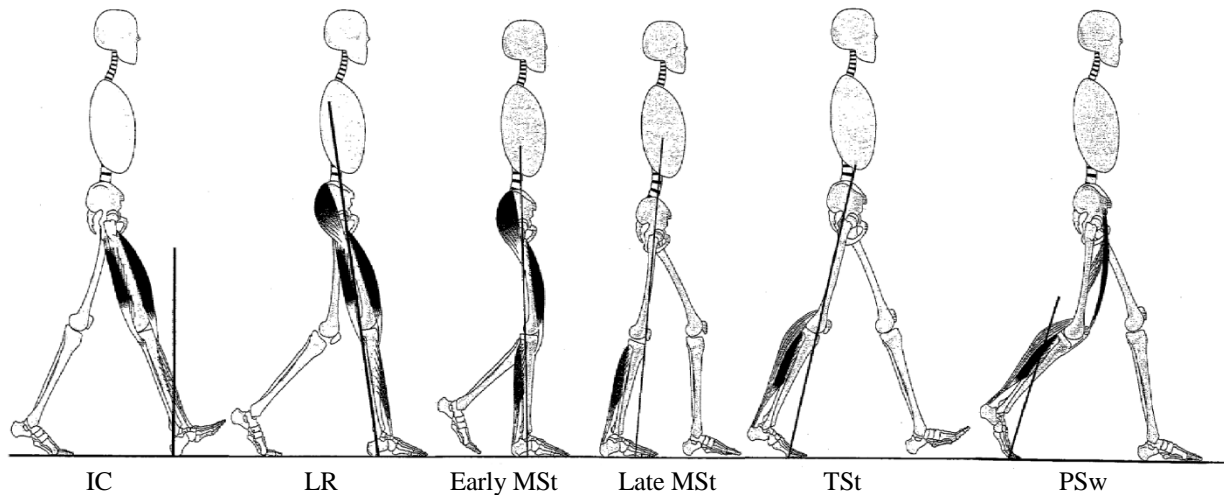


Figure 3.3: The five phases of the stance period of the gait cycle with the line of action of the GRFs on the ipsilateral leg (the leg with the muscles) [Götz-Neumann 2006]

The swing phase consists of (Figure 3.4):

- a- Initial Swing (ISw): It is about one third of the swing phase (62-75% of gait cycle). It starts with the lift of the foot and ends when the swing foot (the ipsilateral foot) is opposite to the stance foot. By lift-off of the foot a clearance from the floor is obtained which allows the limb to advance forward.
- b- Mid Swing (MSw): It begins at the end of the previous period and continues until the tibia of the swinging limb is vertical. It takes the period 75-87% of the gait cycle and has the same function of the previous period.
- c- Terminal Swing (TSw): The last interval of the whole gait cycle (87-100% of the gait cycle). Starts with the tibia of the swinging limb vertical and ends when the foot makes contact with the floor. The purpose of this period is further advancement of the limb and preparation for new stance phase of the limb.

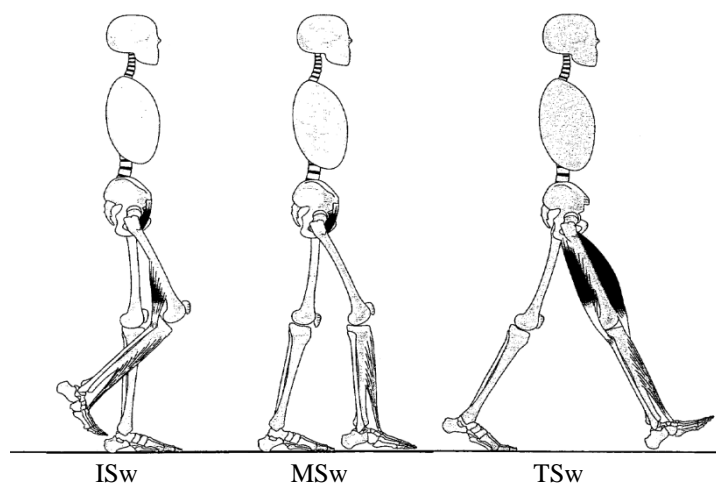


Figure 3.4: The three phases of the swing period of the gait cycle with the swinging ipsilateral leg [Götz-Neumann 2006]

The body divides itself functionally in two parts during walking: One consists of the head, trunk, neck and arms. It is called the passenger because it is carried rather than contributing to the act of walking. The second part is the two limbs and called the locomotor since it is the part responsible for the motion. The locomotor functions can be summarized in standing stability, dynamic stability, progression (which is already explained in the gait cycle), shock absorption (through damping the body weight when it makes the initial contact with the floor), and energy conservation.

During one gait cycle the BCoM goes through a rhythmic upward and downward motion. The lowest point occurs at the time of double support and the highest point occurs at the mid-stance, and the average vertical displacement in the BCoM is 50 mm. The lateral displacement is also approximately 50 mm. Figure 3.5 shows the vertical displacement of the BCoM.

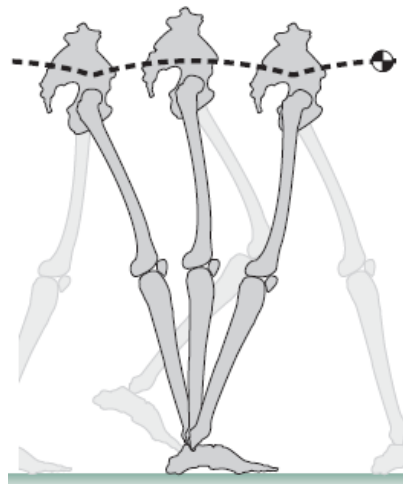


Figure 3.5: BCoM motion [Gordon 2009]

The path of the BCoM is very smooth with no abrupt changes. This smooth path ensures the minimizing of the energy expenditure since abrupt changes in this path will waste energy. The locomotor is the part responsible for this sinusoidal motion of the BCoM. Many researchers have studied this locomotor in order to know the mechanisms responsible for this smooth motion. One of the pioneer studies that was adopted for more than 5 decades and proved by many following researchers was firstly done in 1953 by Saunders et al. [Saunders 1953] and is lightly modified later in 1981 by Inman et al. [Inman 1981]. According to this study the gait determinants in normal gait cycle are the following:

1. Knee flexion during mid-stance phase: The stance limb starts initial contact with the knee in full extension and flexes as the foot moves further and the forefoot contacts the ground. This flexion reaches approximately 15 degrees then starts to extend keeping some flexion at the mid-stance. Since this flexion occurs when the body is at its peak point and the shank is almost vertical, then a reduction in the BCoM elevation of about 11 mm is achieved.
2. Pelvic tilt: The pelvis tilts about 5 degrees downward from vertical to the swing side lowering the BCoM about 5 mm. A suitable clearance of the swing leg is necessary to prevent the foot of the swing leg from contacting the ground.
3. Pelvic rotation: The pelvis rotates in a position of 4 degrees rotation from the progression line before the initial contact occurs. During the opposite contra-lateral leg swing phase the pelvis rotates in the opposite direction about 4 degrees building up a rotation rang of 8 degrees. Through this rotation that uses the pelvic width both the ipsi-lateral and contra-lateral legs are lengthened since the support points are extended. The rotation of the pelvis prevents about 9.5 mm of downward displacement of the BCoM.

Without the mechanical advantage of these three determinants the BCoM will move vertically like an inverted pendulum and the displacement will be about 75 mm instead of 50 mm. Then the summation of reductions due these three determinants is about 25 mm. These factors reduce the BCoM vertical displacement but alone will lead to abruptness in the BCoM pathway. These abruptness are smoothed by the second three determinants:

4. Foot and ankle motion: The ankle is elevated at initial contact by the heel lever arm and falls down as the forefoot contacts the ground. At terminal stance the heel rises and the ankle is again elevated by the forefoot lever and continues through pre-swing. These ankle motions smooth the BCoM pathway during stance phase.

5. Knee motion: This is associated with foot and ankle assembly motion. At initial contact the knee is in full extension and directly after that starts to flex and continues so until full extension again at mid-stance. At the beginning of the terminal stance the knee flexes again until the leg comes into swing phase. These motions of the knee smooth even further the BCoM pathway.

6. Lateral pelvic displacement: This reduces the muscular and balancing demands of the body by shifting the pelvis over the support point of the stance limb, which also improves the position of BCoM over the support leg.

During walking the two feet are the elements making contact with the ground. The GRFs are transmitted to the whole body through them. In Figure 3.6 is shown the sequence of foot support area during stance. This support area is combined with three components of ground forces. The vertical component is the largest and most important component to support the weight of the body. The horizontal component is important to protect the foot from slipping.

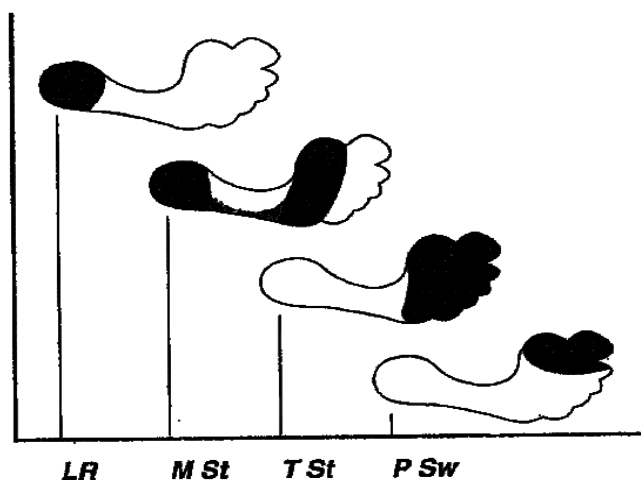


Figure 3.6: The sequence of foot support area during stance. Heel only in loading response (LR), foot flat in mid stance (MSt), forefoot and toes in terminal stance (TSt), medial forefoot in pre-swing (PSw) [Perry 1992]

### 3.2 Basics of Prosthetic Limbs

Prosthesis is a replacement for a missing body part. In lower limb amputation the prosthesis is an external replacement fitted on the residual limb to provide the amputee with functional requirements combined with maximum possible comfort and appearance of normality.

As it is shown in the literature review the prostheses had developed marvellously in the previous decades. The lower limb amputations can occur at many levels, such as pelvic level, hip joint, femur, knee joint, tibia, and within foot level. For a lower limb above knee amputation (transfemoral) which is the concern of this thesis, a large number of models and forms of prostheses purposed for walking could be found. The most of new prostheses are modular

constructed and called modular (endoskeletal) prosthesis. The benefits of such a system is the utilization of standardized interchangeable components that when assembled build the prostheses that meets the needs of the individual. Despite the large number of modular systems available in the market, they have some similarity:

1. Utilization of a tubular structural member that constitutes the internal skeleton and to which all other elements (knee, ankle, sockets ...) can be easily attached.
2. A covering of soft materials over the skeleton structure to provide a better appearance.
3. Means of adjusting the alignment of the prosthesis at the ends of the shank tube.

All these models and forms consist of the following basic components: foot ankle assembly, shank, knee joint (assembly), thigh piece, socket, and suspension devices. Figure 3.7 shows a modular prosthesis with its different components.

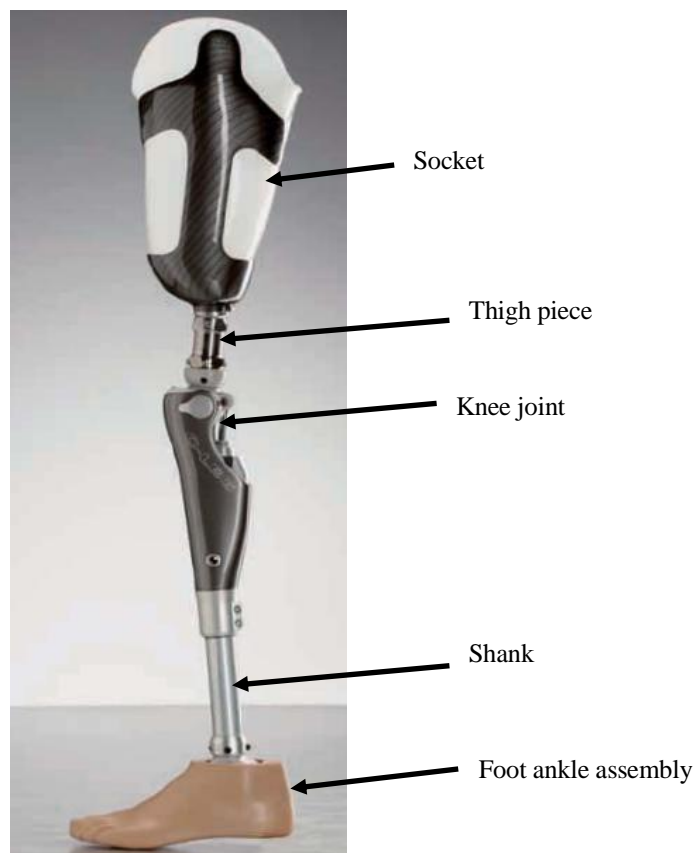


Figure 3.7: A modular lower limb above knee prosthesis [Otto Bock 2009b]

**The foot ankle assembly** has the function of providing a contact area with the ground and transmitting the GRFs to the residuum. There are many models of foot ankle assembly and they can be divided into three categories; conventional, multi-axial, and energy storing foot assemblies.

The conventional models are solid and have great stability. They are simple and have no moving parts and therefore they need very little maintenance. In the heel there is a cushion wedge that compresses during gait and absorbs a part of the transient shock of impact at initial contact.

Multi-axial foot assemblies permit movements in all three anatomical planes, namely, sagittal, transverse, and frontal. They accommodate to uneven walking surfaces better than the solid types and also absorb a part of the torsion forces which leads to an enhanced comfort.

The energy storing prosthetic feet are designed to work like a cantilever spring. They store energy in the mid-stance phase and during energy storing they reduce the kinetic energy and release this energy in the pre-swing phase. Since these feet are elastic they allow accommodation to uneven terrain. Energy storing prosthetic feet allow a small increase in the stride length and respectively walking speed. Due to these characteristics they are suitable for active users with high motion demands. The amputees spend more time in single support on the energy storing foot compared to the conventional foot, which improves the symmetry of the gait and makes the trunk motion more uniform. This suggests an increase in the biomechanical efficiency.

The universal criteria in deciding on a prosthetic foot are the shoe size, heel height, patient weight, left or right, maintenance and activity level. The activity levels are described through the prosthetic K levels from K0 for non-Prosthetic candidate to the high level athletes K4.

**The shank** is basically a structural member that connects the foot-ankle assembly and the knee unit. It has two major forms:

**Exoskeletal Construction:** The space between the ankle assembly and the knee joint is hollow and the load is sustained by the walls of the shank. The walls also serve as a part of the knee joint.

**Endoskeletal (central-support) construction:** This is the form in most modular prostheses. Here the shank consists of a metal or plastic tube that connects the foot-ankle assembly and the knee joint. In the modular prosthesis an axial and/or torsional shock absorbing mechanism can be inserted in the shank to reduce vertical and/or torsional impacts by allowing a small vertical/rotational movement.

**The knee assembly** should provide control and stability during the stance phase of locomotion, the bend during the later part of the stance phase, swing control during swing phase, and to enable the amputee to sit down and kneel.

The currently available knee components are passive systems replacing the human knee. Many prosthetic knee types are available and can be classified depending on the assembly form such as, single-axis knee joint and polycentric knee joint, or depending on the knee motion control system, such like constant friction, variable friction (here the friction is controlled through many mechanisms like dry friction, hydraulic and pneumatic Systems) and the modern microprocessor-controlled systems which offer control of stance and swing phase of hydraulic or pneumatic knee joint over a wider range of walking speeds.

During a level walking the following functions are required from a prosthetic knee [Zahedi 2004]:

- At initial contact (heel strike) the knee must be stabilized allowing the foot to start plantar flexion.
- During the loading response period the knee joint should undergo a yielding flexion with high flexion resistance in order to support the body weight and reduce the impact of the initial contact.
- During the mid stance and terminal stance phases, the motion of the body over the stabilized leg follows the motion of an inverted pendulum, and the ground force changes its position from the heel to the forefoot and the moment around the knee joint changes its direction leading to an extension in the knee. In this phase an appropriate extension resistance is required to prevent hyper extension in the knee joint.

- At the pre-swing phase the moment around the knee joint changes its direction leading to a flexion in the knee which prepares for the swing phase. At this phase the knee resistance to flexion should be minimal allowing large deflection in the knee.
- The swing phase starts with a 30 degrees flexed knee and this should flex up to 55-65 degrees and then in a short period of time should extend back to be fully extended. The extension of the knee is achieved through the inertia forces of the shank since it changes its direction of motion at mid-swing. At the terminal swing phase the terminal impact should be minimal.

**The prosthetic socket** is one of the most important components of lower-limb prostheses. It forms the human-device interface. A comfortable, secure and well-fitted socket is a primary requisite for the successful use of an artificial limb. A comfortable and good fitted socket leads to the feeling that the prosthesis is an integrated part of the body. Socket design should meet the comfort and functional requirements. The comfort requirements can be summarised in pain-free operation and minimized damage of the underlying tissues and skin. The functional requirements are:

- 1- Transmission of the inertial forces and body weight from the residual limb to the prosthesis and to the floor. These forces may be up to 120% of the body weight.
- 2- Allowance for amputees to satisfactorily control the prosthesis and maintain the stability of the suspension of the prosthesis limb on the residuum without excessive slippage.
- 3- Contain and protect the tissues of the stump. The interface material between the socket and the residuum provide a cushioning effect and protect the pressure sensitive areas of the residuum by redistributing the interface pressure.
- 4- It also provides an attachment point for the thigh piece (pylon).

To meet the comfort and functional requirements two major crucial points should be considered. The first is to effectively distribute the ambulatory loads on the residuum. The second is to achieve an optimized fitting tightness between residuum and socket which leads to a good control on the prosthesis.

Sockets can be classified according to their interior shape, the design of their distal end (open-end socket or with contact support at the distal end), contact area (total contact or non-total contact), and the materials used in the socket and socket-interface design (wood, leather, silicon and gel-like interface, thermoplastics, advanced composites).

**Suspension systems** just like pelvic belts and Silesian Bandage are auxiliary systems to help hold the prosthetic limb in position. Nevertheless some systems are suspended just by the use of suction alone but there are many cases where this suspension is not sufficient. For example: if the residuum is very short or not available at all (trans-pelvic amputations).

Many amputees like the robotic appearance of the prosthetic limb, however, for most amputees, a lifelike appearance of the prosthetic is as much important as a prosthetic with high functionality. This is achieved through external covering that protects the internal components of the prosthetic, and could be coloured to match the surviving leg colours. The present state of the art is the creation of a sculpted match for the opposite limb with individual colouring to give it lifelike finish but unfortunately such covers are costly and need to be replaced after a few years as a result of wear. This cosmetic-overlooked need is very helpful for the acceptance of the prostheses by many patients and has a positive psychological effect.

### 3.3 Dynamics of Flexible Multibody Systems

The human body and many other biosystems can be modelled as a system of flexible and rigid bodies connected with joints, similarly to many mechanical systems (cars, robots, etc). A multibody system can be defined as a number of connected rigid and elastic bodies that move relative to each other. The connection between the bodies is done through joints and constraints limiting the motion of the bodies relative to each other in a predefined way. Every free body has six degrees of freedom but through the joints and constraints these degrees of freedom are reduced. Working forces, springs and dampers can also be introduced between the bodies.

The multibody systems classify themselves into two groups, namely, open-chain systems, when the bodies of the system are entirely connected without building close loops, and closed-chain systems (see Figure 3.2). The open-chain systems are the simplest and most restricted systems compared to the others.

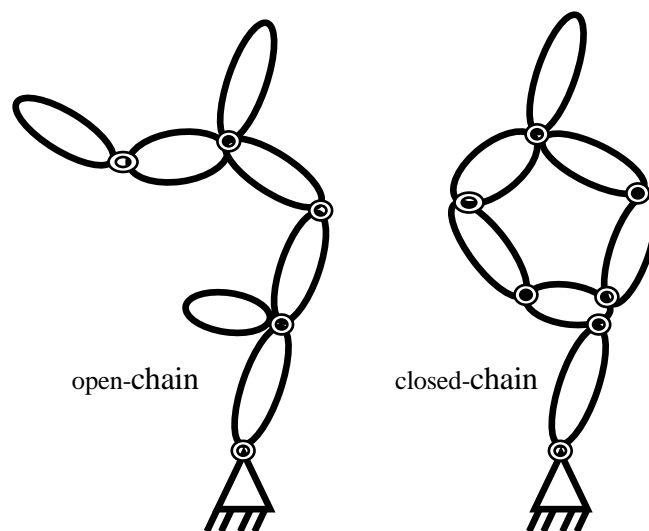


Figure 3.8: Open-chain and closed-chain systems

The study of the dynamics of a multibody system includes the developments of the governing equations of motion. These governing equations are built based upon many principles describing the dynamical behaviour of a physical system. Some of these principles for example are the well-known Newton's laws of motion and Lagrange equation of motion which is based on the kinetic energy of the system.

The energy principle of Hamilton - which can be used in obtaining Lagrange equation of motion - is another principle describing the dynamic behaviour of physical systems. The Hamilton principle states that the time integral of the difference of the kinetic and potential energies of a system is a minimum.

Another principle that is used by many works in dynamics is d'Alembert's principle which is based on the concepts of inertia forces. D'Alembert's principle is similar to Newton's second law and states that the summation of the active forces and inertia forces are zero.

All these methods and principles are equivalent in their sense but in the application of these methods for solving large multibody systems they are markedly different.

Some of the difficulties encountered in these different approaches in building the equations of motion or solving them are:

1. The introduction of non-working constraint forces between adjoining bodies.

2. The tedious calculation of derivatives.
3. The geometrical description of the system.
4. The solution of the governing equation.

In order to avoid these difficulties many methods were developed. Kane developed in the early 1960s a new principle that has got more recognition in its application with multibody systems and it was called Lagrange's form of d'Alembert's principle or Principle of virtual power. This principle states that the sum of the generalized active and inertia forces for each generalized coordinate (or alternatively, each generalized speed) is zero. The benefit of this form is that it automatically eliminates the non-working internal constraint forces without introducing any tedious differentiations [Huston 1990].

Lagrange's equations can be stated in the form:

$$\frac{d}{dt} \left( \frac{\partial K}{\partial \dot{x}_r} \right) - \frac{\partial K}{\partial x_r} = F_r \quad r = 1, 2, \dots, n \quad (3.1)$$

$$K = \sum_{i=1}^N m_i (\mathbf{v}_i^R)^2 \quad (3.2)$$

Such that  $x_r$  ( $r=1,2,\dots,n$ ) are the generalized coordinates describing the system configuration and  $n$  is the number of degrees of freedom.  $F_r$  is the generalized active force associated with the coordinate  $x_r$ .  $K$  is the system kinetic energy where  $P_i$  is a particle of the system and  $m_i$  is its mass.  $\mathbf{v}_i^R$  is the velocity of  $P_i$  in an inertial reference frame  $R$ , and  $N$  is the number of particles in the system.

Lagrange's form of d'Alembert's principle for a generalized coordinate system  $x_r$  ( $r=1,2, \dots, n$ ) is then

$$F_r + F_r^* = 0 \quad , \quad r = 1, 2, \dots, n, \quad (3.3)$$

where  $F_r^*$  is the generalized inertia force for the generalized coordinate  $r$  and is expressed in the form

$$F_r^* = -a_{rp} \ddot{x}_p - h_r, \quad (3.4)$$

where  $a_{rp}$  and  $h_r$  are

$$a_{rp} = m_k v_{krm} v_{kpm} + I_{kmn} \omega_{krm} \omega_{krm} \omega_{kpn}, \quad (3.5)$$

$$h_r = m_k v_{krm} \dot{v}_{kpm} \dot{x}_p + I_{kmn} \omega_{krm} \dot{\omega}_{kpn} \dot{x}_p + e_{lsm} I_{ksn} \omega_{krm} \omega_{kql} \omega_{kpn} \dot{x}_q \dot{x}_p \quad (3.6)$$

,

$a_{rp}$  is called the generalized inertia coefficient,

$h_r$  is called the generalized inertia force coefficient and it contains the Coriolis and centrifugal force terms,



$m_k$  is the mass of the particle  $P_k$ ,

$v_k$  and  $\omega_k$  are the velocity and the angular velocity of the particle  $k$ , respectively,

$I_{kmn}$  is the mass inertia dyadic,

$e_{lsm}$  are the components of the permutation symbol, and the repeated indices indicate a sum over the range of the index (from 1 to 3).

The dynamical equation may be written as:

$$a_{rp} \ddot{x}_p = f_r \text{ where } f_r \text{ is defined as } f_r = F_r - h_r. \quad (3.7)$$

Equations (3.3) and (3.7) are applicable for unconstrained multibody systems with six degrees of freedom at each joint (three translational and three rotational). For the case of systems with fewer degrees of freedom the same equations also apply. With the reduction of a translational degree of freedom, the generalized coordinate associated with this degree of freedom must be zero. If a rotational degree of freedom is reduced then the terms associated with this degree cancel out from the dynamical equations. In case the movement at a joint is known then the generalized coordinate associated with that movement becomes a known variable.

By referring to the floating frame of reference formulation the introduction of the flexible bodies motion into a rigid bodies dynamic system is done by considering small linear body deformations relative to a local reference frame on the flexible body, while that local reference frame is undergoing large, non-linear global motion with respect to the other bodies in the dynamic system. Figure 3.9 shows an example of a flexible body with a body fixed local reference frame at one end called  $B$ , a vector  $s$  representing the position of a point  $P$  on the body before the deformation, and a vector  $u_P$  representing the deformation in the body at that point. The global coordinate system is called  $G$ .

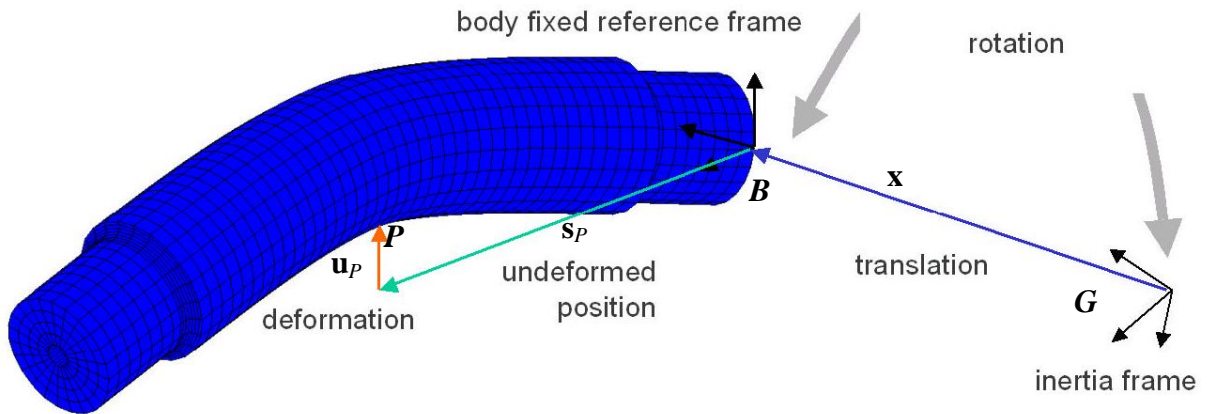


Figure 3.9: The position vector of a deformed point  $P$  on a flexible body relative to the body fixed local reference frame  $B$  and the global coordinate system  $G$  [Intec 2005]

The flexible bodies are usually discretised into a large number of finite elements using the finite element method. In this method the infinite number of DOF of the flexible body are represented in a large finite number of DOF of the finite elements. Since the number of DOF in a finite element model is very large (it is time consuming in simulation of dynamic load cases) it is desirable to represent the deformation of the flexible body into a reduced model and derive the

governing equation of motion of the flexible body for this reduced system. One of the well-known and often used reduction methods is the Guyan reduction method, which is explained here and used in this research. In the Guyan method, a set of master nodes in the finite element model of the flexible body is defined by the user and retained. The rest of the nodes (slave nodes) are removed by condensation. This method is also called static condensation since the stiffness properties are considered during the condensation but the inertias coupling of master and slave nodes are ignored.

Through Guyan reduction the large, sparse FEM mass and stiffness matrices are condensed down into small, dense pair of matrices, with respect to the master DOF. The deformation here is described by a modal representation with a comparatively small number of modal coordinates. The following equations and derivations are based on data from the following resources [Wallrapp 1999, Adams 2008, and Intec 2005].

Firstly the linear deformations of the nodes of the finite element model,  $\mathbf{u}$ , are approximated in a linear combination of a small number of shape vectors (or mode shapes),  $\boldsymbol{\phi}$ , which is also called modal superposition:

$$\mathbf{u} = \sum_{i=1}^M \boldsymbol{\phi}_i q_i, \quad (3.8)$$

where  $M$  is the number of mode shapes and  $q$  are the modal coordinates. This equation can be represented in matrix form as:

$$\mathbf{u} = \boldsymbol{\Phi} \mathbf{q}, \quad (3.9)$$

where  $\boldsymbol{\Phi}$  is the modal matrix containing the mode shapes.  $\mathbf{q}$  is the vector of the modal coordinates. The modal matrix  $\boldsymbol{\Phi}$  becomes after modal truncation a rectangular matrix which is the transformation matrix from the modal coordinates to the physical coordinate  $\mathbf{u}$ .

Since the free selection of the modes can lead to accidental constraints in the system a technique called Craig-Bampton method is to be used. In this method the system DOF are divided into two groups: the first group is the boundary DOF. These DOF are not subject to modal superposition and are preserved exactly in the Craig-Bampton modal basis. In these modes there are no losses of resolution when higher order modes are reduce and truncated. The second group is the interior DOF. Also two sets of mode shapes are defined in this method: Constraint modes gained by giving each boundary DOF a unit displacement while holding all other boundary DOF fixed. These modes are static shapes and span all possible motions of the boundary DOFs. The second group contains the fixed boundary normal modes obtained by fixing the boundary DOF and computing the eigen solutions.

The physical DOF and the Craig-Bampton modes with their coordinates are illustrated in the following equation

$$\mathbf{u} = \begin{Bmatrix} \mathbf{u}_B \\ \mathbf{u}_I \end{Bmatrix} = \begin{bmatrix} \mathbf{I} & \mathbf{0} \\ \boldsymbol{\Phi}_{IC} & \boldsymbol{\Phi}_{IN} \end{bmatrix} \begin{Bmatrix} \mathbf{q}_C \\ \mathbf{q}_N \end{Bmatrix}, \quad (3.10)$$

where,

$\mathbf{u}_B$  is the boundary DOF,

$\mathbf{u}_I$  is the interior DOF,

$\mathbf{I}$  and  $\mathbf{0}$  are the identity and zero matrices, respectively,

$\boldsymbol{\Phi}_{IC}$  is the physical displacement of the interior DOF in the constraint modes,

$\boldsymbol{\Phi}_{IN}$  is the physical displacement of the interior DOF in the normal modes,

$q_C$  are the modal coordinates of the constraint modes,

$q_N$  are the modal coordinates of the fixed-boundary normal modes.

By the use of modal transformation, the generalized mass and stiffness matrices corresponding to the Craig-Bampton modal basis are:

$$\hat{\mathbf{K}} = \Phi^T \mathbf{K} \Phi = \begin{bmatrix} \mathbf{I} & \mathbf{0} \\ \Phi_{IC} & \Phi_{IN} \end{bmatrix}^T \begin{bmatrix} \mathbf{K}_{BB} & \mathbf{K}_{BI} \\ \mathbf{K}_{IB} & \mathbf{K}_{II} \end{bmatrix} \begin{bmatrix} \mathbf{I} & \mathbf{0} \\ \Phi_{IC} & \Phi_{IN} \end{bmatrix} = \begin{bmatrix} \hat{\mathbf{K}}_{CC} & \mathbf{0} \\ \mathbf{0} & \hat{\mathbf{K}}_{NN} \end{bmatrix}, \quad (3.11)$$

$$\hat{\mathbf{M}} = \Phi^T \mathbf{M} \Phi = \begin{bmatrix} \mathbf{I} & \mathbf{0} \\ \Phi_{IC} & \Phi_{IN} \end{bmatrix}^T \begin{bmatrix} \mathbf{M}_{BB} & \mathbf{M}_{BI} \\ \mathbf{M}_{IB} & \mathbf{M}_{II} \end{bmatrix} \begin{bmatrix} \mathbf{I} & \mathbf{0} \\ \Phi_{IC} & \Phi_{IN} \end{bmatrix} = \begin{bmatrix} \hat{\mathbf{M}}_{CC} & \hat{\mathbf{M}}_{NC} \\ \hat{\mathbf{M}}_{CN} & \hat{\mathbf{M}}_{NN} \end{bmatrix}. \quad (3.12)$$

The subscripts  $I$ ,  $B$ ,  $N$ , and  $C$  denote the internal DOF, boundary DOF, normal modes, and constraint modes, respectively.  $\hat{\mathbf{M}}$  and  $\hat{\mathbf{K}}$  are the generalized mass and stiffness matrices.

Now for the reduced system the eigenvalues can be calculated from the following equation for each modal coordinate  $q$

$$(\hat{\mathbf{K}} - \lambda \hat{\mathbf{M}})q = 0. \quad (3.13)$$

From Figure 3.9 the location of a point  $P$  on the flexible body at some point of time is the sum of the three vectors,  $\bar{x}$  is the translation of body fixed local reference frame  $B$  with respect to a global inertia frame  $G$ ,  $\bar{s}_p$  the position of the point  $P$  before deformation with respect to the local body fixed reference frame, and  $\bar{u}_p$  is the translational deformation vector of the point  $P$  from its undeformed position to the new deformed position.

$$\bar{r}_p = \bar{x} + \bar{s}_p + \bar{u}_p \quad (3.14)$$

and in matrix form:

$$\mathbf{r}_p = \mathbf{x} + {}^G \mathbf{A}^B (\mathbf{s}_p + \mathbf{u}_p), \quad (3.15)$$

where the values  $\mathbf{s}_p$  and  $\mathbf{u}_p$  are expressed in the local body coordinate system.  ${}^G \mathbf{A}^B$  is the transformation matrix from the local body reference frame  $B$  to the ground. From Eq. (3.9) the deformation  $\mathbf{u}_p$  is a modal superposition as in the following equation:

$$\mathbf{u}_p = \Phi_p \mathbf{q}. \quad (3.16)$$

$\Phi_p$  is a slice from the modal matrix that corresponds to the translational DOF of node  $P$ .

The generalized coordinates of the flexible body are:

$$\xi = \left\{ \begin{array}{c} x \\ y \\ z \\ \psi \\ \theta \\ \varphi \\ q_{i,(i=1\dots M)} \end{array} \right\} = \left\{ \begin{array}{c} \mathbf{x} \\ \boldsymbol{\psi} \\ \mathbf{q} \end{array} \right\}. \quad (3.17)$$

$M$  is the number of modes and  $q_i$  are the generalized coordinates of the flexible body.

In order to compute the governing equation of motion of the flexible body the following terms are required:

The velocity of the point  $\mathbf{P}$  in the system

$$\mathbf{v}_P = \dot{\mathbf{x}} - {}^G \mathbf{A}^B (s_P + \mathbf{u}_P) \mathbf{B} \dot{\boldsymbol{\psi}} + {}^G \mathbf{A}^B \boldsymbol{\Phi}_P \dot{\mathbf{q}}, \text{ where } \mathbf{B} \dot{\boldsymbol{\psi}} = {}^G \boldsymbol{\omega}_B^B. \quad (3.18)$$

${}^G \boldsymbol{\omega}_B^B$  is the angular velocity of the flexible body relative to the global coordinate system expressed in the body coordinates. This velocity is displayed in terms of the time derivative of the generalized coordinate vector  $\xi$  in the form:

$$\mathbf{v}_P = [\mathbf{I} - {}^G \mathbf{A}^B (s_P + \mathbf{u}_P) \mathbf{B} + {}^G \mathbf{A}^B \boldsymbol{\Phi}_P] \dot{\xi}, \quad (3.19)$$

and the angular velocity of a marker on a flexible body at the point  $\mathbf{P}$  with respect to the global coordinate system is

$${}^G \boldsymbol{\omega}_B^P = {}^G \boldsymbol{\omega}_B^B + {}^B \boldsymbol{\omega}_B^P = {}^G \boldsymbol{\omega}_B^B + \boldsymbol{\Phi}_P^* \dot{\mathbf{q}}, \quad (3.20)$$

where  $\boldsymbol{\Phi}^*$  is the slice from the modal matrix that corresponds to the rotational DOF of node  $\mathbf{P}$ .

Now that the velocity and angular velocity are calculated, the governing equations of motion of flexible bodies are derived from Lagrange's equations which are function of the kinetic energy and the potential energy. This derivation needs to calculate the following terms:

The kinetic energy is

$$T \approx \frac{1}{2} \sum_p m_p \mathbf{v}_P^T \mathbf{v}_P + {}^G \boldsymbol{\omega}_P^B \mathbf{I}_P {}^G \boldsymbol{\omega}_P^B, \quad (3.21)$$

which can be displayed in the generalized mass matrix and generalized coordinate system as

$$T = \frac{1}{2} \dot{\xi}^T \mathbf{M}(\xi) \dot{\xi}. \quad (3.22)$$

The mass matrix

$$\mathbf{M}(\xi) = \begin{bmatrix} \mathbf{M}_{tt} & \mathbf{M}_{tr} & \mathbf{M}_{tm} \\ \mathbf{M}_{tr}^T & \mathbf{M}_{rr} & \mathbf{M}_{rm} \\ \mathbf{M}_{tm}^T & \mathbf{M}_{rm}^T & \mathbf{M}_{mm} \end{bmatrix}, \quad (3.23)$$

where the subscripts  $t$ ,  $r$ , and  $m$  are for the translational, rotational and modal DOF, respectively. For further information on the elements of this mass matrix see [Wallrapp 1999], [Adams 2008], [Intec 2005].

The potential energy, which comes out of two sources (the gravity and the elasticity), is:

$$V = V_g(\xi) + \frac{1}{2} \xi^T \mathbf{K} \xi, \quad (3.24)$$

where  $\mathbf{K}$  is the generalized stiffness matrix, and it is constant. Since the modal coordinates contribute to the elastic energy it can be reduced into the form

$$\mathbf{K} = \begin{bmatrix} \mathbf{K}_{tt} & \mathbf{K}_{tr} & \mathbf{K}_{tm} \\ \mathbf{K}_{tr}^T & \mathbf{K}_{rr} & \mathbf{K}_{rm} \\ \mathbf{K}_{tm}^T & \mathbf{K}_{rm}^T & \mathbf{K}_{mm} \end{bmatrix} = \begin{bmatrix} \mathbf{0} & \mathbf{0} & \mathbf{0} \\ \mathbf{0} & \mathbf{0} & \mathbf{0} \\ \mathbf{0} & \mathbf{0} & \mathbf{K}_{mm} \end{bmatrix}. \quad (3.25)$$

$\mathbf{K}_{mm}$  is the generalized stiffness matrix of the structural components with respect to the modal coordinates.

The gravitational energy is then

$$V_g = \int_V \rho [\mathbf{x} + \mathbf{A}(s_p + \Phi(P)\mathbf{q})]^T \mathbf{g} dV, \quad (3.26)$$

and the gravitational force is then calculated from the gravitational energy in the generalized coordinate system as

$$\mathbf{f}_g = \frac{\partial V_g(\xi)}{\partial \xi} = \begin{bmatrix} \left[ \int_V \rho dV \right] \mathbf{g} \\ \left[ \int_V \rho (s_p + \Phi(P)\mathbf{q})^T dV \right] \frac{\partial \mathbf{A}^T}{\partial \Psi} \mathbf{g} \\ \left[ \int_V \rho \Phi^T(P) dV \right] \mathbf{A}^T \mathbf{g} \end{bmatrix}. \quad (3.27)$$

The damping in the system is represented in the form of damping force through Rayleigh's dissipation function, where  $\mathbf{D}$  is the modal damping matrix. This function contains the damping coefficients and is generally constant

$$\mathbf{F} = \frac{1}{2} \dot{\mathbf{q}}^T \mathbf{D} \dot{\mathbf{q}}. \quad (3.28)$$

Now the final form of the governing differential equation of motion of a flexible body in the generalized coordinates is

$$\mathbf{M} \ddot{\xi} + \mathbf{D} \dot{\xi} - \frac{1}{2} \left[ \frac{\partial \mathbf{M}}{\partial \xi} \dot{\xi} \right]^T \dot{\xi} + \mathbf{K} \xi + \mathbf{f}_g + \mathbf{D} \dot{\xi} + \left[ \frac{\partial \Psi}{\partial \xi} \right]^T \lambda = \mathbf{Q}, \quad (3.29)$$

where  $\lambda$  are Lagrange multipliers of the constraints,  $\Psi$  are the algebraic constraint equations, and  $\mathbf{Q}$  are the generalized applied forces.

## **4 Evaluation Criteria for the Functionality of Prostheses:**

The evaluation of the human gait depends on subjective and objective measures. The subjective measures could not be evaluated from numerical models but they may be partially estimated through the use of objective measures. After describing the human movement mechanically and anatomically, it is important to decide which criteria and objective measures are the most important and useful in identifying the performance of the human motion. Improving these criteria and measures ensure the refinement of the anatomical and mechanical ideals and reduce the gait deviation. The selection of these criteria is very important since it determines the modelling strategy that will be followed later. Gait deviation is defined as walking differently from the normal pattern. However, normal patterns vary from one individual to another and also change with walking speed, age, and other factors. Here it is very important to keep in mind the most outstanding characteristic of normal locomotion, which is the symmetry. For the case studied in this work, i.e. a unilateral amputee, gait deviation can be identified by observing the deviations between the prosthetic side and the sound side.

From the literature it is found that the most discussed values and measures of the normal and deviated gait are the GRF, the motion of the BCoM, and the energy expenditure.

The energy expenditure is usually measured through metabolic energy costs and relatively  $O_2$  cost. This energy expenditure is a function of the mechanical efficiency of the muscles and the optimal use of the available muscles and muscles fibres by the user. The goal of this work is to build a numerical mechanical model of the human gait without modelling the muscles but just the joints and the torques working at these joints and the model will simulate a part of the gait cycle and not the whole cycle. Accordingly, it is not advantageous in this work to study the energy expenditure directly. It will be more appropriate at this stage to select other kinematic and kinetic parameters of the gait to be the evaluation criteria.

Accordingly, the BCoM and the GRF are selected as the main criteria for evaluating the human gait and for studying the effect of changing the adaptive foot properties on the gait. Since the GRF changes its action position with respect to the foot, it is important to study the torque resulting from this GRF. This is done by selecting the ankle joint moment as an additional evaluation criterion. Another important factor is the hip joint rotation and moment of the prosthetic side. The hip joint is the only part of the prosthetic leg that still has muscles and can be controlled by the amputee. In modelling the human gait, the hip joint moment or rotation should be selected as an input for the system. In this work the hip joint moment is selected to be one of the inputs, accordingly, the rotation of the hip joint will be one of the outputs, this rotation is selected as the fourth criterion in evaluation of the human gait.

In the following sections the four selected criteria are explained, and some figures of them are also shown. The data in the figures is experimental data from a female unilateral amputee weighting 60 kg. These parameters are also used in the rest of the work in the different evaluation processes.

### **4.1 The Displacement of the BCoM**

The location of the centre of gravity of a human being in the normal standing position varies with body build, age, and sex. By many studies it was found to be ranging from 55 to 59% of the standing height. The average value for men was found to be 56% and for women 55.5% of standing position height [Hamilton 1997]. This BCoM is also called sacral BCoM because its position is anatomically just anterior of the second sacral vertebra. During walking the configuration of the body undergoes changes and the actual BCoM changes its position with respect to the anatomical marker accordingly but the sacral BCoM stays fixed. However, in this study the sacral BCoM is used in studying the displacement during walking since it provides a

reasonable approximation of the vertical BCoM motion at slow and free selected speeds through the motion of one single marker.

From perusal of the literature it is reported that the oscillation of the BCoM shows certain asymmetries and is related to the normal gait. In case of abnormality the symmetry of the oscillation is reduced. Also the oscillation can be closely approximated to sinusoidal waves. Crowe et al. derived the BCoM from the GRFs and showed that it can be displayed as a function of purely sinusoidal components [Crowe 1995].

This will be utilized in this study by evaluating the deviation of the model centre of mass oscillation from the sinusoidal form, as an indication of symmetry and agreement to the normal gait. The horizontal displacement of the BCoM represents the horizontal travelled distance of the body and the walking speed. Changes in walking speed can be considered as a preliminary indication of energy costs. Figure 4.1 shows the sinusoidal behaviour of the BCoM. The two curves differ due the amputation on one side.

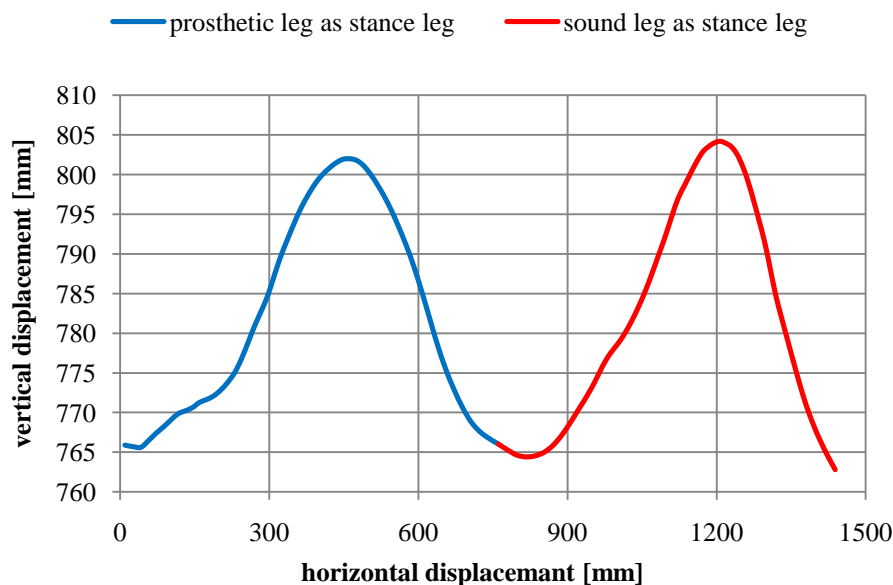


Figure 4.1: BCoM motion in sagittal plane.

## 4.2 Ground Reaction Forces

The GRF is the basis for evaluating the gait by most orthopaedics workers. The loads applied on the prosthetic leg are determined by the weight of the amputees and their walking patterns, which may differ from those of non-amputees. There are many approaches used to determine the forces (loads) applied on the prosthesis during walking. One of these approaches is the use of force plates and motion analysis systems. The motion analysis system records the kinematics of the human body and of the prosthesis components. The force plate, which is embedded in the floor, measures the GRFs and moments. From this data and by using inverse dynamic analysis the forces and moments acting at the components of the prosthesis can be calculated.

If the GRFs acting on the prosthetic side are symmetric to the forces on the sound leg then the sound leg will not be overloaded to contribute to the loss of forces and energy on the amputated leg which results in an energy saving motion and more symmetric gait.

In Figure 4.2 it is clear that the sound leg is loaded more than the prosthetic leg to compensate for the loss in the muscles at the amputated side. Also the sound leg's contact with the ground is

longer than that of the prosthesis. The minimum value between the two peaks is when the body is at its highest point and lowest horizontal velocity.

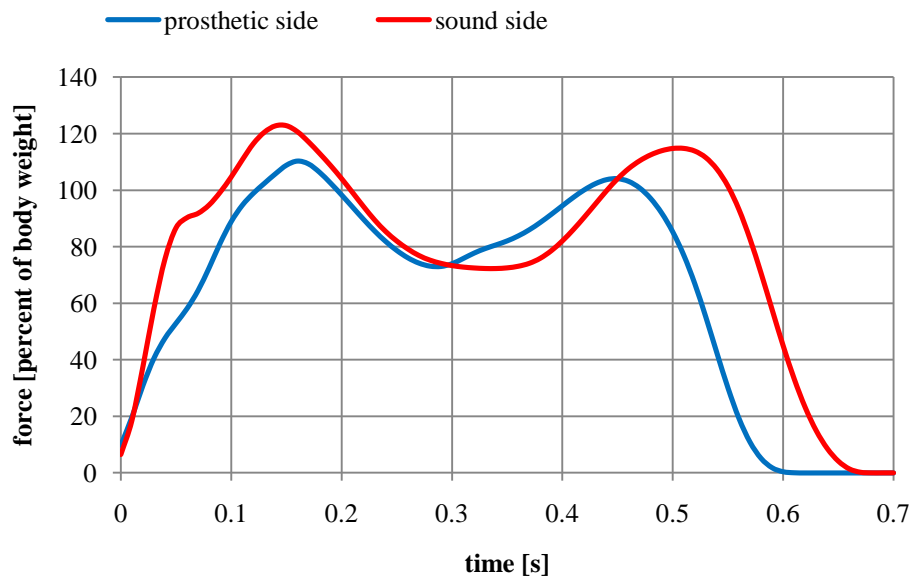


Figure 4.2: Vertical GRFs

### 4.3 Ankle Joint Moment

The ankle torque of both the amputated and the sound leg are important to insure a harmonic roll-over during the load response, mid and terminal stance phases of the gait cycle. A comparison of the prosthetic foot ankle moment with the healthy ankle moment is an effective evaluation measure of the improvements required for the prosthetic foot to reach a level of performance similar to that of the sound foot.

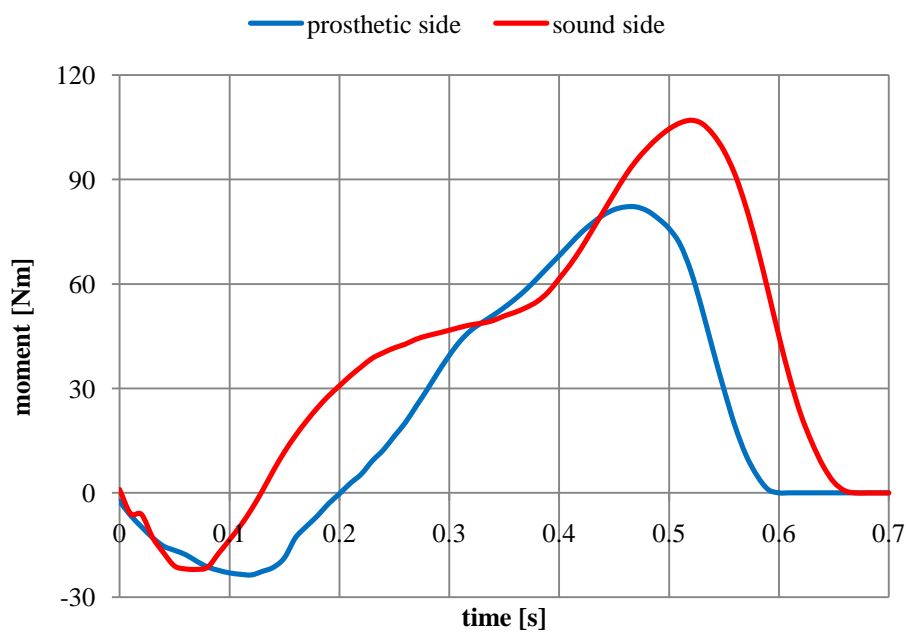


Figure 4.3: Ankle joint moment



In Figure 4.3 the sound side torque at the ankle is higher than the prosthetic side and this suit the results of the GRF which is expected since the torques result from these GRFs. The point of zero torque represents the situation when the BCoM is vertical over the ankle joint centre such that the forefoot and the heel are bearing the body weight with zero resultant torque at the ankle.

#### 4.4 Hip Joint Rotation

As it is already mentioned in this work the hip joint moment will be given as an input in the model. The rotation angle of the hip joint depends on this moment and on the other parameters of the model which make it an evaluation parameter of the gait. The rotation angle of the hip is important for the body advancement since a large rotation (within the anatomic limits) is combined with extra advancement of the body. Also the work done by the hip joint is a function of the joint rotation and moment. In Figure 4.4 the hip joint rotations of both the prosthetic and sound sides are displayed. The figure shows good consistency between the two curves such that the rotation of the prosthetic side has the same form as the sound side. The hip joint at the prosthetic side rotates more than the sound side during the swing phase in order to give the passive artificial limb more energy and inertia, which helps in extending the artificial knee joint and prepares the leg for a new step. This extra rotation of the hip is not required in the sound leg since the already existing muscles acting around the sound knee extend the joint to start a new step.

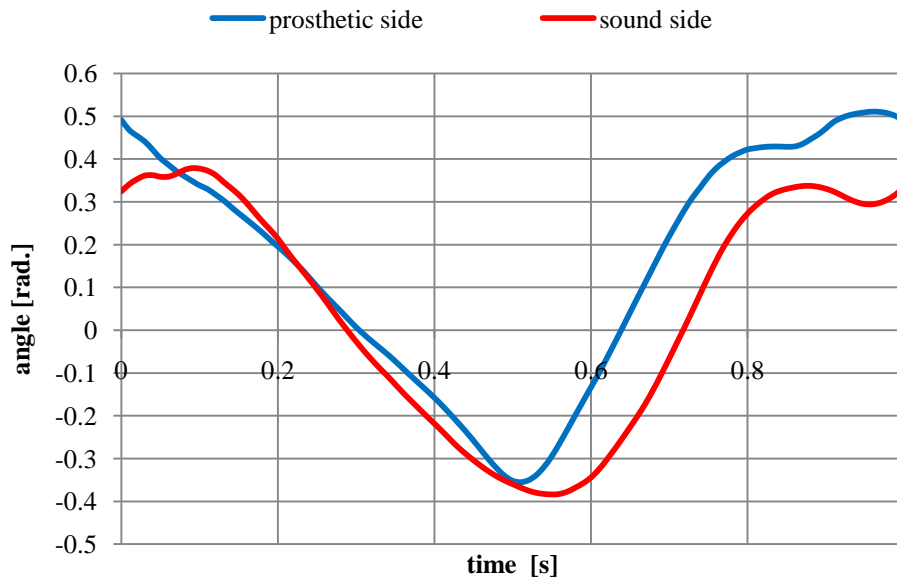


Figure 4.4: Hip joint rotation

## 5 Numerical Modelling of the Human Gait

In order to study the effect of changing the properties of the prosthetic foot on the human gait a model of the stance phase of the gait cycle is necessary. The human gait consists of many parts and many forces are working on the body during walking. It would be very complex to build an analytical model of the body to get the governing equations of motion and to solve them analytically. The integration of elastic elements in the system would make this task also more complex. Accordingly the decision was to use a multibody simulation program in building a numerical model of the gait in the stance phase. At the beginning of the work two MBS programs were studied called SIMPACK and ADAMS and some simple examples were built using them.

The choice was then to use the MBS program SIMPACK due to its abilities in dealing with elastic bodies imported from different FEM programs, and simulating them further in the multibody system.

The modelling is done after that in the following order. The body is separated into a number of rigid bodies, joints, and forces and then a model is set up using these elements. A model of the contact with the ground is developed according to the design parameters and used further in the human gait model. Before modelling the elastic elements and integrating them in the rigid bodies model a pre-evaluation is done. In this pre-evaluation the input data of a rigid bodies model, which was done using ADAMS simulation program, is used in the simulation. The results are then compared with the experimental data to insure the model's functionality. Since the results of the rigid bodies model shows good consistency with the experimental data the step of modelling of the elastic foot is followed. A model of an elastic prosthetic foot (here C-Walk foot from the company Otto Bock) is built in a FEM program and then integrated in the multibody model. The model is run with inputs from a gait analysis of a woman using an above knee prosthesis and a C-Walk foot at different velocities. The results are analysed and compared with the experimental results. The following sections explain these steps in details.

At the end of the modelling a design and evaluation tool (numerical simulation model) of an above-knee lower limb prosthesis during the stance phase was available to be further improved and used in the simulation of elastic models. It is yet to be seen that this model is able to:

1. Describe the motion of human being with lower limb prostheses that matches the experimental results.
2. Evaluate new designs of prostheses and give output data that could be used for comparison between the new designs and the old designs or with the experimental data.
3. Model and evaluate designs done with elastic elements (for the foot part).
4. The use of this tool in estimating the possible improvements of the amputee comfort, mobility and safety throughout the gait cycle with the minimum required energy and effort.

The following Figure 5.1 shows the pre-processing stage of modelling any mechanical system in the SIMPACK program. In this modelling stage the gait cycle model is built up and all the inputs are given and saved. Also in this stage the elastic foot is to be integrated in the system after modifications. This modelling process (called model setup) is followed by the processing step where the differential equations of motion are built and solved for static equilibrium, eigenvalues calculations or time integration based on the inputs.

The third step is the post-processing that gives the outputs in many forms like animations, state and general plots and mode shapes. These outputs are to be used in the evaluation of the adaptive properties and further development of prosthesis.

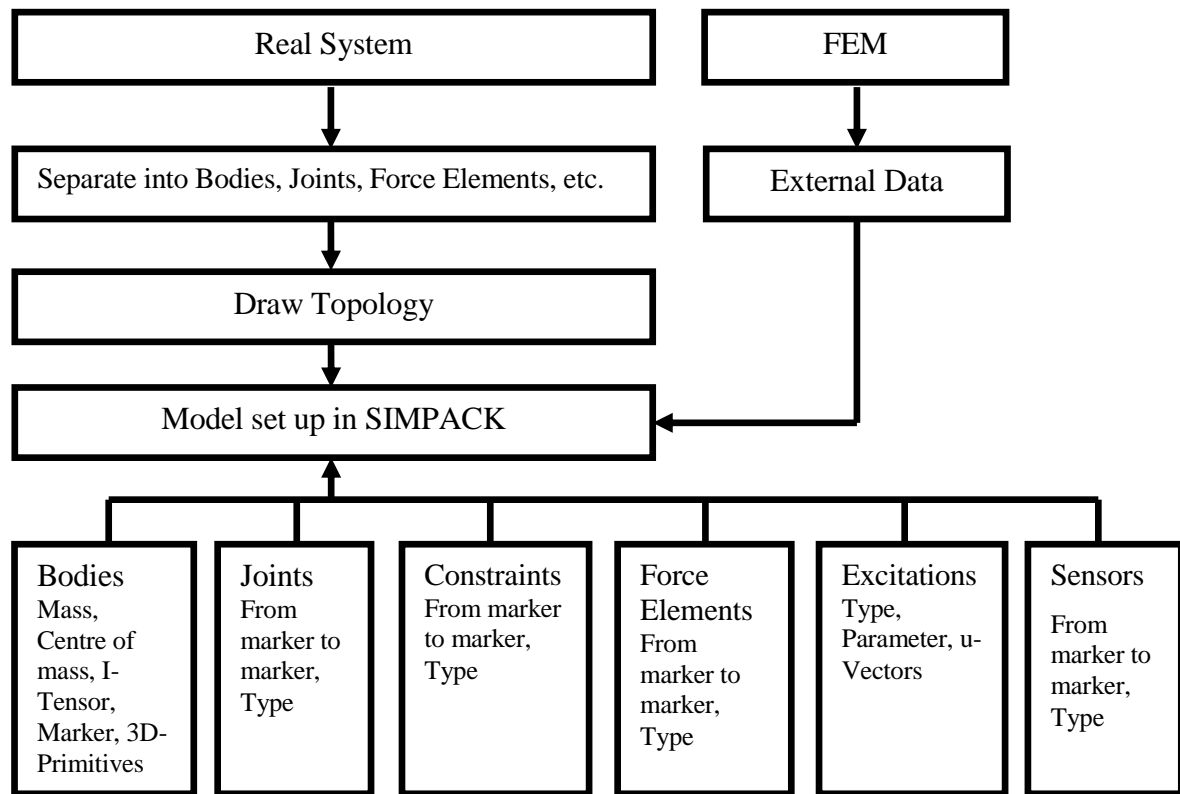


Figure 5.1: Flow chart of pre-processor module of the multibody simulation program SIMPACK

### 5.1 Building the Rigid Bodies Model

The first step in building the model is to separate the real system into a number of bodies, joints and force elements. As it was already explained in the theoretical background the body is divided into two main parts: One is the locomotor consisting of the two legs and the hip, the second is the passenger consisting of the trunk, head and the two arms. Since the passenger here is a passive part and also because the motions of the two arms have no significant effect on the whole locomotion during walking [Perry 1992, Götz-Neumann 2006, and Waters 1992] the passenger is modelled as one body containing the head, neck, two arms and the trunk. This reduction has the advantage of making the dynamic system simpler and respectively the solution of the governing equations of motion easier.

The locomotor is divided into six parts. Three parts for the sound leg (foot, shank, and thigh). These three parts are joined through two hinge joints that approximate the knee and ankle joints. The second three parts are for the artificial limb (the artificial foot assembly, the pylon, and the thigh piece with the socket and residue as one part). The pylon and the thigh are joined by a hinge joint representing the artificial knee. The foot is fixed to the pylon with no movable joints such that the only motion in the ankle comes from the elasticity of the prosthetic foot. This is the case in most prosthetic feet. Figure 5.2 shows the model of the human gait where the red parts are the artificial limb parts. The artificial limb makes the contact with the ground and represents the stance phase of the gait cycle.

The model is two dimensional and built in the sagittal plane. The two legs are joined together with the passenger through hinge joints approximating the function of the hip joints in the sagittal plane. A multibody system must have a reference frame to describe its motion with reference to this frame. In human gait this reference is the ground. Two translational joints are added to the system at the hip joint position and these two joints allow the body to move freely forward and backward, up and down. These two translational joints are very important and

necessary to give the body its initial position and velocity (initial condition) with respect to the reference frame in both the vertical and horizontal directions.

The weight of the body is divided on the different segments according to some percentage values. These percents are calculated from the average values given in the study of Silva and Ambrosio [Silva 2002]. Every leg weighs 18% of the body weight which is the average value for human adults. The weight of the legs is important to the whole gait cycle because the legs accelerate during the swing phase much more than the other parts of the body and thus increases the body inertia in the forward direction, which helps the body to roll over the stance leg.

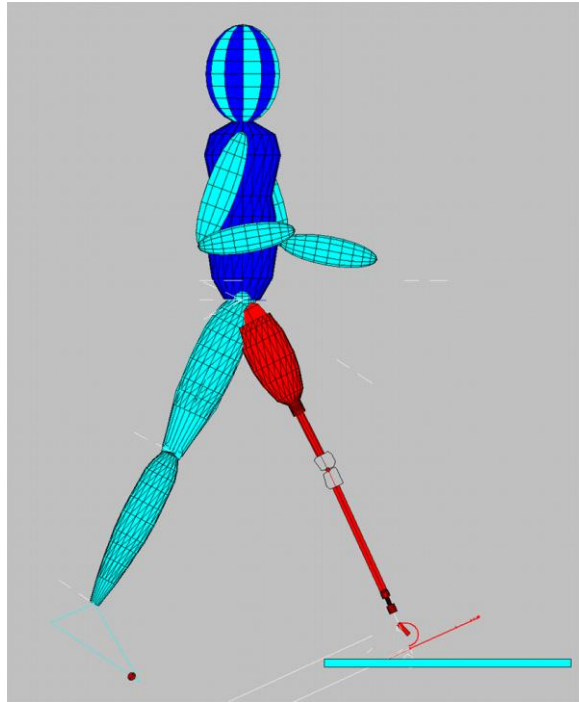


Figure 5.2: The human gait model with the different parts assembled together

Now that the body elements are all built, it is necessary to define their motions and the forces acting on the body. The forces acting on the body come from the muscles' activities. Here there are two concepts that can be followed in designing this system: One is to model and simulate the muscles and their activities. The second is to utilize the measured GRFs acting on the body and calculating the external moments of the joints resulting from the muscles' activities by inverse dynamic analysis. Then these forces and moments can be used as inputs to the system with the rotations of the joints. It is decided to use the second concept because the simulation of the large number of muscles in the model through special functions will make the model more complex. This will not have any extra benefits within the limited purposes of this work, which is the evaluation of adaptive properties of an elastic foot.

For a transfemoral (above knee) amputee the hip joint of the prosthetic side still has muscles that apply moment on the system. This motor is the only internal source of moment in the prosthetic side and due its action the body continues its motion forward during the stance period. As it is explained in the previous chapter this moment will be used as one of the inputs in the model. To achieve the goal of the work, i.e. building a tool that can be used to evaluate the adaptive properties of artificial limbs, the forces acting on the artificial foot must be calculated from the model itself and should not be given as inputs to it. Accordingly a model should be adopted and developed for the contact between the prosthetic foot and the ground.

For the sound leg all muscles are active and due to their action the joints of the sound leg rotate. Also these forces/torques (additionally to the body weight) generate the GRFs at the sound leg, when the foot makes contact with the ground. In this model the vertical and horizontal GRFs acting on the sound foot will be given as inputs in the system on a movable point along the sound foot. The point of application of the force changes its position according to the gait phase such that the resulted torque stays equivalent to that measured with the force plate. Accordingly, there is no need to build a model for the contact with the ground at the sound side to develop these external forces and this reduces the need to define the moments of the joints of the sound leg in the system.

Now that the forces are already determined the motion of the whole system is achieved through the rotational relative motions of the different joints. For the prosthetic side the rotation of the prosthetic knee joint is given from experimental data. For the sound leg all the rotational motions of the hip joint, the knee joint, and the ankle are also given from experimental data.

At the beginning of the simulation all joints are given an initial position and angular velocity. The simulation starts as the heel of the stance leg contacts the ground.

## 5.2 Ground Contact Model

For the contact with the ground a trial was done to model the contact between the foot and the ground through a movable marker on the foot that changes its position along the foot sole to keep the foot continuously in contact with the ground (in a way similar to that used for the input forces of the sound foot). This trial was not successful for elastic bodies since they consist of previously selected master points separated from each other (as it will be shown later) and the selection of a very large number of points on the elastic body makes the solution of the governing equation of the system impossible. Another point that should be taken into consideration is that the foot makes contact with the ground at many points at the same time. These contacts have elastic and damping properties, and this requires representing the contact with a visco-elastic model.

The contact of the foot with the ground starts at the heel and ends at the toes. To simulate the contact of the foot with the ground, a number of force application points were introduced at the forefoot and at the heel. The number of contact points was determined to give a smooth rollover of the foot on the ground and to describe the geometry and area of the lower surface of the artificial foot. Combinations of spring-damper elements are modelled at the force application points. They represent the GRFs acting on the body. Figure 5.3 shows the modelling principle with two vertical spring-damper elements acting at two points.

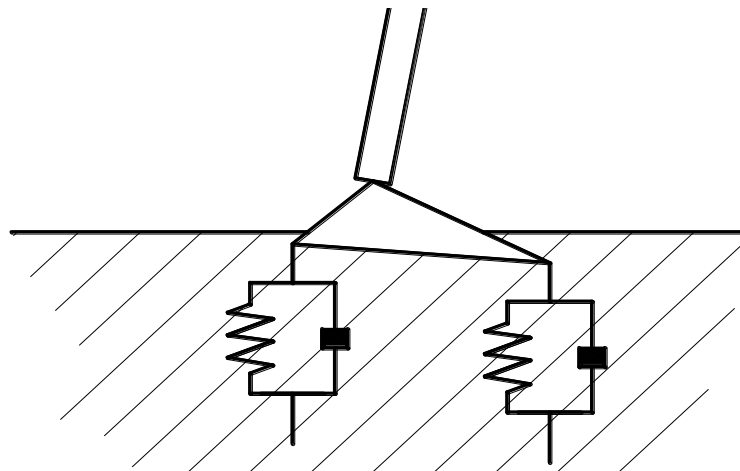


Figure 5.3: Modelling of the vertical GRFs as spring-damper elements at two points

The foot during walking is also facing horizontal forces preventing it from slipping. These forces represent the friction between the foot and the ground and without it the model will slip and fall down due the body horizontal forces acting on the ground. Figure 5.4 shows the vertical and horizontal forces acting on a point at the foot heel.

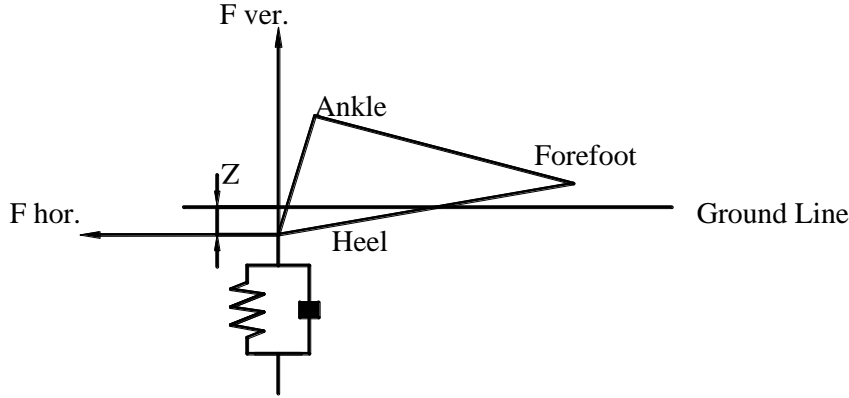


Figure 5.4: Vertical and horizontal GRFs at the foot's heel

Many researchers have defined the contact with the ground through visco-elastic elements [Gerritsen 1995, Gilchrist 1996, and Wojtyra 2000].

In this study 14 contact points were used (seven at the heel and seven at the forefoot) in order to give the prosthetic foot a smooth roll over surface that better approximates the reality. The vertical force is modelled using the following function

$$F_{ver} = \begin{cases} 0 & z \geq 0 \\ -(k_g z + c_g \dot{z}) & z < 0 \end{cases}, \quad (5.1)$$

where

$z$  is the vertical penetration of the contact point in the ground,

$k_g$  is the stiffness of the ground contact model and it stays constant,

$c_g$  is the damping coefficient of the model. This damping is non-linear and a function of the contact point penetration in the ground. The damping value is represented in the following function [Gilchrist 1996, and Wojtyra 2000]

$$c_g = \begin{cases} c_{g \max} \left( \frac{z}{z_p} \right)^2 \left( 3 - 2 \left( \frac{z}{z_p} \right) \right) & |z| < |z_p| \\ c_{g \max} & |z| \geq |z_p| \end{cases}, \quad (5.2)$$

where  $z_p$  is a constant value, when the penetration exceeded this value then the damping coefficient stays constant with its maximum value  $c_{g \max}$ .

To determine the proper values of stiffness  $k_g$ , and damping parameters  $c_{g \max}$ , and  $z_p$  it is important to determine the maximum allowable penetration of the foot in the ground (displacement of the foot with respect to the ground). The model of contact with the ground represents the deformations of the prosthetic foot's soft tissues and the deformation of the shoe sole. The heel pad deforms differently for different gait patterns and this deformation ranges from 2.9 to 9.11 mm. For the shoe this deformation depends on the shoe type and it is considered to be higher for the heel compared with the forefoot. An estimated value of 10 mm

for the heel and 6 mm for the forefoot is considered in this modelling. These two structures contribute to a maximum penetration of 19 mm at the heel and 15 mm at the forefoot.

Notice: The model in this study is also two dimensional and consists of rigid bodies. This means a part of the body's vertical displacement is lost through the modelling. These vertical displacements help in damping the forces acting on the body. They sum up to 15 mm reduction in body vertical displacements (for example 9.5 mm due to the loss of the pelvic rotations and 5 mm due to the loss of pelvic tilts). This value cannot be taken completely as additional contributor to the maximum penetration in modelling the ground. However they contribute to the energy absorption.

Accordingly the displacement of the foot with respect to the ground surface can be assumed to have a maximum value of 19 mm at the heel and 15 mm at the forefoot. A number of test simulations are done to find out the values of the stiffness and damping parameters. The resulted values were: At the heel  $k_g = 4200$  N/m and  $c_{gmax} = 60$  Ns/m, at the forefoot  $k_g = 6500$  N/m and  $c_{gmax} = 60$  Ns/m and  $z_p$  is for both sides 0.005 m.

The horizontal reaction force represents the friction and is defined as a function of the horizontal velocity  $\dot{y}$  and the vertical force

$$F_{hor} = -c_h \cdot F_{ver} \cdot \dot{y}, \quad (5.3)$$

where  $c_h$  is a constant value that could be changed to give the foot stability on the ground and prevent it from slipping against the ground. Through many trials a value of 1.0 s/m was found to be an appropriate value.

These equations are active when the foot is in contact with the ground, otherwise there are no forces acting on the foot.

### 5.3 Pre-evaluation of the Rigid Bodies Model

Before the elastic elements are integrated in the multibody model it is necessary to evaluate the model's functionality in a simpler system of rigid bodies. For this purpose a model of the gait already built by Pflanz in his work with Otto Bock [Pflanz 2001] is used. The model of Pflanz was built using the multibody simulation program ADAMS. In this model the prosthetic foot Flex-Walk, which is a flexible foot made of carbon fibre reinforced plastic (CFRP) and functions as a spring, is modelled through a system of rigid bodies connected with springs and dampers. Figure 5.5 shows the prosthetic foot Flex-Walk.



Figure 5.5: The prosthetic foot Flex-Walk [Össur 2009]

This foot is modelled as an assembly consisting of four rigid segments connected together by three hinge joints. The elastic properties are represented in the form of torsional springs and dampers at the hinge joints. The foot contacts the ground at a number of points in two regions;

the heel and the forefoot. The whole foot complex is fixed with the shank pylon (see Figure 5.6).

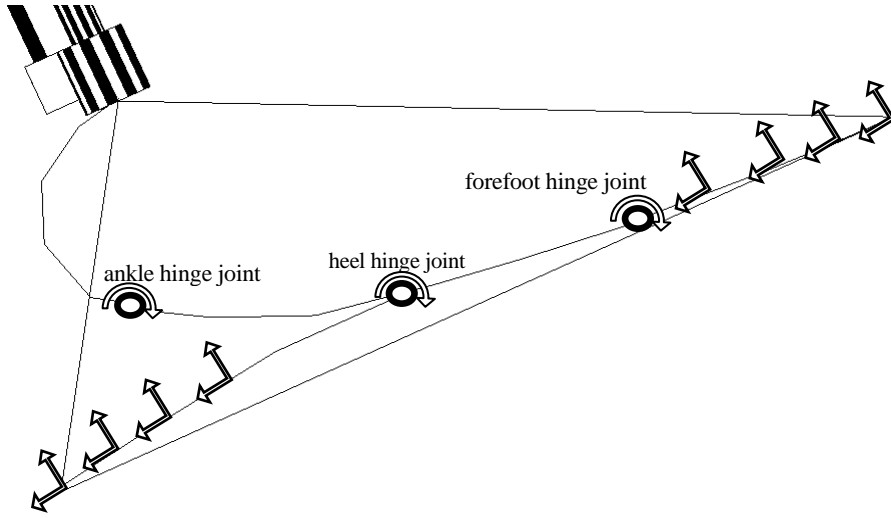


Figure 5.6: The foot Flex-Walk modelled as a complex of four rigid bodies and three hinge joints. The arrows at the heel and forefoot represent the forces acting on the foot. The arrows at the joints represent the torques.

The data used in the simulation of this foot are from an above-knee female amputee using a Flex-Walk foot. The properties of the dampers and torsion springs are taken as they were in the study of Pflanz without any changes. This is because the purpose of this simulation model was to pre-evaluate the model's validity and to compare the results with the experimentally measured ones.

For the vertical reaction force representing the stiffness and damping of the contact between foot and ground in this model the following equations are used

$$F_{ver} = a|z|^3 \cdot (1 - b\dot{z}), \quad (5.4)$$

where,

$$a = 2.5 \cdot 10^8 \text{ N/m}^3, \quad b = 1.0 \text{ s/m},$$

and  $z$  is the vertical coordinate. These equations and the values of  $a$  and  $b$  are calculated by Gerritsen [Gerritsen 1995] through simulating the behaviour of the foot in a numerical model and changing the constants of the model until it matches the experimental results of a mass of 1 kg bounce against a human heel.

The horizontal reaction force represents the friction and is defined by

$$F_{hor} = -c \cdot F_{ver} \cdot \dot{y}, \quad (5.5)$$

where  $c = 1.0 \text{ s/m}$ , and  $\dot{y}$  is the horizontal velocity. The friction equation represents a dry friction that is a function of the velocity and the vertical force.

The duration of the step is 0.64 s. Figure 5.7 shows the vertical GRF acting on the body of an amputee using Flex-Walk foot. As it is seen in the figure the experimental and numerical results show an acceptable consistency. This makes the model an acceptable tool for evaluation and development of the adaptive properties of prosthetic feet. The differences are assumed to occur due to the fact that the elastic Flex-Walk foot is modelled as rigid bodies connected with torsional springs. Also the foot in reality makes a continuous contact with the ground and not



just at some points as it was simulated here. The difference in the step duration that can be seen at the end of the figure is about 5%. This is estimated to be a result of modelling the gait in a two dimensions instead of three dimensions as in reality.

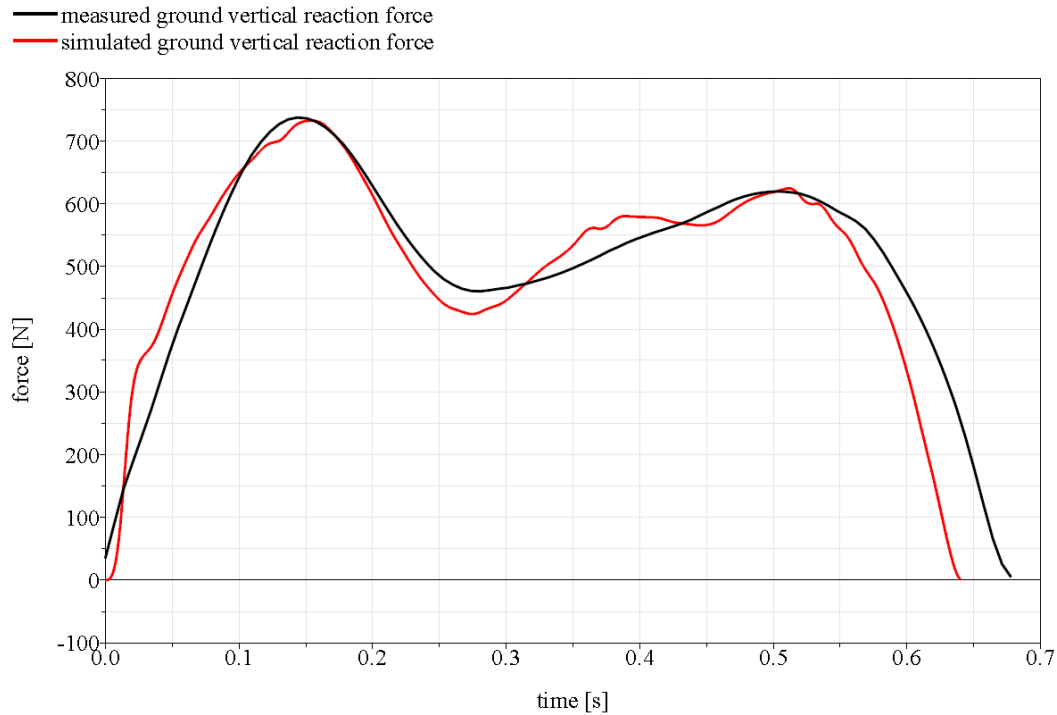


Figure 5.7: Experimentally measured and simulated GRFs acting on the foot Flex-Walk

In Figure 5.8 the torques at the ankle are displayed. The consistency between the experimentally measured and simulated torques is very good, similar to the case of the GRFs. The intersection with the x-axis shows that the foot in the numerical multibody model reaches its stable position (zero torque) before that of the measured. This can be an indication that the system initial velocity in the model and the torques at the hip joint were large such that the body has got an extra moment in the forward direction.

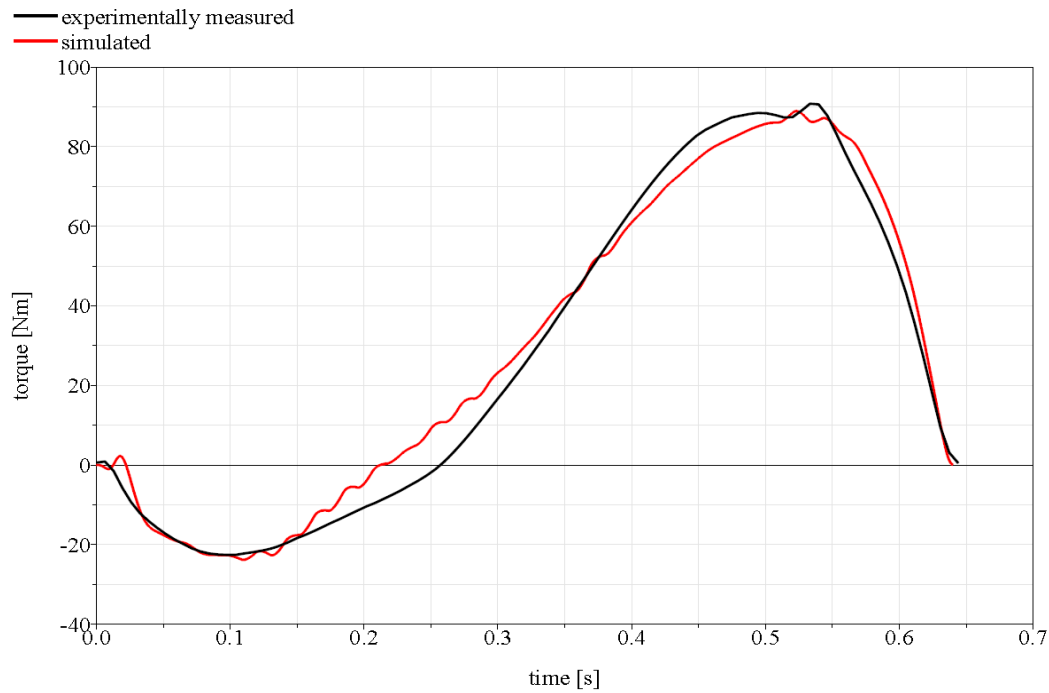


Figure 5.8: Experimentally measured and simulated torque at the ankle of the foot Flex-Walk

Similarly the consistency between the rotation of the thigh at the hip joint for both simulated and experimentally measured values is also very good. At the end of the motion the thigh in the simulated model rotates slowly compared with the measured values of the real system. This can be a result of the input data of the torques at the hip joint and the foot properties.

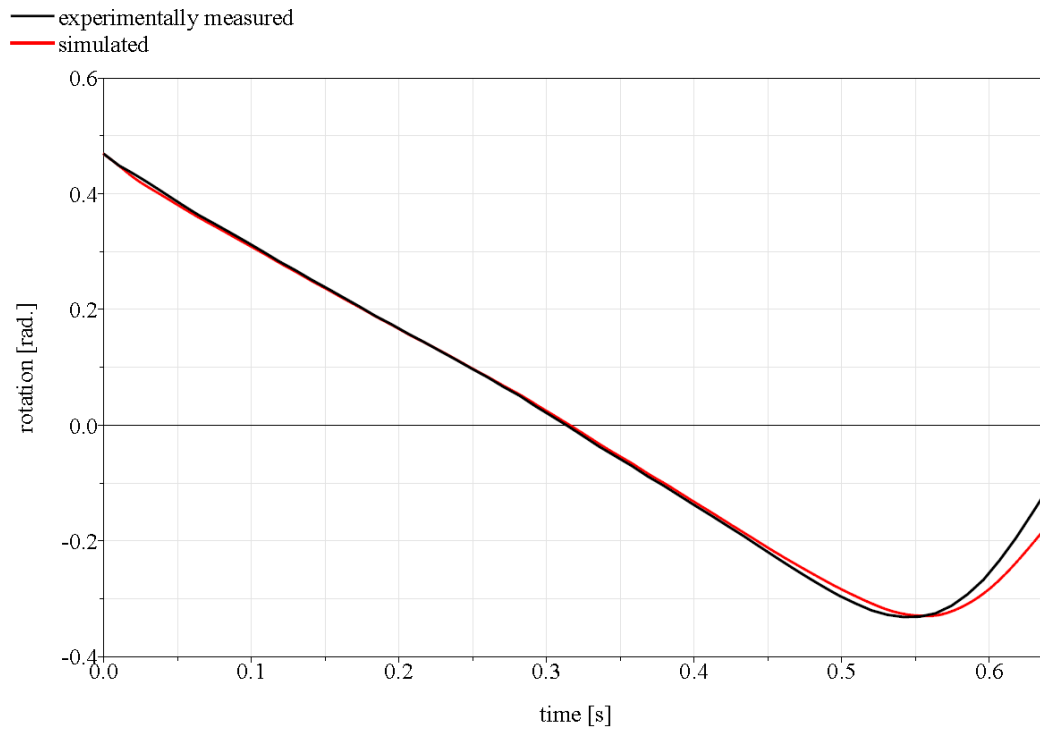


Figure 5.9: Experimental and simulated rotation of the thigh at the hip joint

A symmetrical BCoM is a very important characteristic for minimum energy consumption and comfortable walking. The simulation results show a very good motion of the BCoM such that

the beginning and end of the step are at the same level (see Figure 5.10). The whole vertical displacement is 55 mm which is within the upper limits of the range of displacement for healthy people.

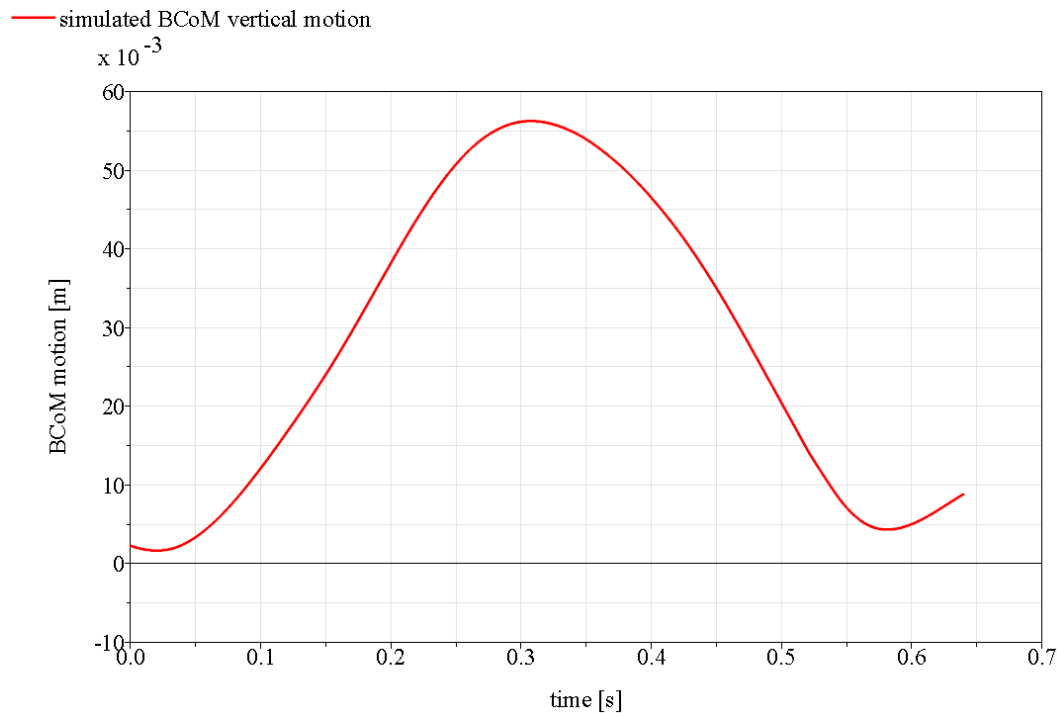


Figure 5.10: Simulated BCoM vertical motion

#### 5.4 Integration of the Elastic Elements in the Model

As it was shown in the previous section, a multibody model of the human gait was built using rigid bodies, and its results were compared with an existing model. The model was able to simulate the stance phase of the human gait using a prosthetic leg simulated as a rigid body, and the results were acceptable to be further adopted and improved. In order to go closer to the reality, the model is to be used further in simulating amputees' locomotion using elastic prosthetic feet since most of the modern prostheses are flexible. This gives the amputees more mobility, comfort, and reduces their energy consumption.

The C-Walk foot from the company Otto Bock is selected as a reference prosthetic foot to be simulated in this multibody numerical model. The C-Walk foot is recommended for active users with high mobility grade 3 and 4 (non-restricted outdoor walker with especially rigorous needs). It is found to be comfortable for walking on uneven grounds and at different speeds.

Figure 5.11 shows this foot which consists of the following elements:

1. C-spring of carbon fibre CFRP
2. Base spring of carbon fibre CFRP
3. Control ring with polymer insert
4. Heel element
5. Modular adapter
6. Clamp pieces with bolt assembly
7. Cosmetic shell
8. Foam cover connection cap

## 9. Overload wedge

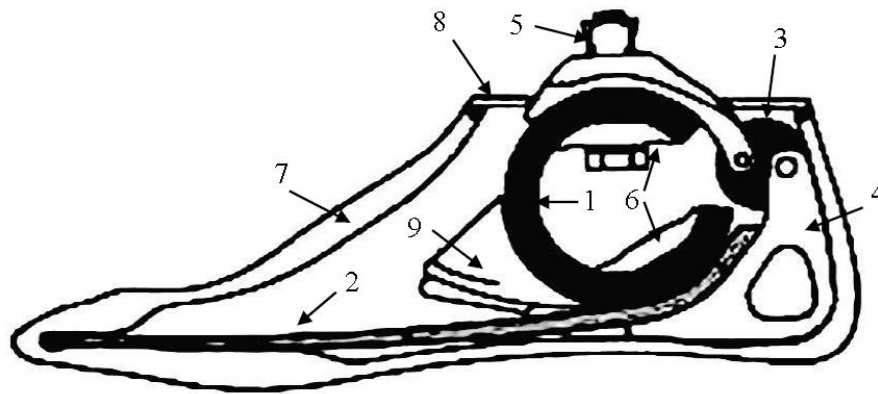


Figure 5.11: The C-Walk foot from Otto Bock. Source: Otto Bock GmbH

The main features of this foot are the two carbon fibre reinforced plastic (CFRP) springs, the heel element and the control titan ring. The C-spring saves the energy by the initial contact during gait cycle and releases this energy back when the forefoot makes contact with the ground. After that both the C-spring and the base spring save the energy of the terminal stance phase and release this energy again in the pre-swing phase. Through this energy release - controlled through the titan ring - the gait cycle and ambulation become more harmonic and comfortable. The flexibility of the foot in different directions due to the C-spring makes it also easier to walk on uneven grounds without causing extra loads on the other parts of the prosthesis.

### 5.4.1 Building the finite element model

In order to integrate this elastic foot in the rigid bodies' dynamic numerical model with its elastic properties, an elastic model of the foot must be built and introduced into the model. For this purpose the FEM program ANSYS was selected. This program is also compatible with the multibody simulation program SIMPACK already used in building the rigid bodies dynamic gait model.

The C-Walk foot consists of two elastic elements: the C-spring and the base spring. All other elements are much stiffer and can be considered as rigid bodies.

In order to build a FE model of the C-spring with properties consistent with the real foot, the deformation of the spring is measured experimentally. In the experimental measurements the spring is loaded with vertical loads since the vertical loads are the largest and most dominant in the human gait. The deformation shows a linear relation with the applied vertical force. This curve is used in selecting a modulus of elasticity for the FE model of the spring that will lead to a deformation matching the real case. According to these experimental results the modulus of elasticity (Young's modulus) of the equivalent spring is found to be 57 GPa. The C-spring deflection is studied without the titan ring, which in reality influences the deformation of the C-spring since this ring is to be modelled in the multibody model later. The FE model of the spring is constructed with two c-shaped shell elements to match the real shape as much as possible. The load deflection relations for both the measured and the numerically calculated values are plotted in Figure 5.12.

The FE model of the spring is shown in Figure 5.13. The holes represent the position of the bolts in the spring. The loading points are at the top and bottom of it. At the top is the pylon mounting point and at the bottom is the base spring mounting point.

Since this elastic model of the C-spring is to be used in the multibody model, it will be very difficult and time consuming to integrate it using all its finite but very large number of elements. A limited number of nodes are to be selected that are the most important and have the most influence on the deformations of the whole system, and the rest of the model should be reduced through the condensation process already explained in the theoretical background. Accordingly, the most important nodes are the mounting nodes, which make contact with the other elements in the system. Two points are selected: one at the top in the centre of the upper hole and the second at the bottom in the middle of the spring's lower surface (at the global coordinate reference system lines in Figure 5.13). These points are called the master degrees of freedom.

Also here it is considered that the deflection of one point can be misleading when all the forces are applied at just one point instead to be distributed all over the mounting area also when this point is at the centre of the force application area. This problem is solved through defining the force application points – which are master degree of freedom points - as a pilot point connected to many neighbouring elements in the FE model. This distributes the acting forces on the whole area and the deflection of these pilot points is combined with the deflection of all neighbouring elements connected to them with the same amount. Now that the FE model of the C-spring is completed and it can be further condensed and reduced into a single element that contains the dynamic characteristic of the original system and can be integrated after that in the dynamic multibody model.

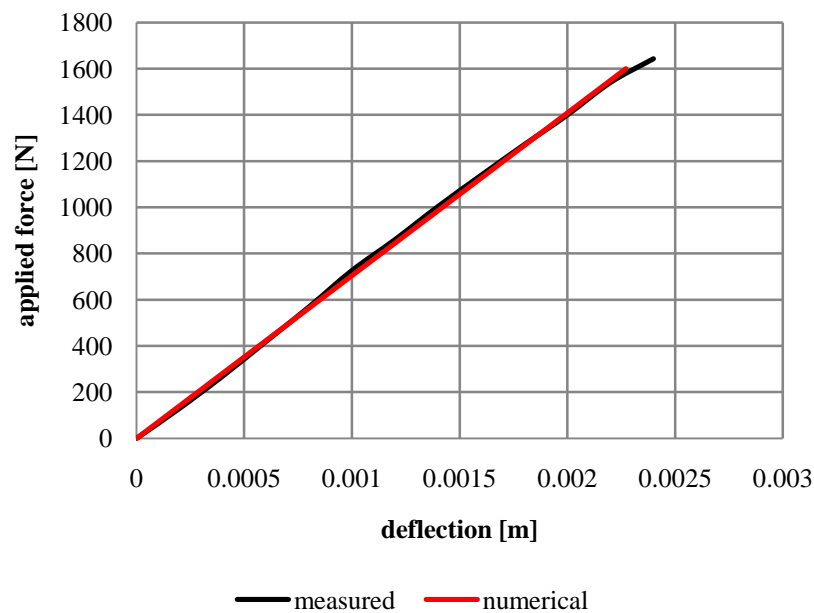


Figure 5.12: The deflection of the C-spring for the real and the numerical model

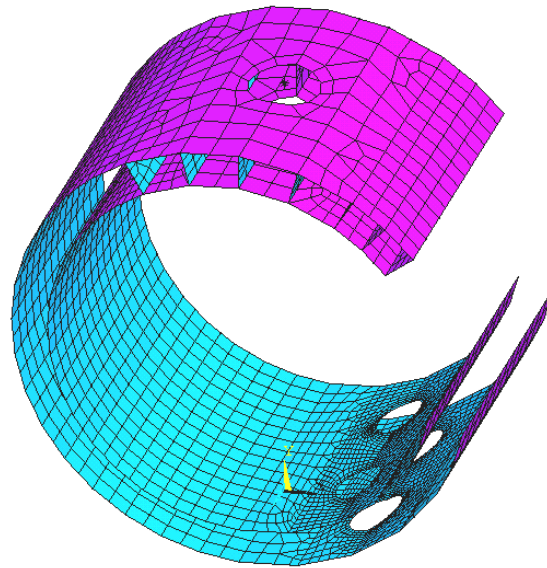


Figure 5.13: The C-spring

As in the case of the C-spring also the foot base spring is to be modelled in FEM with properties consistent with that of the real base spring. The deformation of the spring is measured experimentally. The spring is loaded with vertical loads since the vertical loads are the largest and most dominant in the foot of the human during normal gait. The deformation shows a linear relation with the applied vertical force. This curve is used in selecting a modulus of elasticity for the FE model of the base spring that will lead to a deformation matching the real case. According to these experimental results the modulus of elasticity (Young's modulus) of the equivalent spring is found to be 28.5 GPa. The deformation was measured at a point located 128 mm from the mounting edge. The FE model of the spring is built of one shell element but the form of this element was not built like the real one but rather in a symmetric form as it is shown in Figure 5.15. The load deflection relations for both the measured and the numerically calculated values are plotted in Figure 5.14. Both are measured at a distance 128 mm from the edge and at the middle line of the foot.

Like in the C-spring this elastic model is to be used in the multibody model and should be reduced. Since the base spring is the part that makes contact with the ground a larger number of master degrees of freedom should be selected to make the contact with ground smooth and closer to reality. Accordingly, eight nodes are selected (some are shown in Figure 5.15), one node is selected as a mounting point for the system with the rest of the multibody model. This point is at the middle of the edge and also defined as a pilot point with contact to many neighbouring points. The other seven points are selected along the axis of the foot also in the middle of the sole. To reduce the effect of local deformation of just one point on the results (since in real system the contact is done at all the surface and not just specific points), the master degrees of freedom are also modelled as pilot points and connected to many neighbouring nodes.

Now, the base spring can be condensed and reduced to a single element that still contains the dynamic characteristic required for the dynamic analysis.

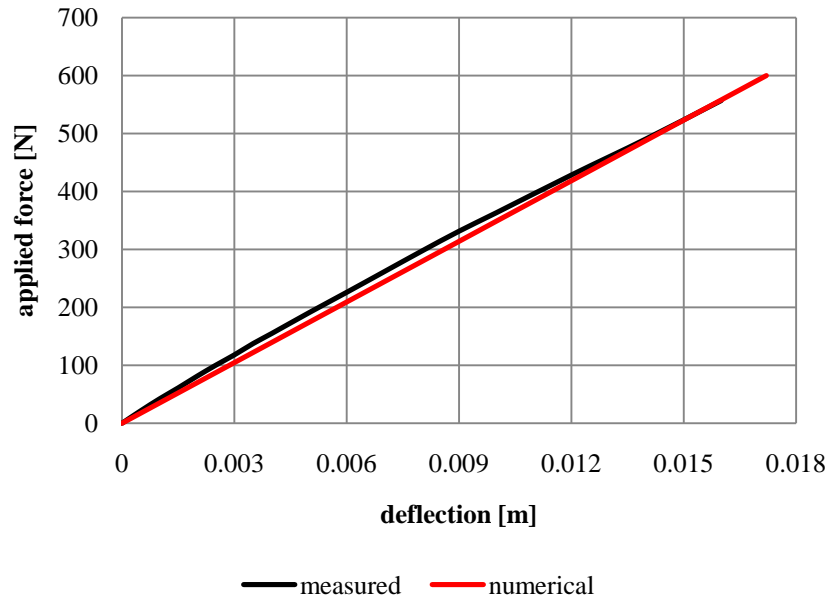


Figure 5.14: The deflection of the base spring for the real and the numerical model

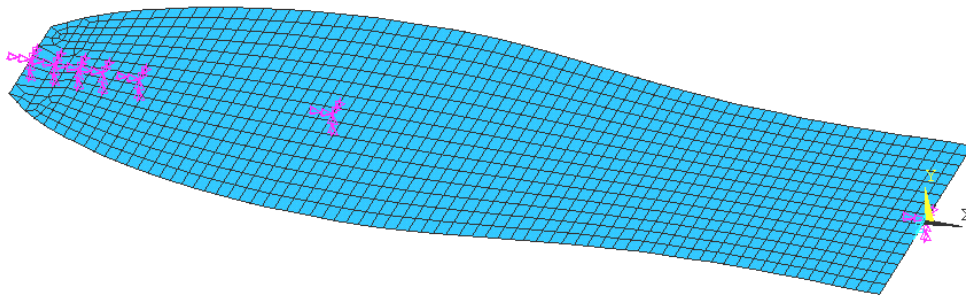


Figure 5.15: The base spring

The spring models built in FEM are three dimensional, and the MBS model is two dimensional. The possible problem of extra torques that may appear when the GRFs act on the whole foot is solved through selecting the contact points with the ground along the middle of the foot such that the torques developed due to these forces are working perpendicularly to the working surface.

#### 5.4.2 Reducing the FE model

In the previous section FE models of the base and C springs were built. These models are reduced in the following steps. Firstly both models are analysed using the substructure analysis. In this analysis the mass and stiffness matrices are built for the elements where all the master degrees of freedom are selected without any constraints. The benefits of this reduction to simplify the complex FE model into a simpler form consisting of fewer elements and can be handled easier in a multibody simulation. The resulting elements of this reduction are analysed again to calculate the eigenmodes of the reduced system. Before calculating the eigenmodes the elements' nodes are constrained in a way equivalent to the form that will be used lately in the multibody system. Here the C-spring is constrained at its top node such that just one node stay free and have 6 eigenmodes corresponding to its 6 DOF. For the base spring the DOF of one

node is completely constrained which will be used in mounting the base spring at the foot complex. The other 7 points are free and have 42 eigenmodes. The result of this modal analysis is a file containing the modeshapes of the constrained finite elements.

#### 5.4.3 Integration of FE model in the multibody system

The reduced FE models and the eigenmodes are read in the MBS program Simpack and converted into a form suitable for multibody dynamics. The nodes that are required to be used in the simulation are all selected (here all nodes are selected). The eigenmodes used in the modal approximation of the deformation of the flexible body are to be selected and the corresponding damping coefficient should be given. Through these steps the elastic model is ready to be used in the MBS.

This foot is modelled in the MBS simulation program as a complex consisting of the two elastic elements. The C-spring is connected with a fixed joint to the pylon that represents the shank, then the foot heel and sole are connected to the C-spring. The titan ring, which has a functional purpose, is modelled as a two-bar mechanism with two rigid elements. The reason for the use of this mechanism is to give the C-spring flexibility to move downward and to limit its motion upward during the rolling of the foot on the ground. Figures 5.16 and 5.17 show the foot complex as it is displayed in the multibody model. The foot contacts the ground at a number of points in two regions; at the heel and at the forefoot. Fourteen contact points are used in the simulation, seven points at each of these two regions.

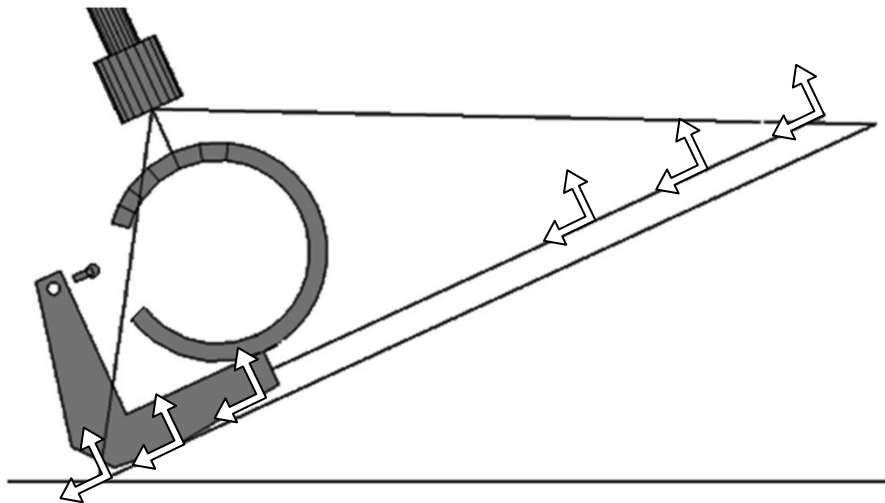


Figure 5.16: The foot C-Walk modelled as a complex of two elastic elements, heel element, and titan ring. The arrows at the heel and forefoot represent the forces acting on the foot



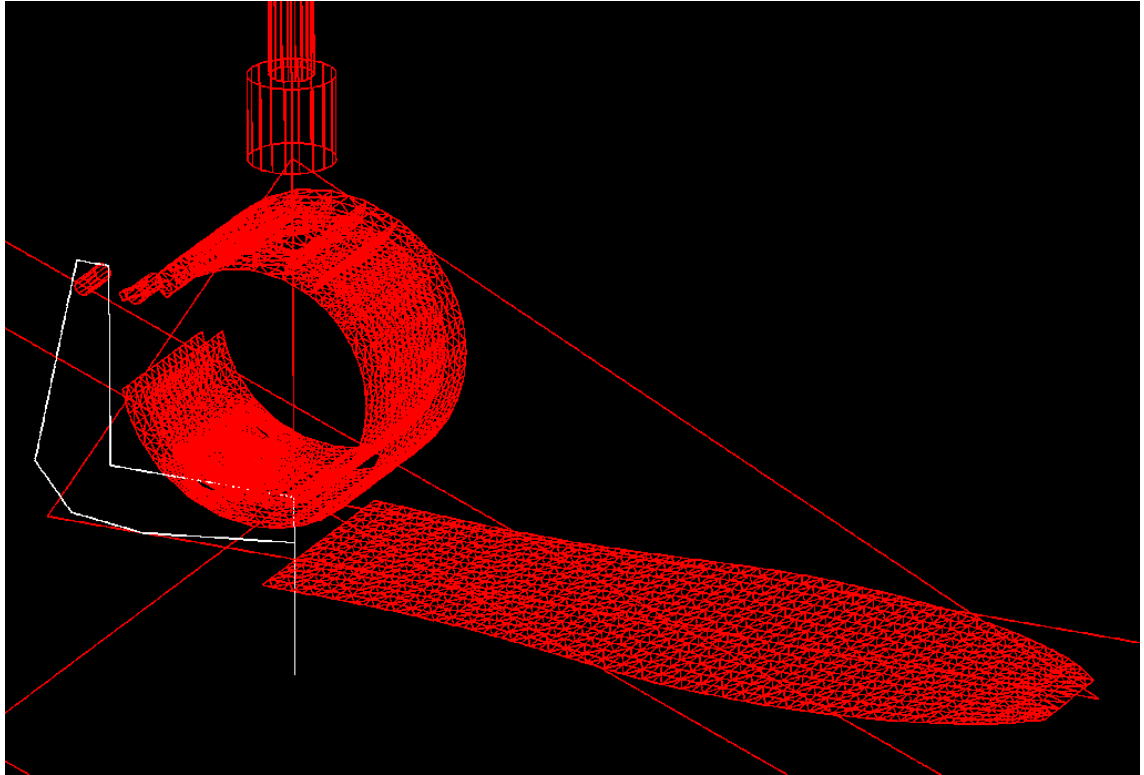


Figure 5.17: The foot C-Walk modelled as a complex of two elastic elements, heel element, and titan ring in the multibody dynamic model

#### ***5.4.4 Some problems faced in the simulation of the human gait***

##### **a. The data used in the simulation**

At the beginning of the work the only available data for the simulation were from a female amputee using the flexible foot Flex-walk. The simulation of the numerical model with the C-Walk foot was done using this data from the Flex-Walk user, and the results of the simulation for the different gait parameters deviated very much from the expected results. Many parameters were modified and changed in order to solve this problem, but these changes have not improved the results enough to an acceptable level for further use. Latterly as the new data for an amputee using the flexible foot C-Walk were available, the simulation was repeated and the numerical model results have shown very good agreement with the experimental results. The reason for this disagreement, when using different data, can be explained by a comparison between the C-Walk and Flex-Walk gait parameters. As an example, in Figure 5.18, the hip joint moments at the prosthetic side for both feet are displayed. From the beginning of the gait cycle the Flex-Walk foot user shows a larger moment at the hip joint compared with the user of C-Walk foot. Nevertheless the weights of the two amputees are 60, 65 kg, respectively (the difference in the weight of the amputees is less than 10%). The difference in the moment at the hip joint was as much as 70%. This applies also for the other gait parameters. From this result it could be partially concluded that the simulation of human gait needs input data from the actual user of the prosthesis and this is consistent with the fact that the use of prosthetic foot includes a learning process. The requirements for using some artificial feet are not necessary the same as some other artificial feet. An amputee needs some time until he can use his prosthesis and utilize it smoothly (in the literature it was found that some amputees feel very satisfied and comfortable with some types of artificial limbs on one hand and find other types of artificial limbs disturbing, but some other group of users have opposite opinion [Mak 2003]).

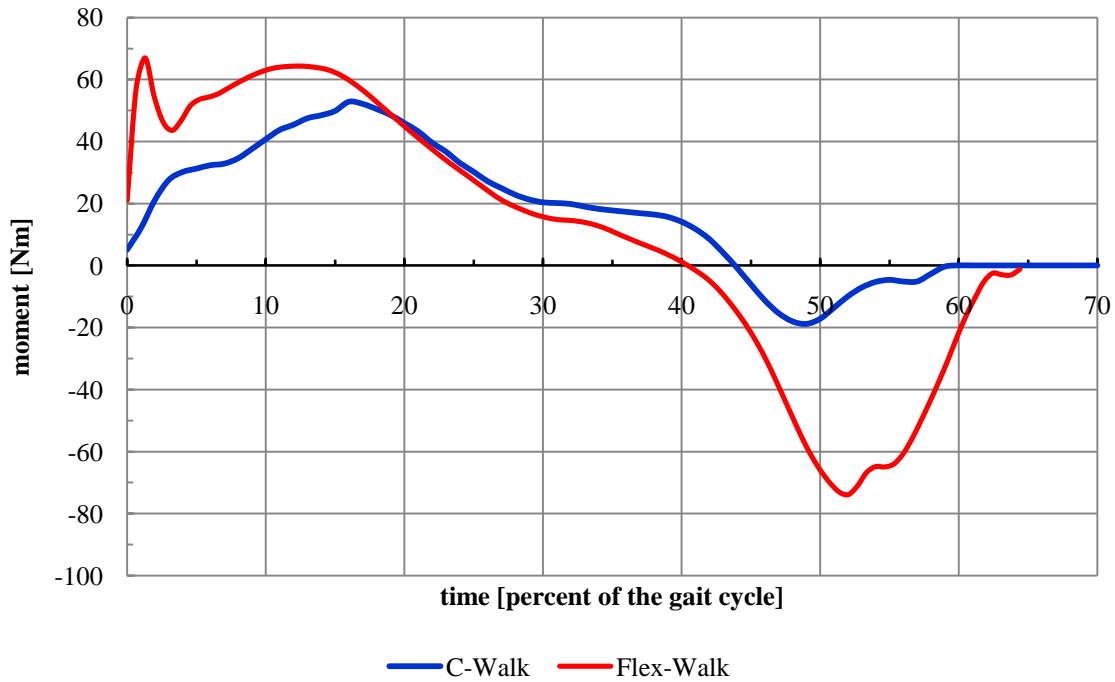


Figure 5.18: The moment of the hip joint at the prosthetic side for two Flex-Walk and C-Walk prosthetic feet users

## b. The contact with the ground

Throughout the simulation of the model with the elastic elements, the following error message had appeared and the simulation was interrupted before it could finish. This error message should not have occurred because the modal matrix of the elastic body is not singular contrary to what is reported in the error message. In addition, the error occurred some point midway through the simulation whereas if the error was valid then it would be expected to occur at the start before any time in the simulation elapses.

```

** ERROR in RHS evaluation, error code =                2
   The elastic Modalmatrix of the body with
   the elastic number NRKE is singular
   NRKE =                2

DASSL--  AT T (=R1) AND STEPSIZE H (=R2) THE
          r1 =  0.4472041694640E+00
          r2 =  0.1797241808354E-15
DASSL--  ITERATION MATRIX IS SINGULAR

** ERROR in Time Integration module
** Singular Jacobian
** The matrix of partial derivatives (Jacobian) is singular,
   integrator failed to solve a system of nonlinear equations.
** This might indicate
   -> loop closing constraints on position and velocity
       level being not compatible (e.g. because of bugs in
       a user routine),
   -> redundant or contradictory loop closing constraints,
   -> rigid body contact conditions between surfaces with

```

identical curvatures in the contact region,  
and / or  
-> something else.

- \*\* a) Check the loop closing constraints for compatibility.
- \*\* b) Eliminate constraints being redundant or contradictory.
- \*\* c) Since contact between surfaces with identical curvatures may not be handled by SIMPACK's default strategy, you might try to modify the definition of the surfaces slightly (if applicable). Otherwise such a contact condition has to be handled completely inside a user routine.

```
CPU-time (integration + write )      :    30.69000      (sec)
integration stopped at T =           :    0.447204169463955
number of all integration steps      :             880
number of function calls (total)     :           37999
number of function calls without     :           1545
      counting those for the
      evaluation of the Jacobian
number of Jacobian evaluations       :             282
number of mass matrix evaluations    :              0
number of root function calls        :              0
number of error test failures        :             134
number of convergence test failures :             29
last step size                      :  1.402379600706886E-006
last used order                     :              4
error code of integrator              :             -8
```

\*\* Prepare model for SBR export ...

\*\* SBR export settings:

- \*\* - File name: Normal07.output/Normal07.sbr
- \*\* - Floating point number precision: Single
- \*\* - Time settings:
- \*\* - Export every time step
- \*\* - Resulting number of steps: 3201
- \*\* - Configured time frame: 0 to 0.64 s
- \*\* - Actually used time frame: 0 to 0.64 s

\*\* Preparation of SBR export finished:

- \*\* - Total number of output channels: 1120
- \*\* - Estimated memory requirement: 13.676 MB

t = 0.447199990000089

Compressing output values ... successfully finished!

\*\* SIMPACK module executed

The three possible reasons for the error reported in the error message were reviewed. The loop closing constraints on position and velocity level were compatible at the time when the simulation is ended and cannot be the reason for this problem. The only loop closing constraint in the model was the two bar mechanism used to model the titan ring function. Many trials were done to change this constraint through other forms of mechanisms. Through the replacement of this mechanism with a spring element the simulation was able to solve the problem for a longer time but not until the end of the required simulation time. The third possible reason reported in the error message was the rigid body contact conditions between surfaces with identical

curvatures in the contact region. Because the model of the foot that make contact with the ground is elastic and its surface curvature was not identical the ground surface, and also because the contact model used is defined by the user through equations for the reaction forces between the points of contact. It is estimated that this could not be the reason of the problem, nevertheless a modification of the contact equation is done and many forms of equations and equation variables were used without giving a reasonable solution to the problem. Also many other design parameters were redefined and modified in order to solve the problem, but all these attempts were of no help.

One assumption is that one or more of the forces acting on the foot change rapidly or sharply and this may cause the problem. To reduce these assumed rapid or sharp changes in the forces it is suggested to change the damping coefficient of the elastic foot. This change in the damping coefficient has solved the problem and the program was able to simulate the gait along the given period of time. The changes in the damping coefficient were done in small steps to ensure that the minimum required change in damping was done and to reduce the effect on the dynamic behaviour of the whole system. After many trials a reasonable values for the damping coefficient of both the C-spring and the base-spring were found and used for all the other simulation processes.

During writing this dissertation a study was published in September, 2009 by Fischer [Fischer 2009]. This study treats the problem called Painlevé Paradox in the modern multibody dynamic. In this study it is shown that for rigid multibody systems making rough contacts, there exist critical friction coefficients, for them the paradox described by Painlevé can occur. The work of Fischer treats the problem for rigid bodies and tries to develop a physically correct method that can deal with the paradox situation in modern multibody systems in a systematic way. It could be that the problem here in this work has the same reason as explained in Fischer work, nevertheless the contact element here is elastic and not rigid.

## 5.5 Simulation Results for Walking on Level Surface

The data used in the simulation of this foot are from the company Otto Bock. They are for a female amputee using a C-Walk foot, the weight of the amputee is 60 kg, her height is 1.61 m, and the amputation side is the left side. The amputation reason is trauma. The measurements are repeated eight times for each walking velocity and in each time two steps of the gait cycle are measured. An average value of the eight trials without filtering is calculated and further used in the simulation. The walking speed used in this part of the results is 1.35 m/s and the duration of the step is 0.62 s.

Figure 5.19 shows the vertical GRF acting on the prosthetic foot of the amputee. It can be seen that there are some differences between the two curves, which are assumed to occur due to various reasons. At the time 0.125 s the ground force shows a small abrupt change and then continues its smooth curve. This occurs when the foot sole starts to make contact with the ground since the simulated foot contact with the ground is modelled through a limited number of contact points and not continuously as in reality. Then the reaction force reaches its first peak value at about 0.16 s which is the end of the load response phase of the gait cycle and the start of the single support period. The maximum vertical reaction force value for the simulation was 661.5 N, and it is just 1.9% higher than the measured value (649.3 N). The curve slope at the beginning in the simulation results is higher than the measured values and this depends on two factors: The first is the foot-ground contact model used in the simulation, since there is still no ideal model that could be adopted for foot-ground contact. Many factors play major effects on this model for instance the shoe elasticity and the cosmetic cover properties. The second factor is the fact that this model is a two-dimensional model and accordingly three of the six gait determinants (namely pelvic rotation, pelvic drop, and the lateral displacement of the pelvis) are

lost. These determinants make the motion smoother and probably reduce the slope of the GRFs at the beginning of the step.

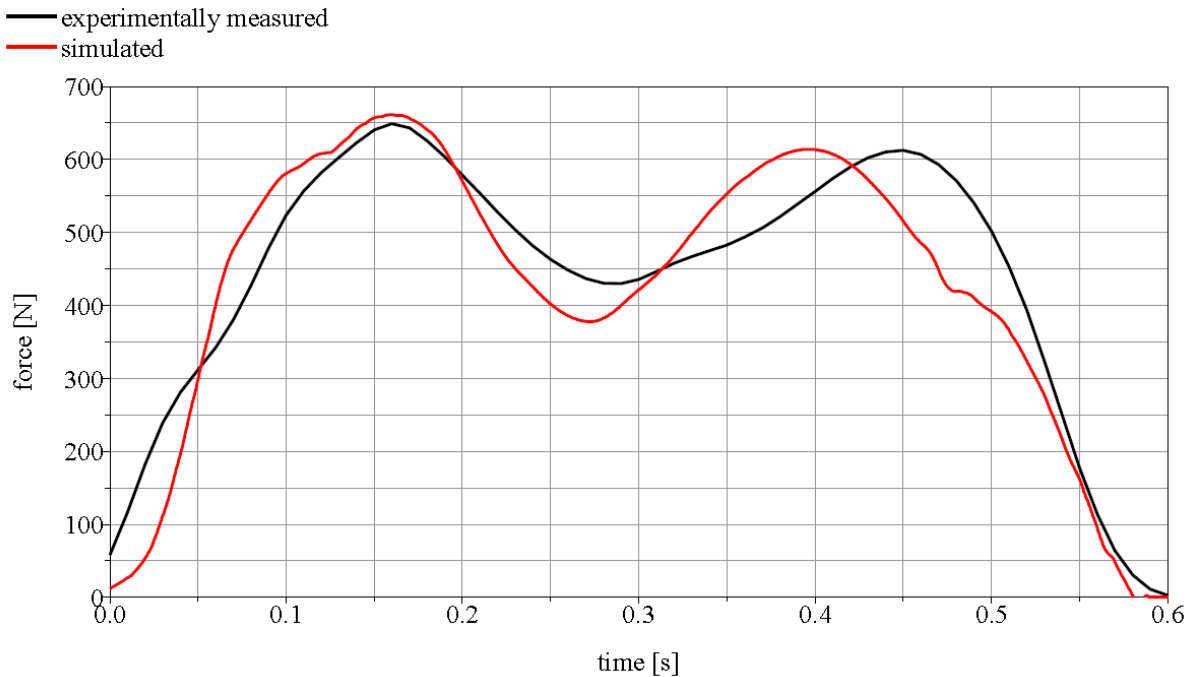


Figure 5.19: The experimentally measured and the simulated GRFs acting on the prosthetic foot

The second peak in the simulation occurs at 0.4 s, which is earlier than the measured values at 0.45 s. This is because the model is a two dimensional model and has no pelvic rotations, which make the step size about 70 mm shorter (this is explained later in the BCoM motion description). The reaction force reaches its second peak earlier since the body rolls over forward earlier with the loss of the pelvic rotation until the second, sound leg contacts the ground. At this point the prosthetic foot starts simultaneously to roll over the ground and leaves it earlier than in the real case but more gradually. This explains the gradual reduction of the force for the simulated model until the prosthetic foot has completely left the ground. The simulated foot leaves the ground 0.02 s earlier than the experimentally measured case. The magnitudes of the vertical reaction forces at the second peak were identical for both simulated (614 N) and measured (613 N).

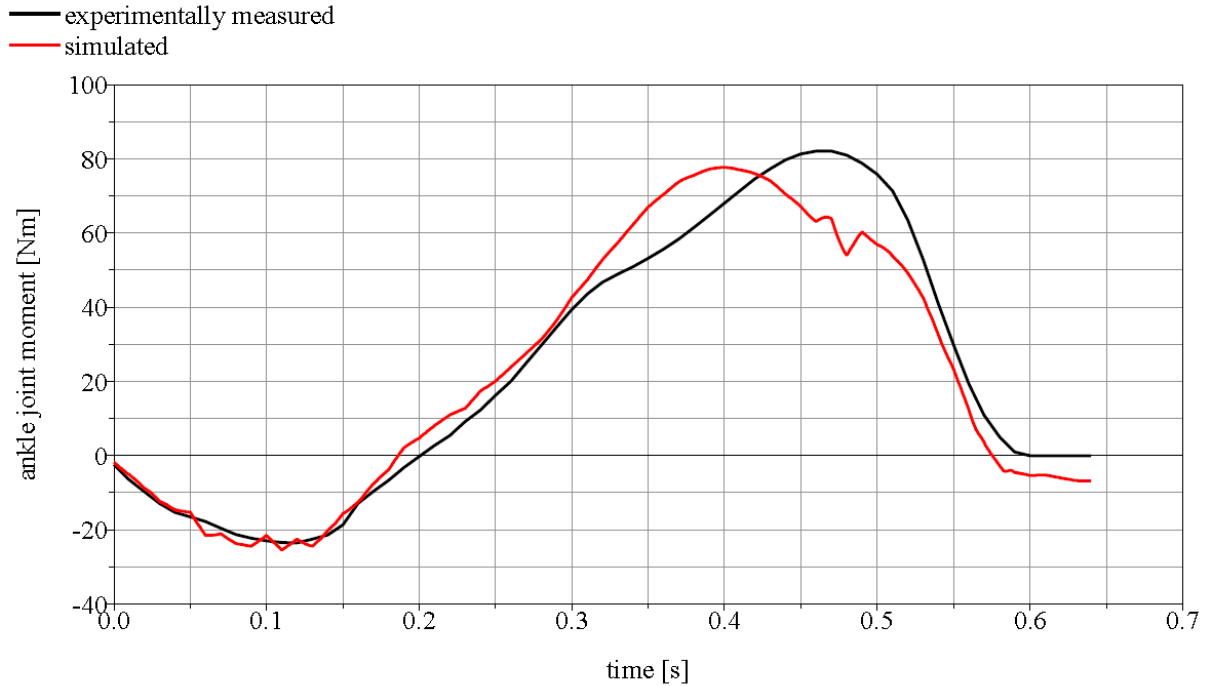


Figure 5.20: The experimentally measured and the simulated moment at the ankle of the prosthetic foot

In Figure 5.20 the moments at the ankle joint are displayed. The consistency between the experimentally measured and the simulated moments is satisfactory and is also consistent with the vertical GRFs. The intersection with the x-axis shows that the foot in the simulated multibody model reaches its stable position (zero moment) shortly before that of the real one, which can be an indication that the body is ambulating faster over the ankle compared with reality and that the body has an extra moment in the forward direction (also due to the shortened step size caused by pelvic rotation loss). The moment reaches its peak value in the simulation at 0.4 s, which agrees with the time of the peak value of the vertical GRFs, and then starts to decrease gradually (but longer than in reality), because the prosthetic foot is leaving the ground and is lifted by the hip joint rotation. This early release from the ground and the point of measuring the torque (in the simulation the torque is measured at the point of mounting the c-spring on the pylon) cause the differences in the peak values of moments, which is for the simulation (77.7 Nm) 5.4% less than the experimentally measured value (82.1 Nm).

The consistency between the rotation of the thigh at the hip joint for both the simulation and experimentally measured values are very good. Both values start and end at the same rotation. The hip extension in the simulation is 3 degrees less than in reality which is 6% from the total hip joint rotation. The minimum value was for both experimentally measured and simulated values at the point in time when the second sound leg starts its contact with the ground (the beginning of the second double stance phase). Figure 5.21 shows the hip rotation in radians for both simulation and experiment.

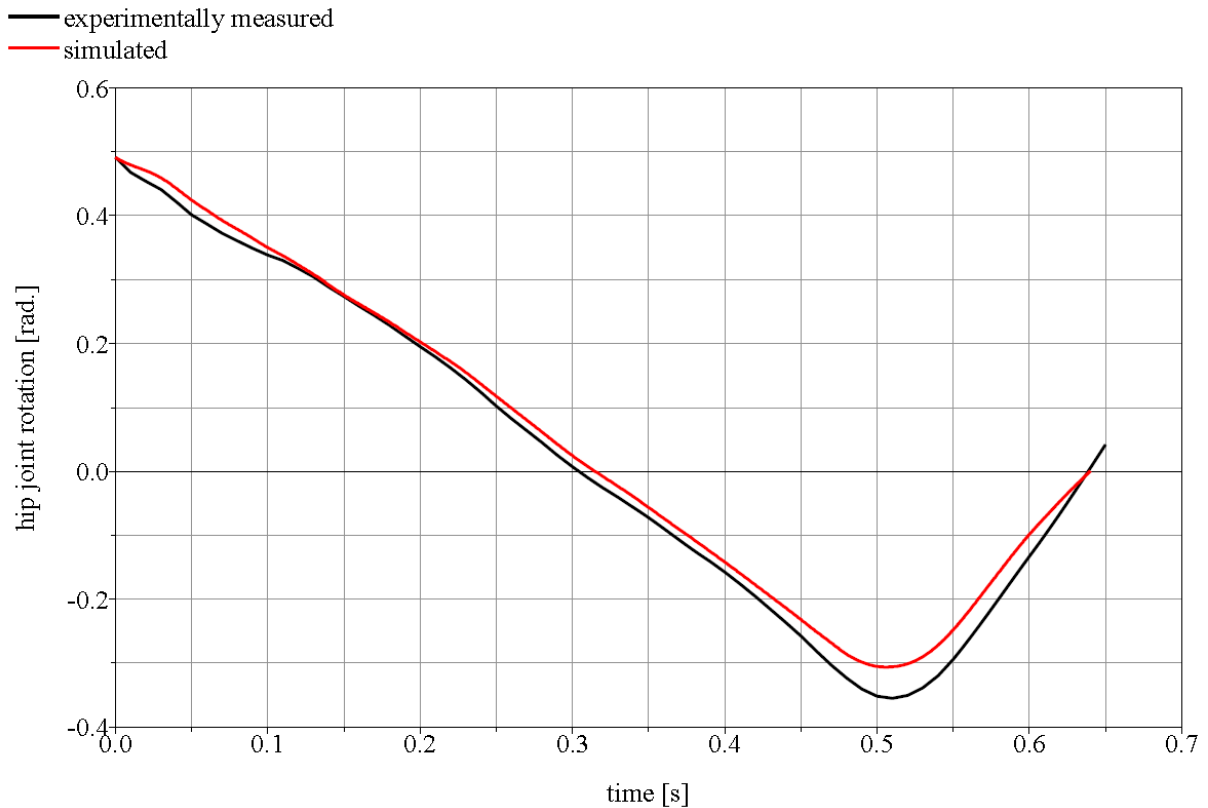


Figure 5.21: The experimental and numerical rotation of the thigh at the hip joint

A symmetrical BCoM is a very important characteristic for minimum energy consumption and comfortable walking. The simulation result for the vertical BCoM motion with respect to the horizontal motion is represented in Figure 5.22. The simulated BCoM motion shows that the beginning and end of the step are almost at the same level, and the maximum vertical displacement is 43 mm. The result shows a smooth curve with no abrupt changes. The comparison between the simulated and measured values gives a 6.5 mm difference in the vertical body motion. This difference, which is 18% of the whole vertical BCoM motion of the real system (36.5 mm), is large but expected. In this two-dimensional model the pelvic rotation is not taken into consideration, and this rotation, which is 4-5 degrees in each direction, is responsible for the prevention of up to 9.5 mm of the total vertical displacement of the BCoM. And the pelvic tilt, which is about 5 degrees, is also not included here in the two dimensional models. This tilt is responsible for up to 5 mm reduction in total vertical BCoM motion. Together both factors reduce the vertical motion up to 14.5 mm (these values are average maximum values for many subjects, references and details are all available in the theoretical background). Then the 6.5 mm increase in BCoM motion in the dynamic simulation model is expected and within the range found in literature. The curves show that the maximum value in the simulation occurs shortly before that in the experimental result. The whole horizontal BCoM motion in the simulation is 0.905 m. This is 6.3% less than the experimental result which was 0.966 m. This is also expected as in the vertical motion. Then the distance between the two hip joints is 200-250 mm, and the rotation of the hip joint in each direction is 5 degrees and repeats itself three times in the stance phase of the gait (which is simulated in the numerical dynamic model). This corresponds to an elongation in step size of 19 mm for each pelvic rotation for a person with hip joints separated at 220 mm. For three rotations it will be 57 mm (the difference between measured and simulated values is 61 mm, which is almost identical to the 57 mm calculated here).

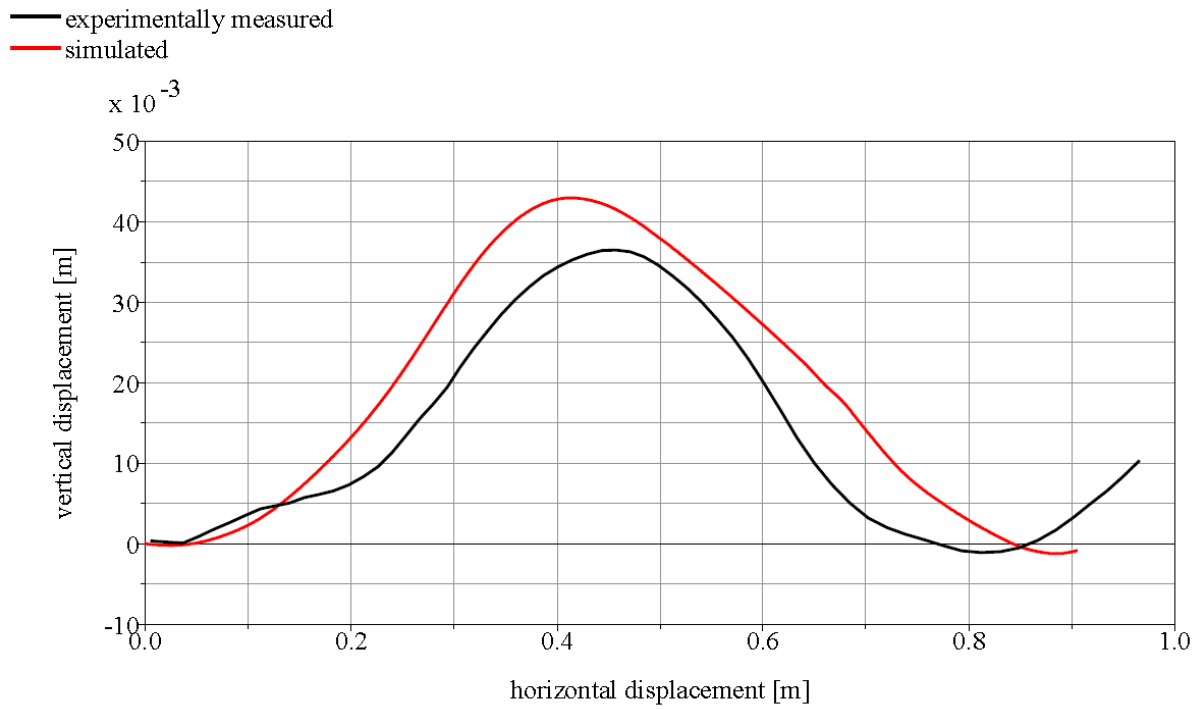


Figure 5.22: The experimentally measured and the simulated sacral BCoM vertical motion with respect to its horizontal motion

As it is seen in the figures and from the already explained reasons for the variations between the experimentally measured and the simulated results, there is an acceptable consistency between the model results and reality, which make the model an acceptable tool for the evaluation of the adaptive properties of prosthetic feet and for the development of adaptive feet.



## 6 Adaptation of Foot Properties with Different Gait Conditions

In this chapter three walking conditions are studied: walking on level surface, entering an uphill inclined surface, and walking on level surface at two different velocities. For these conditions three foot parameters are taken into consideration.

### 6.1 Walking on Level Surfaces

The data used in the simulation for this part are from a female amputee walking on level surface using the C-Walk prosthetic foot (as in the previous chapter). Also here the speed is kept at 1.35 m/s. The results show the effect of changing the foot stiffness and the ankle joint inclination on the gait.

#### 6.1.1 Changing the stiffness of the foot sole

Four FE models of the foot sole are modelled and used in this simulation with four different stiffness values 25.5 GPa, 28.5 GPa, 31.5 GPa, and 34.5 GPa, which represent  $-10\%$ ,  $0\%$ ,  $+10\%$ , and  $+20\%$  changes in the stiffness from normal, respectively.

Figure 6.1 shows the vertical GRFs acting on the body of the amputee at the prosthetic side. As it is seen in the figure there are very small differences between the curves corresponding to the different stiffness values. For the first peak there are almost no differences due to the main weight bearing element here is the heel, which is not changed. For the second peak (where the base spring bears most of the load) the maximum difference corresponding to the two stiffness extremities 25.5 GPa and 34.5 GPa was 14 N (2.3%). This difference is very small and mostly resulted from the reduction in the deformation due to higher stiffness, which reduces the amount of absorbed energy in the damping elements of the system.

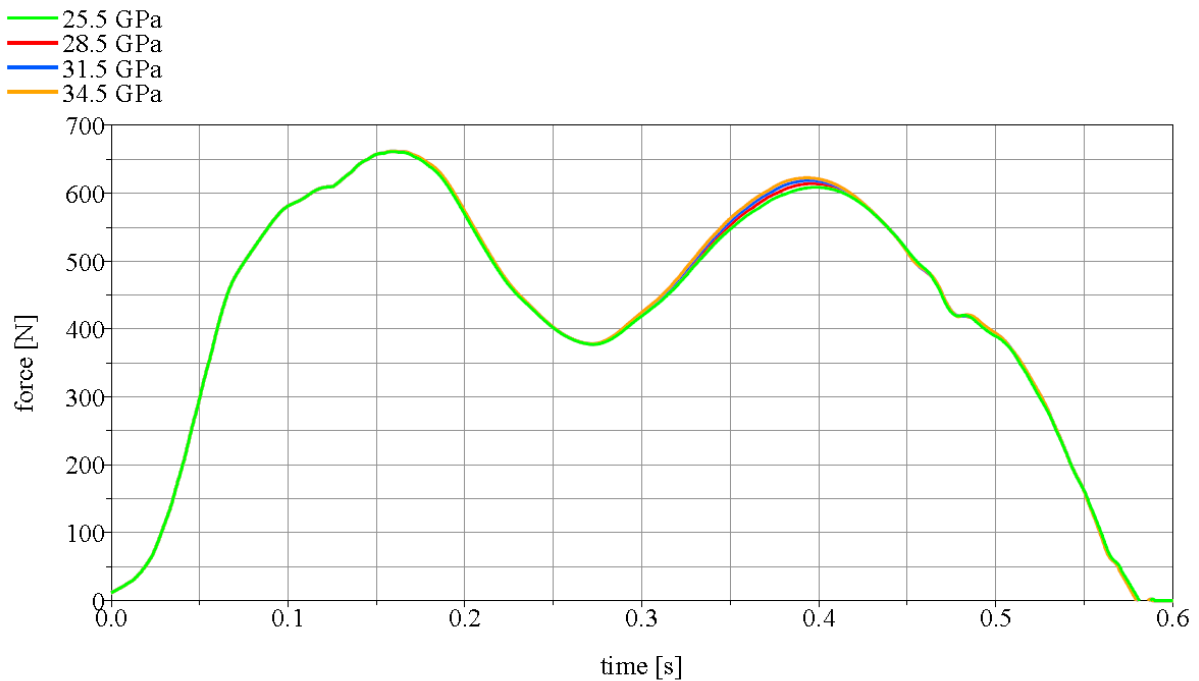


Figure 6.1: The simulated vertical GRFs acting on the prosthetic foot for the different stiffness values of the prosthetic foot sole

In Figure 6.2 the torques at the Ankle are displayed. As in the GRF case the differences are very small and the maximum difference was 4% for a 30% change in stiffness at time 0.4 s. The

same applies to the hip joint rotation, which shows no significant change in its values with the different stiffness values. It is noted that the small differences (maximum of 1 degree) occur at some point and continue until the end of the curve. Figure 6.3 represents the hip joint rotation for the different stiffness values of the sole.

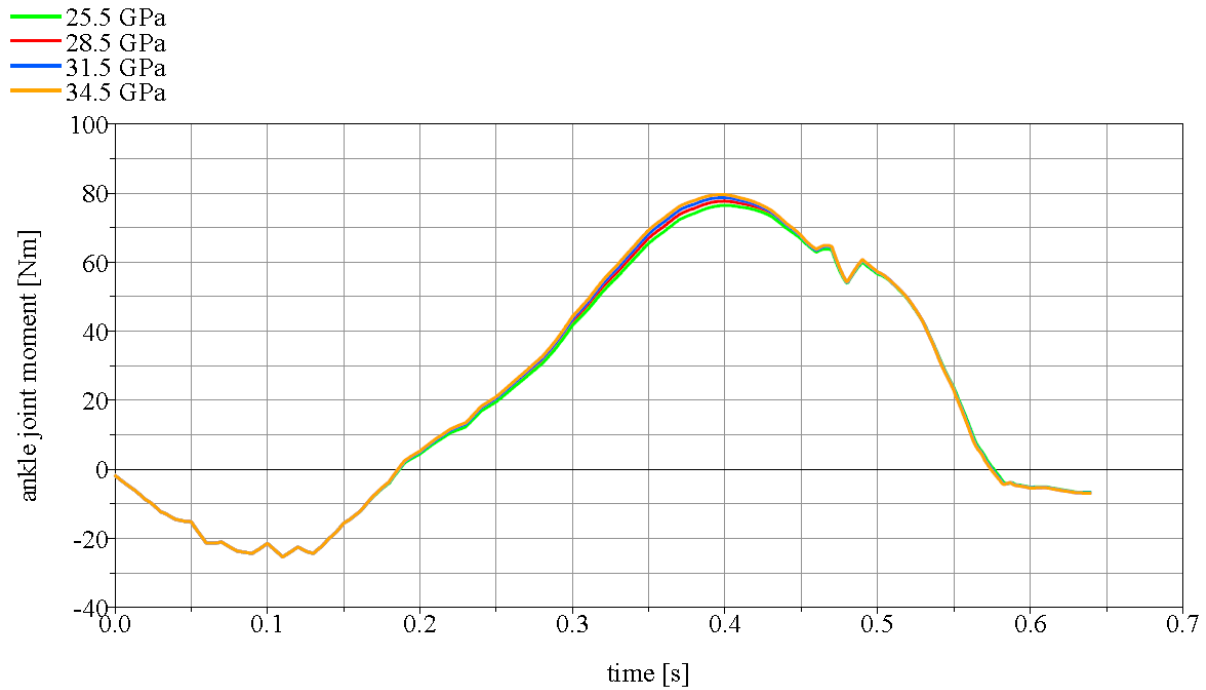


Figure 6.2: The simulated moment at the ankle of the prosthetic foot for different stiffness values of the prosthetic foot sole

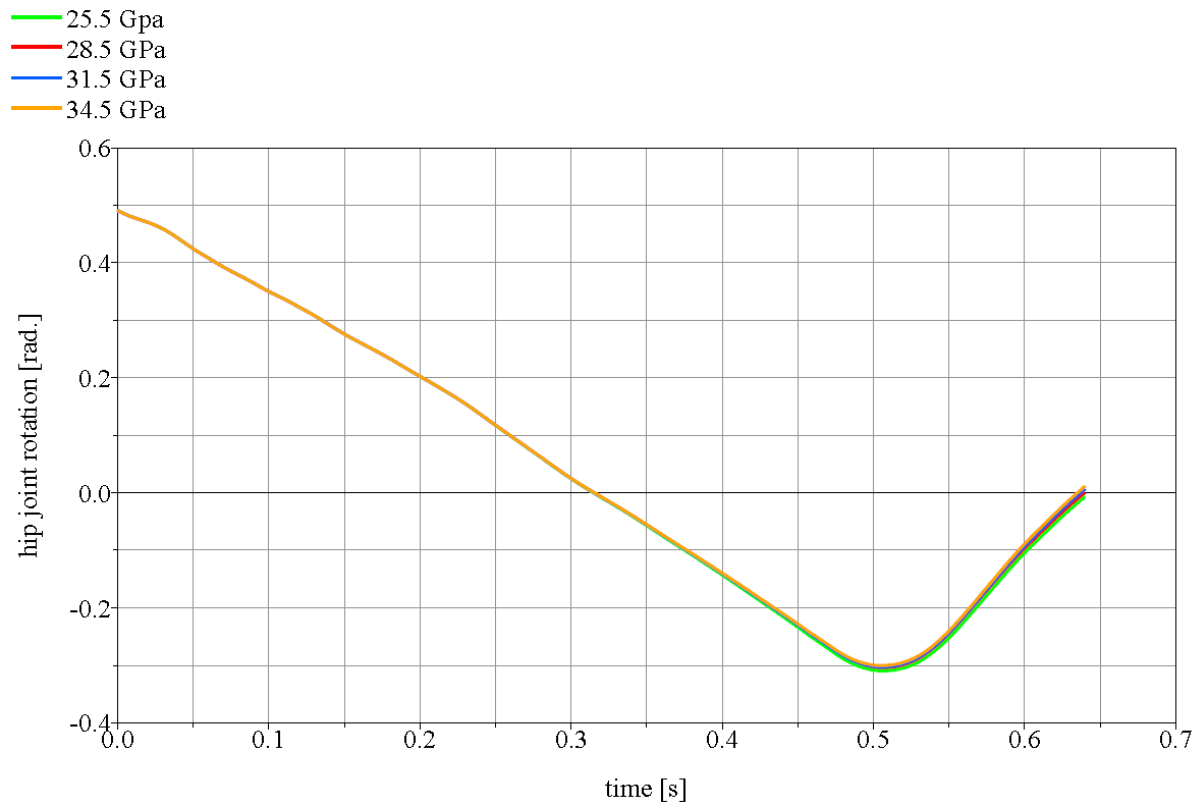


Figure 6.3: The simulated rotation of the thigh at the hip joint for the different stiffness values of the prosthetic foot sole

Observing the BCoM motion shown in Figure 6.4 indicates that changing the stiffness of the foot sole influences the vertical BCoM motion in the second half of the stance period of the gait such that it is ending at a lower or higher vertical position with respect to the start point. These deviations at the end of the simulation time with respect to the results of simulation using the original stiffness value of 28.5 GPa were found to be -9%, +8%, and +14% corresponding to the stiffness values -10%, +10%, and +20% of the original, respectively.

The differences in the horizontal motion of the BCoM at the end of the simulation time were very small. The maximum difference between the results corresponding to the two stiffness extremities 25.5 GPa and 34.5 GPa was 6 mm, which is less than 1% of the total horizontal displacement.

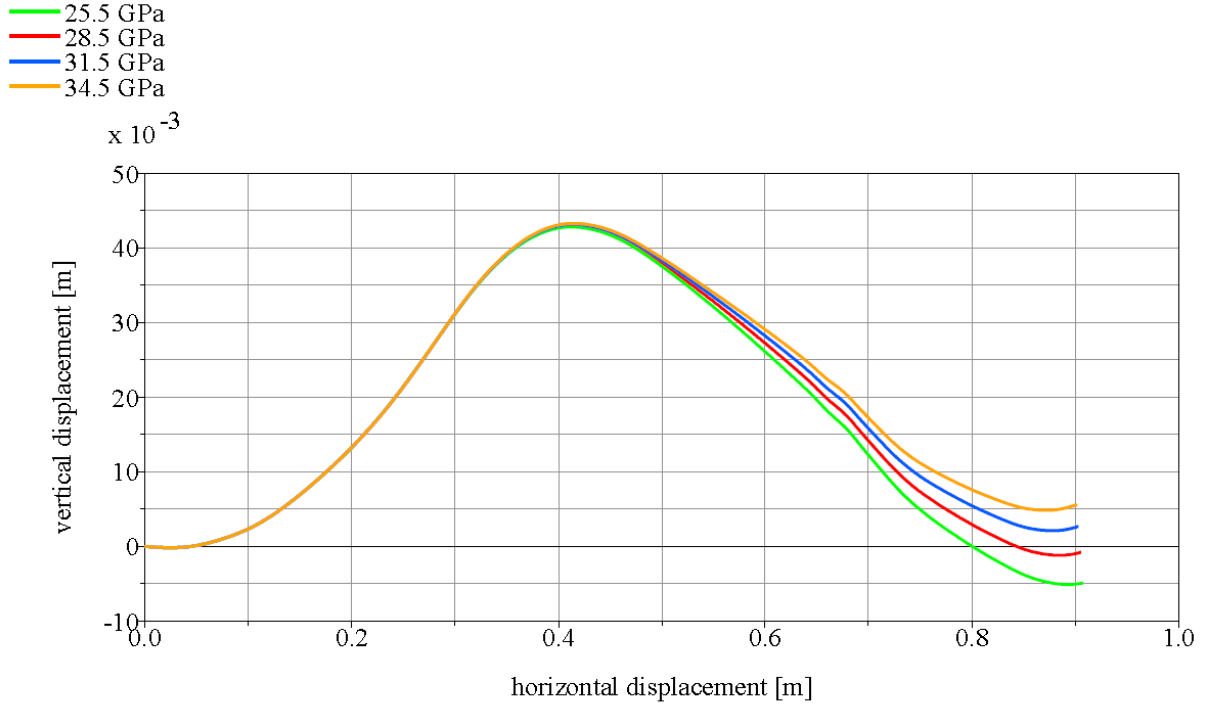


Figure 6.4: The simulated BCoM motion for four different stiffness values of the foot sole

Since the results of changing the stiffness values of the base spring of the prosthetic foot leads to significant changes in the vertical BCoM displacement without causing any significant changes in the forces and moments acting on the body (according to this numerical model), the model will be further used in evaluating the effect of changing the foot sole stiffness on the motions and forces of an amputee at different walking speeds and different surface inclinations.

### 6.1.2 Changing the inclination angle of the ankle joint

In this section the effect of the ankle joint inclination is to be studied. Four inclination angles are considered +3, 0, -3, and -6 degrees. Small changes in the inclination angles are considered since larger rotation values have caused large deviations from the normal gait cycle, which make them not suitable for walking on level surfaces. (Note: -3 and -6 degrees mean rotating the foot in the backward direction and +3 degrees in the forward direction).

Figure 6.5 shows the vertical GRF acting on the body of the amputee at the prosthetic side. The small changes in the inclination angle of the ankle joint have caused large changes in the vertical GRF. The first peak values for the -6 and -3 degrees inclination are 801 N and 732 N,

which are 21.2% and 10.7% higher than the value at the normal 0 degree inclination, respectively. On the other hand increasing the angle up to +3 degrees has reduced the peak force value 11.2% (587 N). Also the timing of the peak values has changed, which is already expected since rotating the ankle joint backward accelerates the load response period. In the case of forward rotation (+3 degrees) of the ankle the system has shown two successive peaks because the foot needs more time until it is completely in contact with the ground. Then the second small peak occurs as the forefoot makes contact with the ground and the sound leg completely leaves the ground.

For the second peaks (where the foot sole bears most of the load) the differences in the forces were small. The maximum difference was 4.6%. In general this figure indicates that the changes in angle of the ankle joint are more dominant than the change in the foot sole stiffness studied in the previous section.

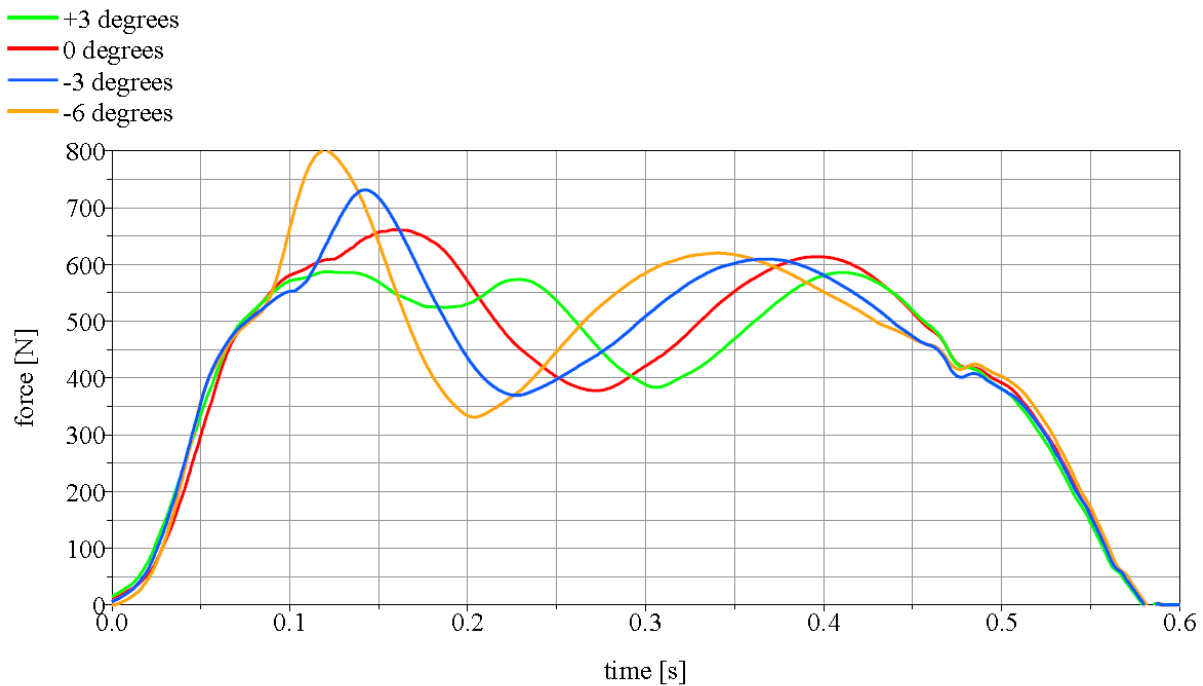


Figure 6.5: The simulated vertical GRFs acting on the prosthetic foot for four different ankle joint inclinations

In Figure 6.6 the torques at the ankle are displayed. The most important difference between the curves is the time when the moments are zero. Increasing the angle of inclination increases the time needed to reach zero moment, which means that the heel of the foot stays loaded for a longer time.

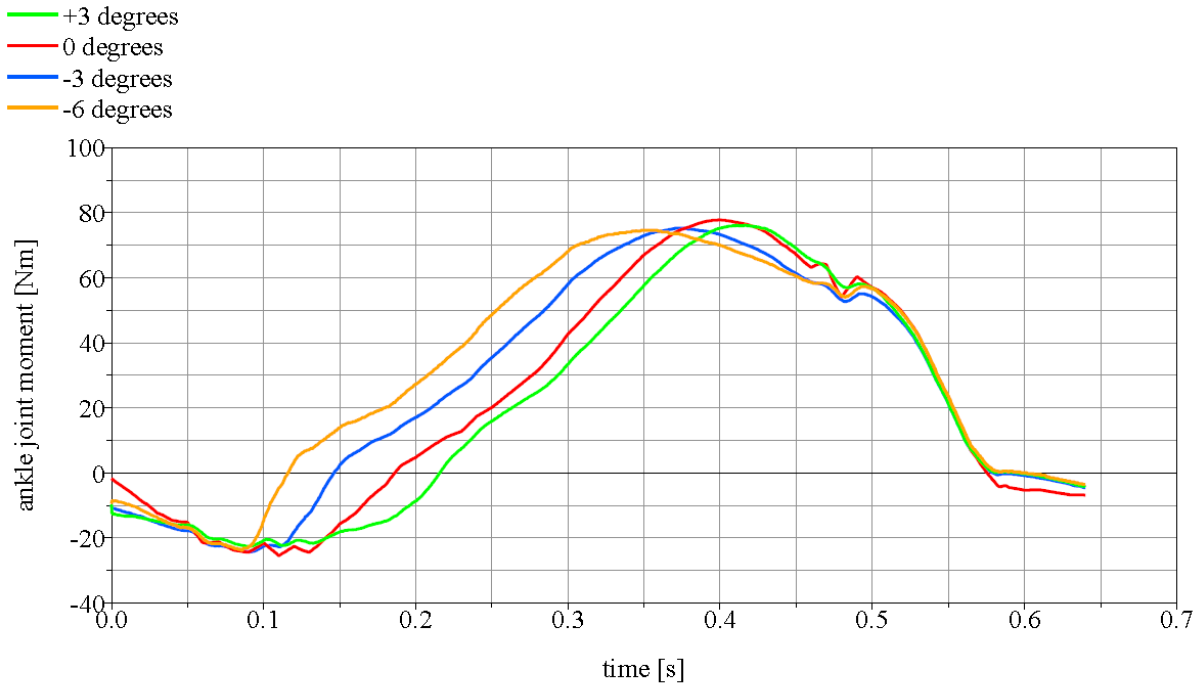


Figure 6.6: The simulated moment at the ankle joint of the prosthetic foot for four different ankle joint inclinations

The hip joint rotation shows very small changes by reducing the angle of the ankle joint  $-3$  degrees but by changing the rotation angle of the ankle joint  $-6$  and  $+3$  degrees, the total rotation of the hip joint has changed  $-7\%$  and  $+7\%$ , respectively. Figure 6.7 represents the hip joint rotation for the different inclination of the ankle joint.

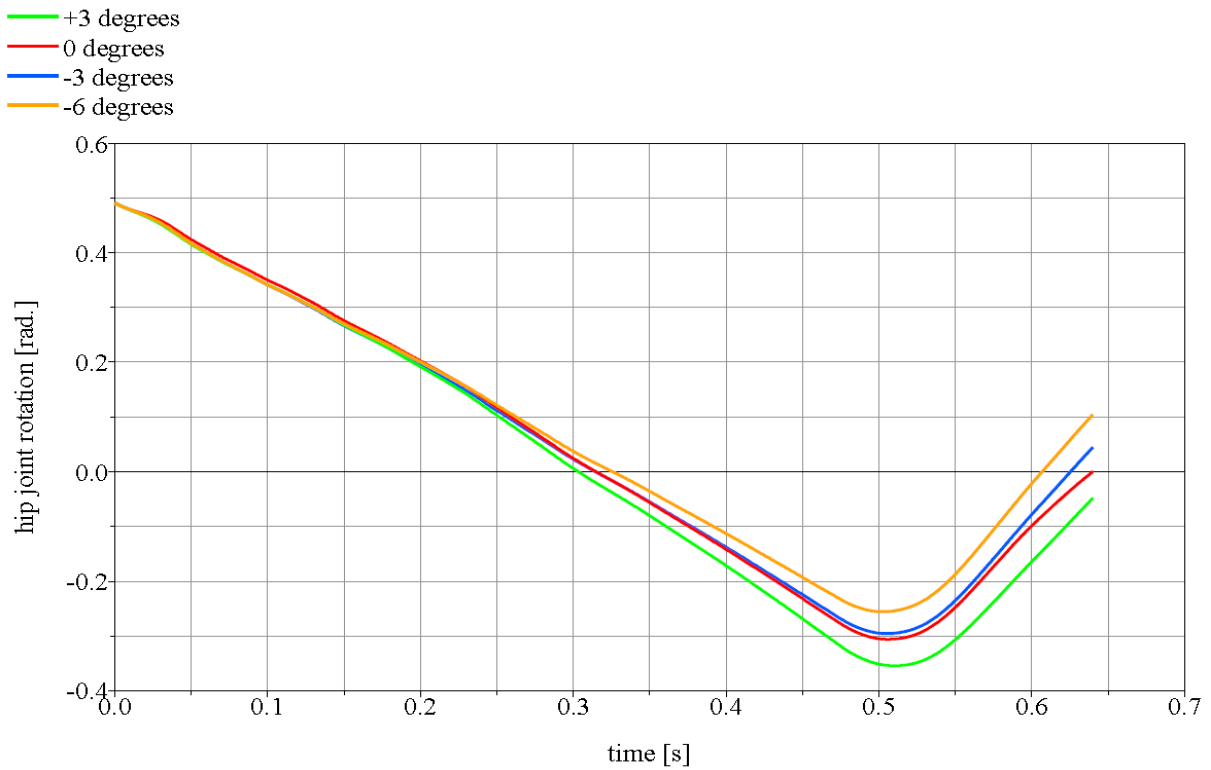


Figure 6.7: The simulated rotation of the thigh at the hip joint for four different ankle joint inclinations

The BCoM motion is shown in Figure 6.8. From the figure it can be clearly recognized that the changes in the BCoM are very significant and occur along the path of the body and not just at the second half of the gait cycle (as the case was in the previous section when the stiffness was changed). The vertical displacement of the BCoM has increased 24 mm for a 3 degrees increase in the ankle joint inclination. This is about 55% of the total vertical displacement. However, reducing the inclination angle by 3 degrees has reduced the BCoM vertical displacement just 11% (5 mm). For  $-6$  degrees change in ankle joint inclination the reduction was 45%. The relation between the inclination angle and the changes in the BCoM displacements is not linear.

The differences in the horizontal displacements of the BCoM at the end of the simulation time were larger than that corresponding to the stiffness changes. The maximum difference between the results, corresponding to the two inclination angles 3 and  $-6$  degrees, is 81 mm, which is 9.0% of the total horizontal displacement.

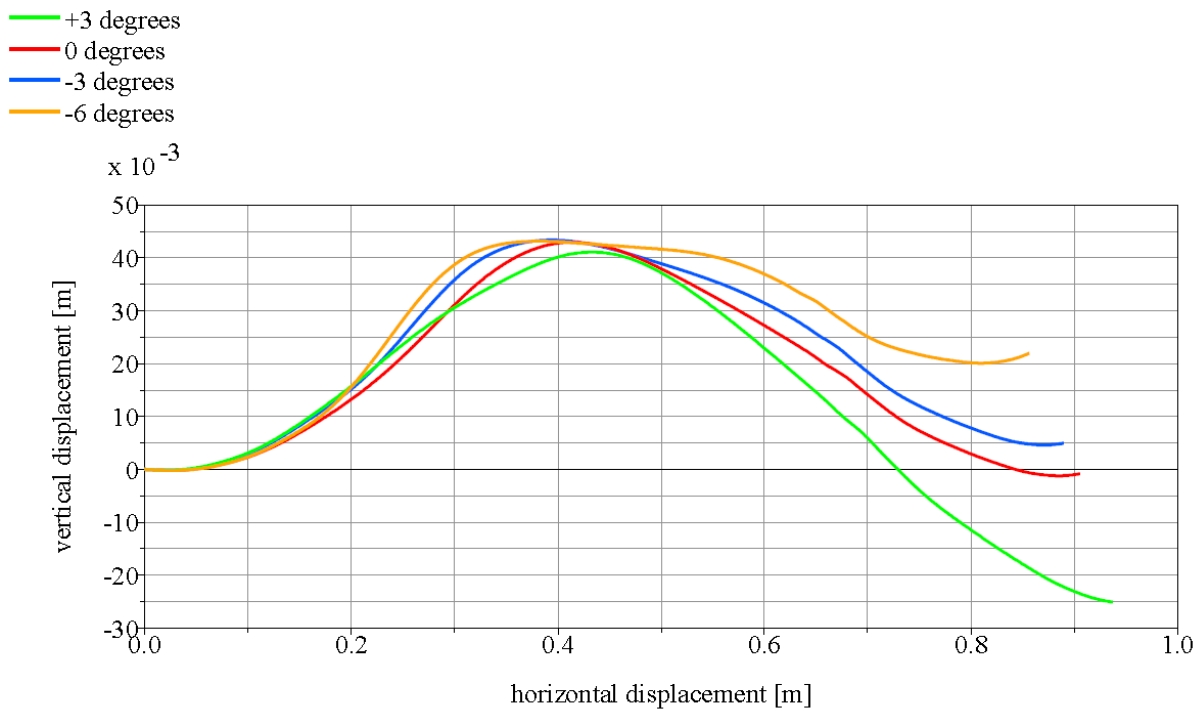


Figure 6.8: The simulated BCoM vertical and horizontal motion for four different ankle joint inclinations

Since the changes in this property of the foot have significantly changed the gait parameters it will also be considered as an important value to be studied in the other gait conditions.

## 6.2 Entering Inclined Surfaces (Uphill) from a Level Surface

The data used in the simulation for this part is from the same female amputee using the C-Walk foot as in the previous section. Also here the speed is kept constant at 1.35 m/s. Although the data is for an amputee walking on level ground, it is used here to study the gait changes while making the first step on inclined surface upward using the prosthetic leg. They are used to evaluate the changes in gait parameters by using adaptive foot properties on inclined surfaces. Here the amputee model starts walking from the level (horizontal) surface and makes one first step on an uphill inclined surface using the prosthetic side.

Two inclinations are used for the surfaces, 6 degrees (10%) and 12 degrees (20%). Three adaptive parameters are considered in the evaluation: the first is the sole stiffness, the second is the ankle joint inclination angle, and the third is the C-spring deformation. The reason for

studying these changes is that some researchers have reported that the ankle-foot roll-over shape changes according to the gait pattern. For example Hansen et al. [Hansen 2004] have reported that during uphill walking on inclined surfaces the ankle-foot roll-over shape changes significantly and the ankle joint rotates upward. Since the changes in the three parameters (stiffness of foot sole, ankle joint angle and the C-spring deformation) also change the ankle-foot roll-over shape, it is studied here to know the effect of these changes on the gait.

### 6.2.1 The effect of changing the stiffness

Two stiffness values are taken into consideration (31.5 GPa and 34.5 GPa) and two inclinations of the surface (6 and 12 degrees). For all cases the model was able to complete the whole stance phase without slipping against the ground or falling down. The discussion in this section will consider the motion until the beginning of the pre-swing phase. At the end of the stance phase period the sound leg contacts the ground again, but the GRFs acting on the sound leg after this time are not known and are taken from the gait of an amputee walking on level surface, which can cause large deviations from reality at the end of the stance phase.

Figure 6.9 shows the vertical GRFs acting on the prosthetic limb of the amputee. Increasing the inclination of the surface causes large changes in the forces acting on the foot. For the 12 degrees inclined surface the maximum force is 861 N which is 30% more than the force for the horizontal surface, and for the 6 degrees inclined surface it is 11% more. The second peak shows no differences in its magnitude for the three inclinations but its long duration indicates that the forefoot bears the largest part of the body weight for the most time while walking on inclined surfaces. This is also noted in the moment of the ankle in Figure 6.10. Since the surface is inclined the foot needs less time to be completely in contact with the ground and the load response phase time is shorter (0.065 s and 0.12 s for the 12 and 6 degrees inclined surfaces, respectively, compared with 0.17 s for horizontal surface).

Changing the stiffness values caused no significant changes in the ground forces acting on the body within the same inclination angle, which means that changing the stiffness of the foot sole leads to almost no changes in the reaction forces.

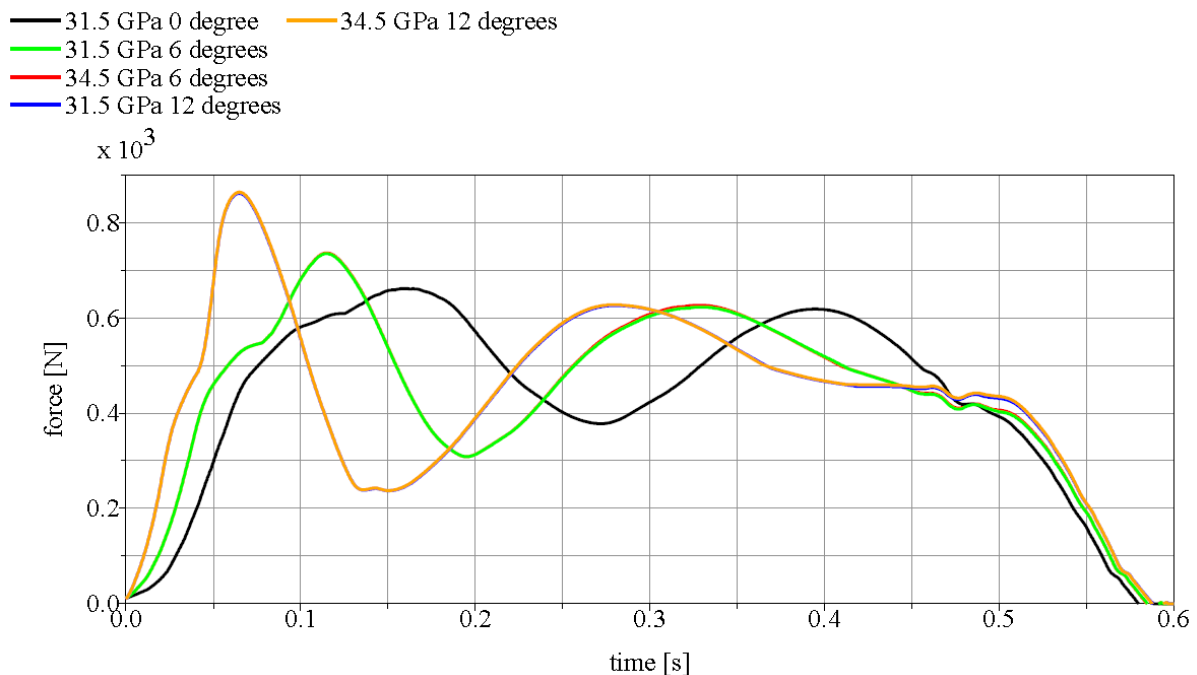


Figure 6.9: The simulated vertical GRFs acting on the prosthetic foot for different stiffness values of the prosthetic foot sole and different ground inclinations

The torques at the ankle are displayed in Figure 6.10. It is clear that the positive moment values are larger and occupy the major part of stance phase time compared with the negative values. This results from more forces acting on the forefoot relative to the heel. From this it is estimated that during walking upward on inclined surfaces the heel contacts the ground for a very short time and increasing the inclination reduces this time. In Figure 6.10 the negative moment lasts for 0.05 s, 0.11 s, and 0.185 s for the 12, 6, and 0 degrees inclined surfaces, respectively, which represent 8%, 18%, and 30% of the stand phase period. The maximum torque values acting on the ankle also increase with inclination. As in the GRF case the differences due to changing the stiffness values are very small.

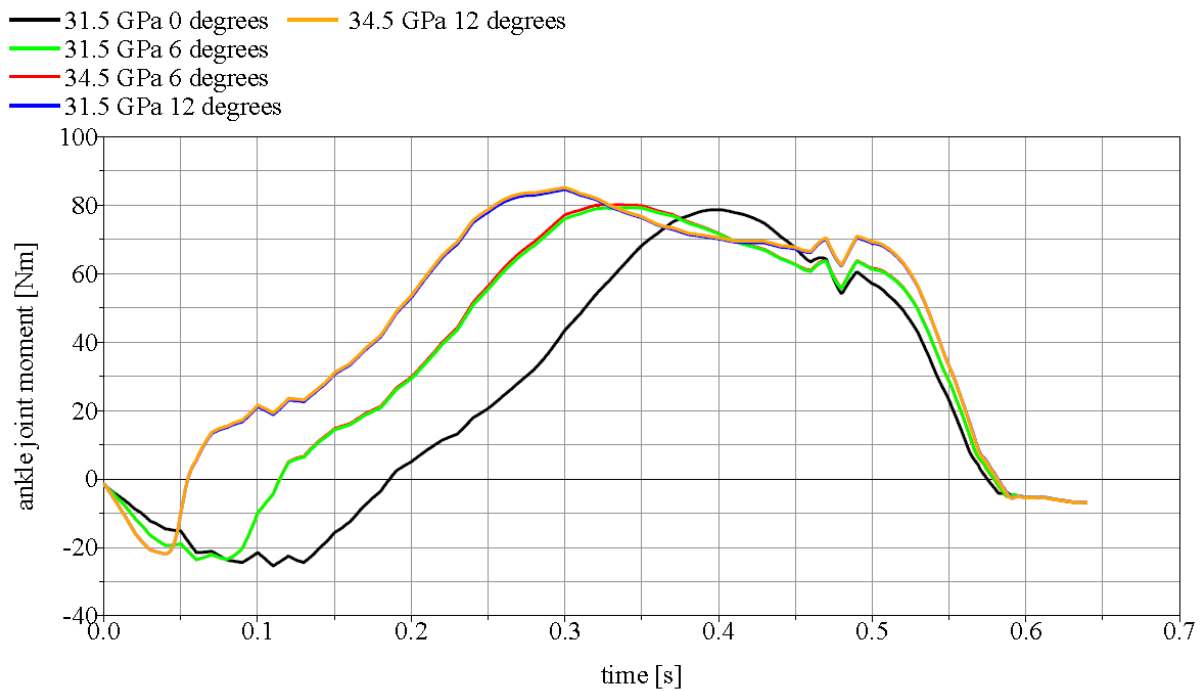


Figure 6.10: The simulated moment at the ankle of the prosthetic foot for different stiffness values of the prosthetic foot sole and different inclinations

Changing the stiffness leads to no significant changes in the hip joint rotations for the same surface inclination as it is shown in Figure 6.11 but by increasing the inclination the total rotation of the hip joint of the prosthetic side is decreased. A 9% reduction of the total range of rotation is calculated for an increase in inclination from 0 to 12 degrees.



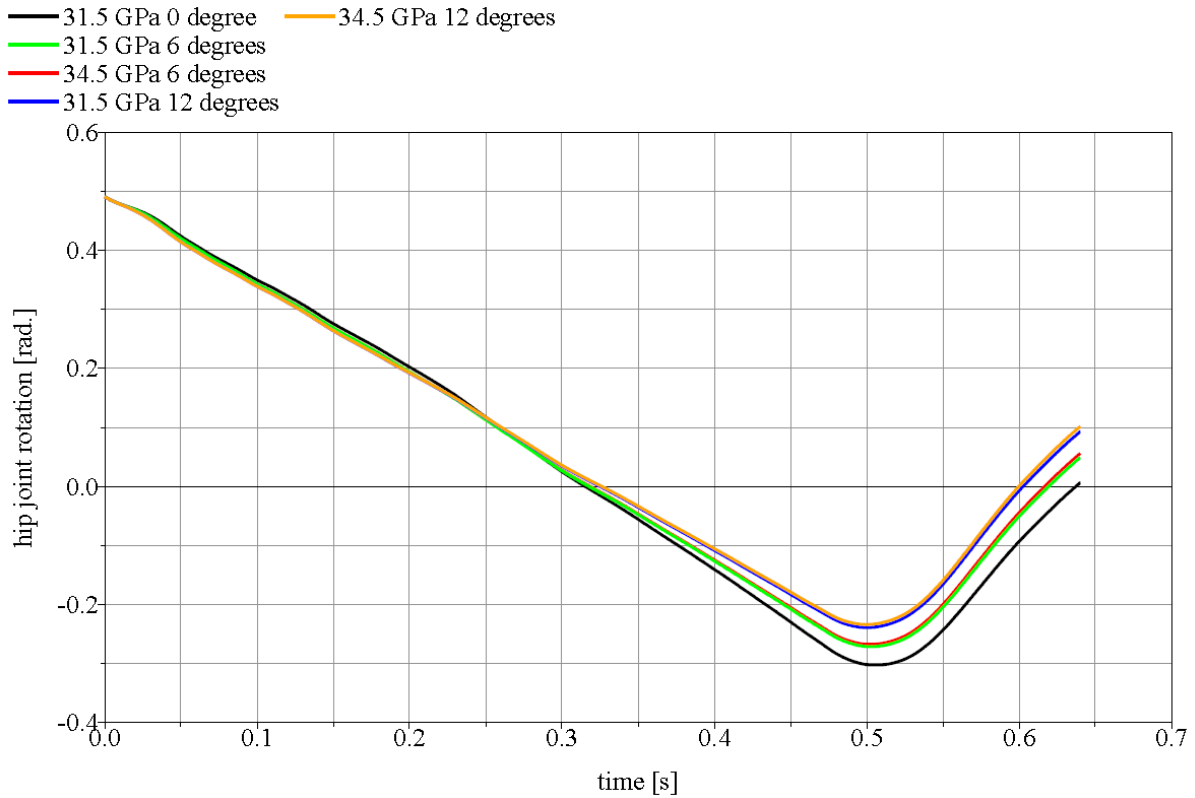


Figure 6.11: The simulated rotations of the thigh at the hip joint for the different stiffness values of the prosthetic foot sole and different ground inclinations

Observing the BCoM motions shown in Figure 6.12 indicates that changing the stiffness of the foot sole influences the vertical BCoM motion. For the 12 degrees inclined surface, reducing the stiffness 10% has reduced the BCoM vertical position 4 mm (9% of the total vertical displacement), and at 6 degrees inclined surface the same stiffness reduction leads to a 3.4 mm reduction (8% of the total vertical displacement). Another very important note is that walking upward on inclined surfaces without applying any extra forces from the sound leg will lead to a dramatic reduction in the total horizontal BCoM motion. The BCoM horizontal motion is 0.72 m for the 12 degrees inclined surface and 0.81 m for the 6 degrees inclined surfaces, which are respectively 80% and 90% of the 0.90 m horizontal motion of BCoM on level surface.

Considering the horizontal motion of the BCoM at the same surface inclinations, the stiffer foot has a 4 mm shorter horizontal displacement, which is a very small difference (less than 1% of the whole motion) but can indicate a tendency that a softer sole increases the foot deformation (roll-over shape), which may improve the gait if this deformation is large enough.

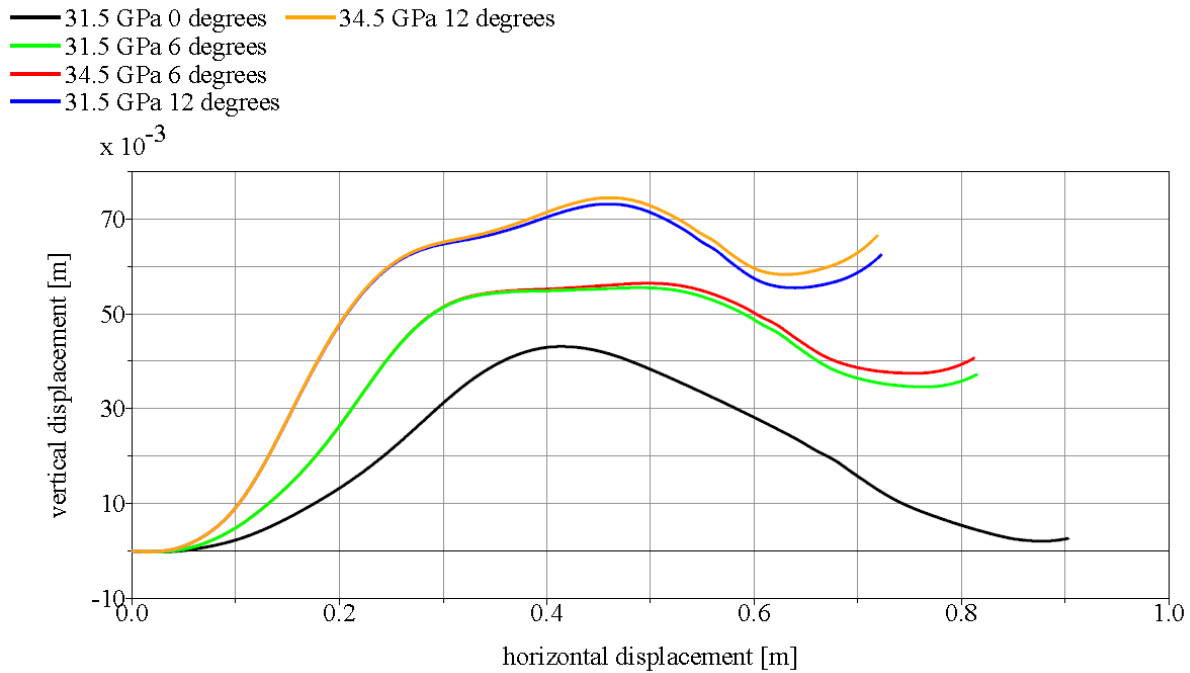


Figure 6.12: The simulated BCoM motion for the different stiffness values of the prosthetic foot sole and different ground inclinations

### 6.2.2 The effect of changing the inclination angle of the ankle joint

In this section the effect of the ankle joint inclination on inclined surfaces was studied. A 12 degrees inclined surface is considered here and the foot sole with 31.5 GPa stiffness. Since the model is to walk uphill on the 12 degrees inclined surface four positive inclination angles for the ankle joint are selected and used in the simulations (0, 3, 6, and 9 degrees). The models are simulated up to 0.5 s.

Figure 6.13 shows the vertical GRF acting on the body of the amputee at the prosthetic side. Increasing the inclination angles of the ankle has reduced the GRF acting on the body but after reaching the 6 degrees inclination there is no more reduction in the GRF value such that the 9 degrees and the 6 degrees inclinations in the ankle joint have the same first peak value of 576 N. This indicates that there are some limits for the reduction in the forces due to changing the ankle angle, and any extra rotation will not reduce the force any more. The reduction in the vertical GRF was 33% of the maximum value. This shows that the small changes in the inclination angle of the ankle joint have caused large changes in the vertical GRF. Also the second peak value of the vertical GRF is reduced through these changes from 627 N at 0 degrees ankle inclination to 551 N at 9 degrees ankle inclination (-12%).

According to these results, it is estimated that making the ankle joint adaptive will reduce the forces acting on the body and improves the comfort of the amputees.

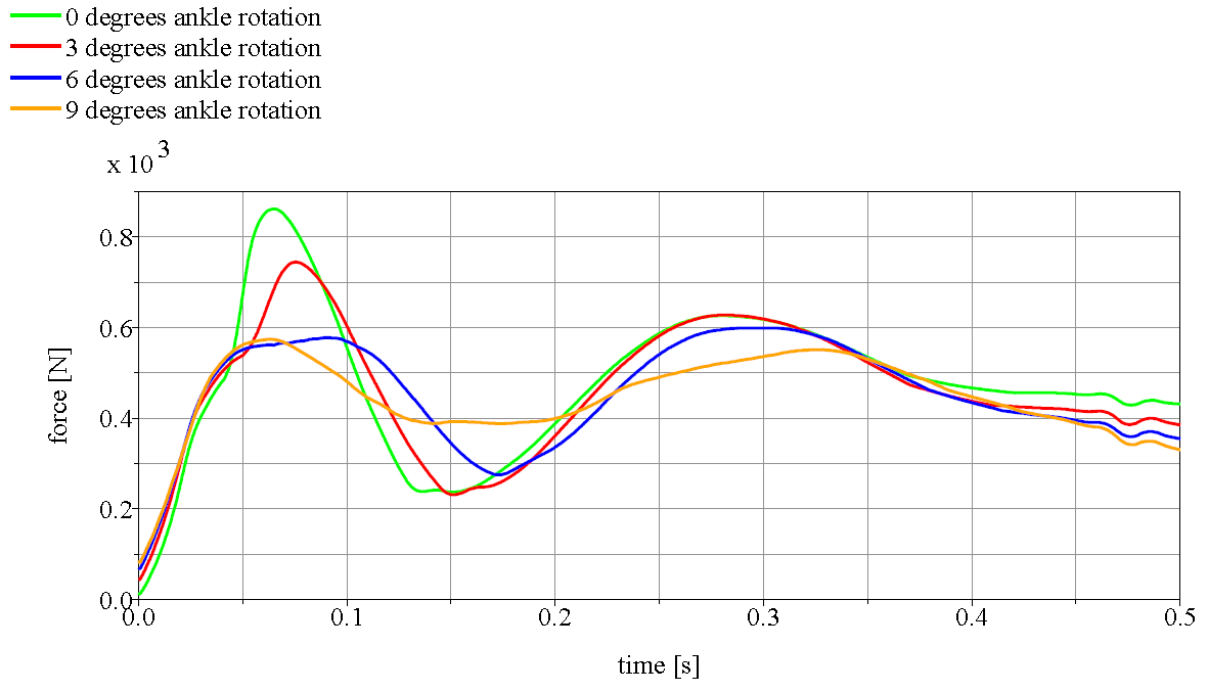


Figure 6.13: The simulated vertical GRFs acting on the prosthetic foot for four different ankle joint inclinations

The most important difference between the curves of the torques of the ankle joint displayed in Figure 6.14 is the time when the moments are zero. For the 0 degree inclination in ankle joint the model simulation and the curve in the figure show that the heel contact with the ground is for a very short time and that the amputee depends on the fore foot in its motion but increasing the angle has increased this contact time for the heel of the foot and reduced the dependency on the forefoot.

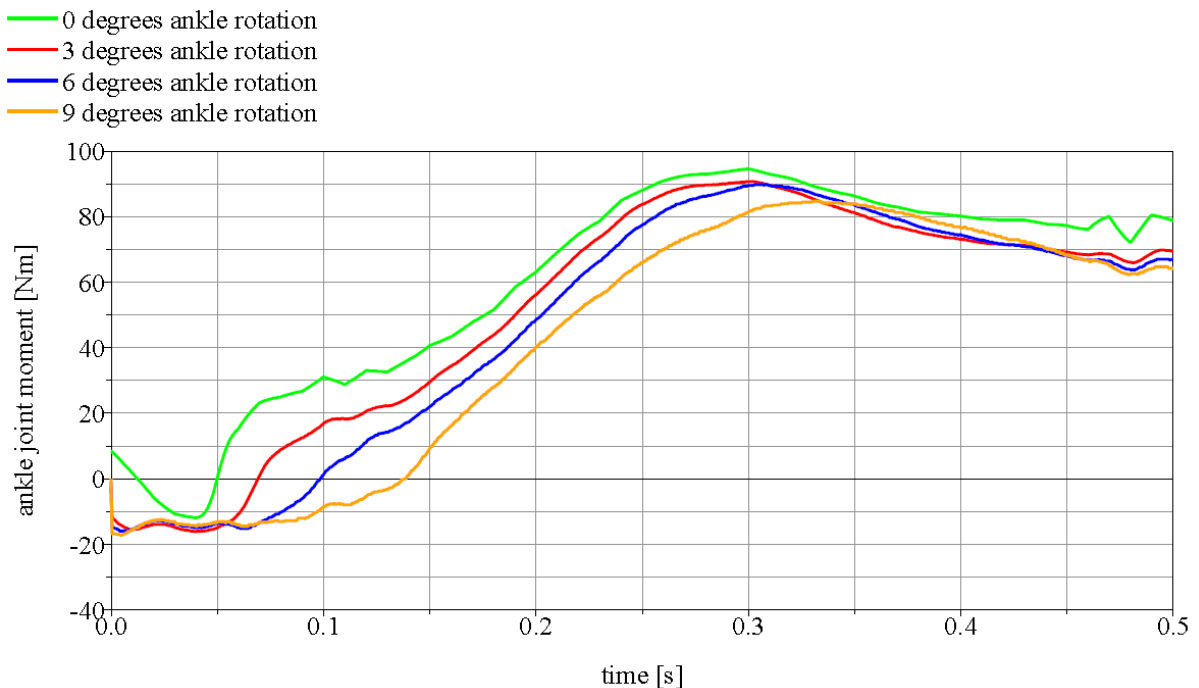


Figure 6.14: The simulated moment at the ankle joint of the prosthetic foot for four different ankle joint inclinations

The hip joint rotation shown in Figure 6.15 changes with the angle such that increasing the angle rotation allows the hip to rotate more. The total increase in the hip rotation was 21% for 9 degrees inclination. It is expected that this will increase the step size of the amputee without the need to exert any extra forces.

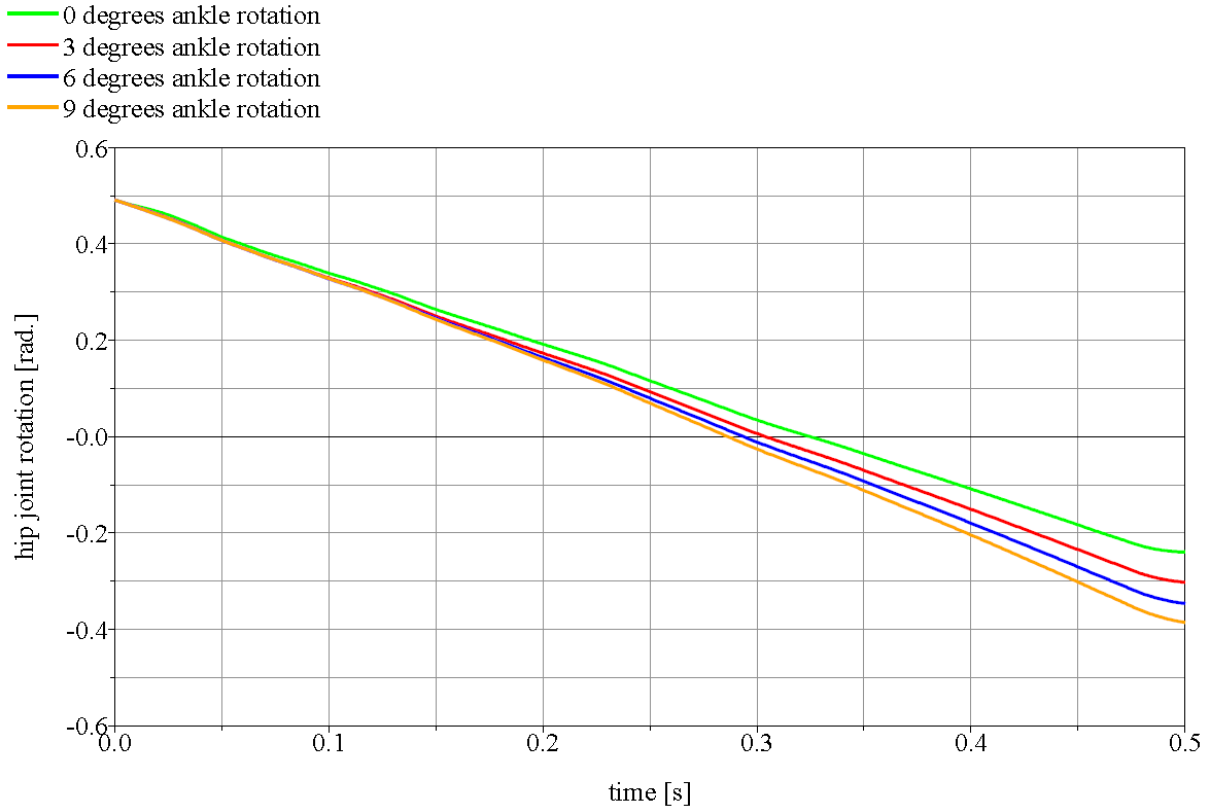


Figure 6.15: The simulated rotation of the thigh at the hip joint for four different ankle joint inclinations

The changes in the BCoM motion are very significant and occur from the beginning of the step along the path of the body. The vertical displacement of the BCoM has changed about 5 mm for every 3 degrees change in the ankle inclination angle. As it is seen in Figure 6.16 the differences in the horizontal displacements of the BCoM at the end of the simulation time (the end of the simulation time of 0.5 s is almost the time when the sound foot start its contact with the ground) are large and indicate an increase in the BCoM horizontal displacement. For the four angles of inclination (0, 3, 6, and 9 degrees) the horizontal displacements were 0.584 m, 0.615 m, 0.639 m, and 0.659 m, respectively, and this corresponds to 5.3%, 9.4%, and 13% increase with respect to the smaller displacement value.

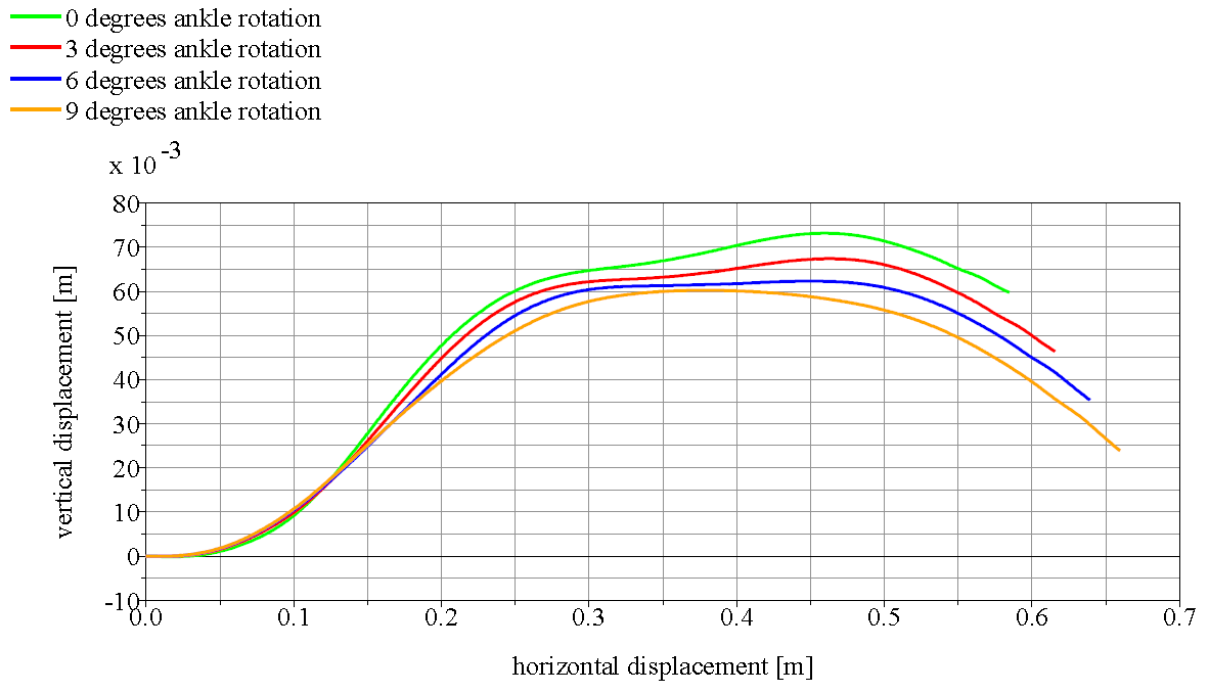


Figure 6.16: The simulated BCoM vertical and horizontal motion for four different ankle joint inclinations

### 6.2.3 The effect of changing the C-spring deformation form

Since the titan ring in the foot C-Walk influences the deformation of the C-spring, and as it was previously mentioned that the ankle-foot roll-over shape changes during walking on inclined surfaces, in this part the effect of changing the titan ring's diameter is studied. The gait is studied for two inclination angles, since the results of changing the diameter on both of them were similar. The results for the 6 degrees inclined surface are displayed here. For the changes in the diameter of the ring four values are used  $-1$  mm,  $0$  mm,  $+1$  mm, and  $+2$  mm.

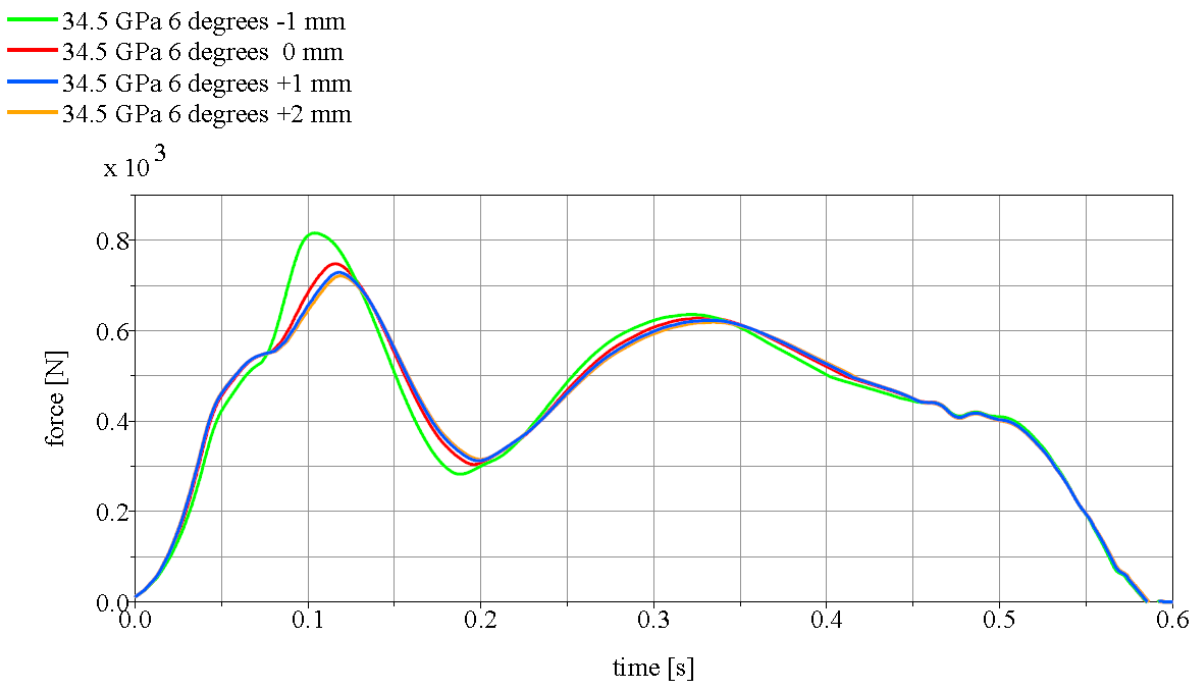


Figure 6.17: The simulated vertical GRFs acting on the prosthetic foot for different ring diameters on a 6 degrees inclined surface

In Figure 6.17 the vertical GRFs acting on the body of the amputee at the prosthetic side shows a significant change at the first peak for the case of  $-1$  mm reduced diameter (this means the C-spring is pre-stressed). The increase in the vertical reaction force is 9%. For the other values the differences are very small and have no significant value.

In Figure 6.18 the ankle moments are displayed. Here also, as in the vertical reaction forces, just for the  $-1$  mm case there was a small difference otherwise the values were identical. This small difference appears since the C-spring is already slightly pre-loaded and by contacting the ground this load increases, which is the reason why the initial absolute values for smaller ring diameter are larger than the other cases. After that the forefoot comes faster in contact with the ground since the ring allows no motion compared with the other cases.

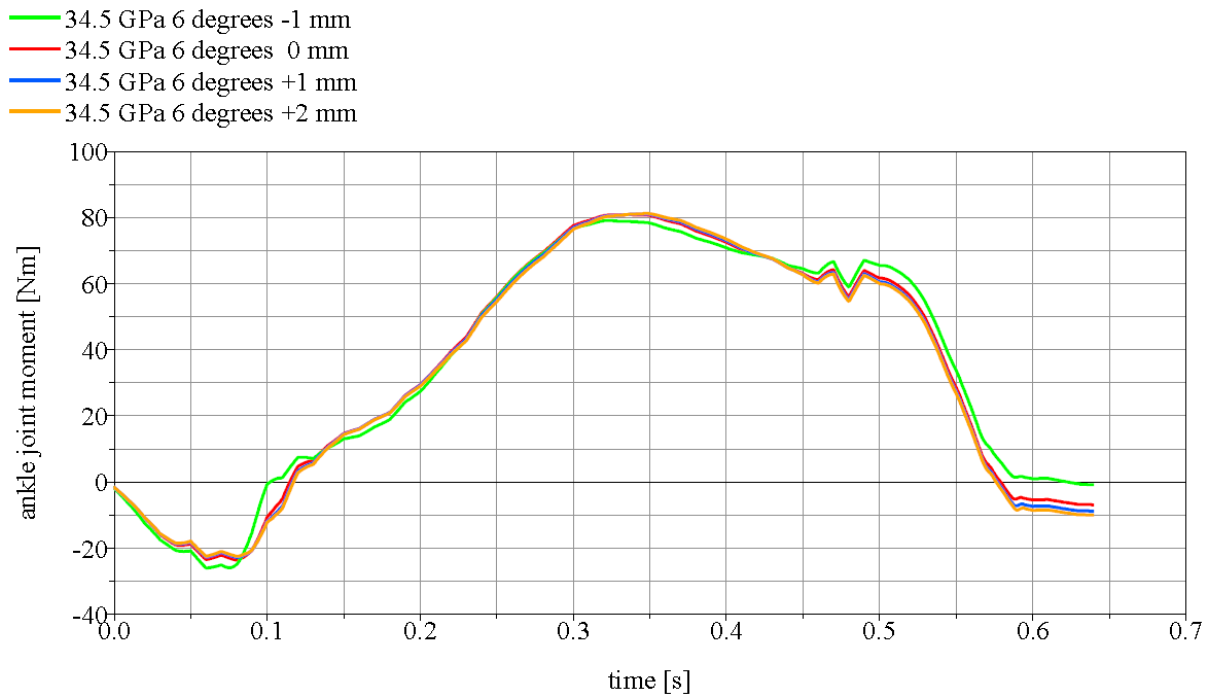


Figure 6.18: The simulated moment at the ankle of the prosthetic foot for different ring diameters on 6 a degrees inclined surface

Changing the stiffness shows no significant changes in the hip joint rotations as it is shown in Figure 6.19.

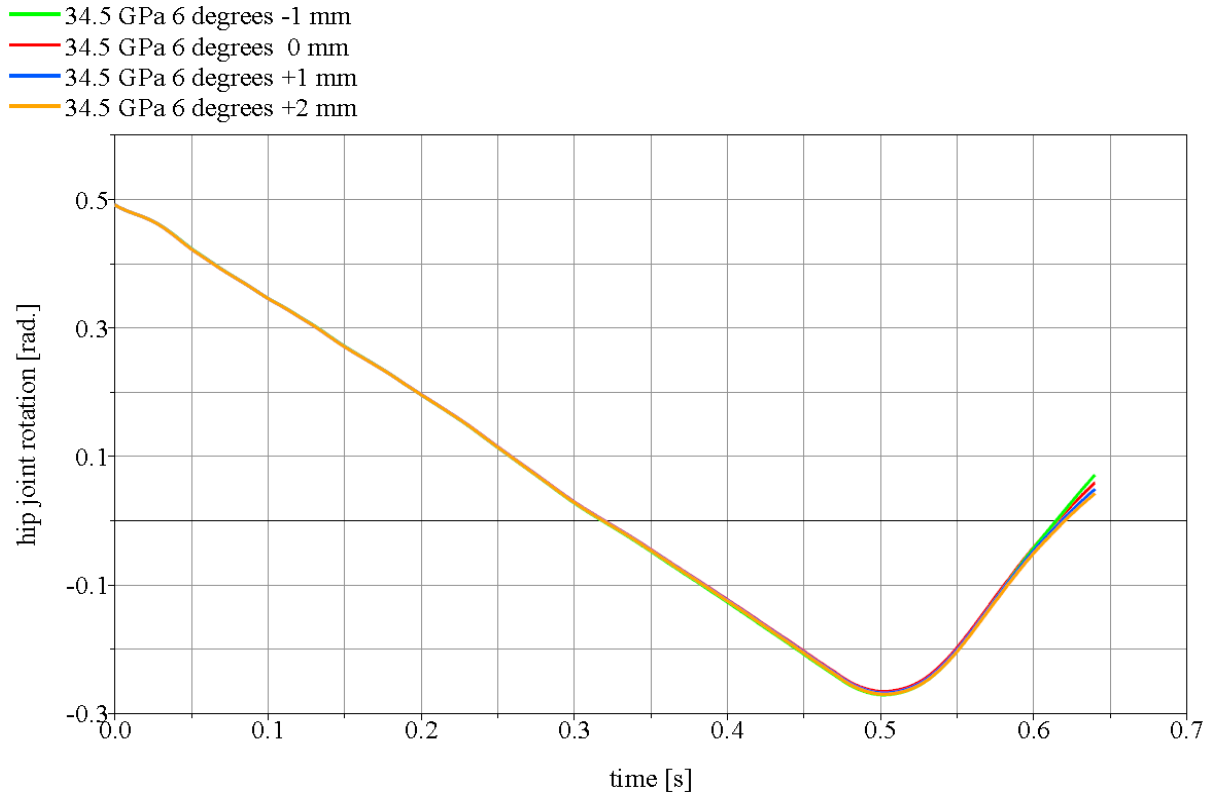


Figure 6.19: The simulated rotations of the thigh at the hip joint for the different ring diameters on a 6 degrees inclined surface

Contrary to the vertical GRFs, reducing the ring diameter has not changed the BCoM significantly compared with the normal position, but increasing it has reduced the BCoM vertical position at the end of the stand phase by 3 mm and 5 mm for the +1 mm and +2 mm diameter increase (see Figure 6.20). These changes are just 5% and 11% of the total vertical displacement and much less than the changes due to changing the stiffness.

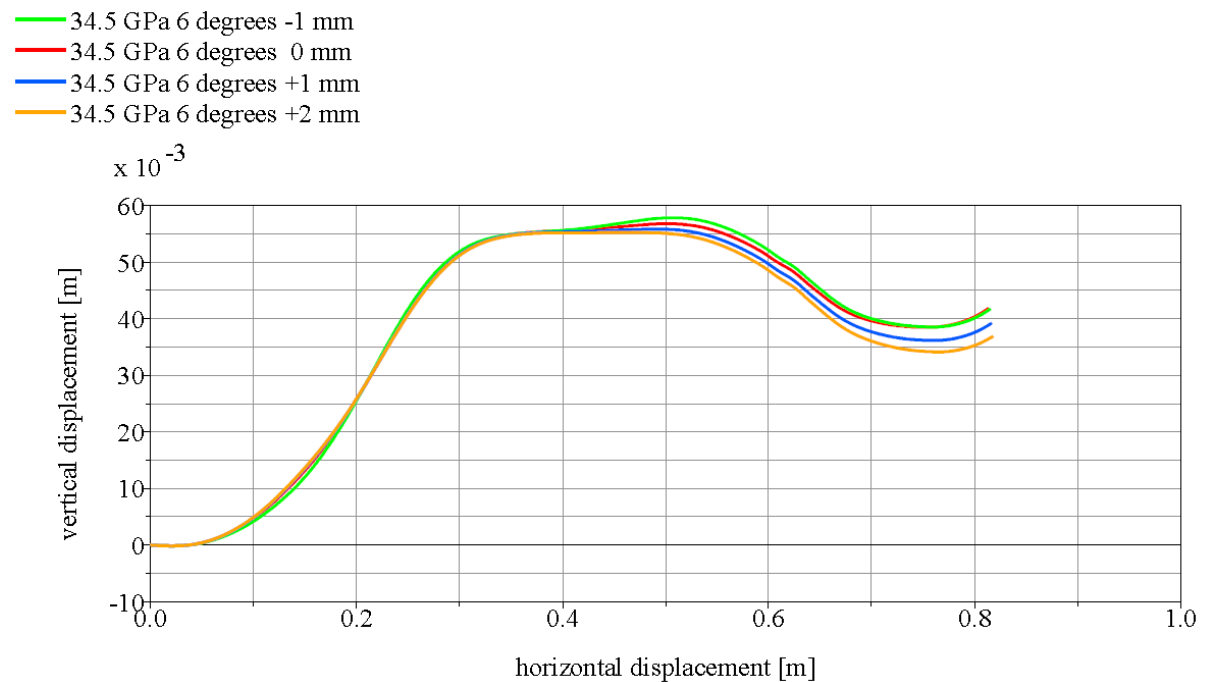


Figure 6.20: The simulated BCoM motion for different ring diameters on a 6 degrees inclined surface

Since the changes in the titan ring diameter have small effect on the gait parameters it will not be further used in evaluating the changes in the other gait conditions.

### 6.3 Walking at Different Velocities

The data used in the simulation for this part are from the same female amputee using the C-Walk foot. Two walking speeds (1.35 m/s and 1.61 m/s) are studied here. The goal of this study is to improve the BCoM motion at the higher speed (1.61 m/s) to match that of the body at the normal speed (1.35 m/s). The reason for this change is that walking faster increases the reaction forces acting on the body which results in a larger deformation of the prosthetic foot compared with the deformations while walking at the normal speed.

According to the results of the previous sections two foot properties offer themselves as a method to change the BCoM motion. Here the required change in the adaptive property is to be determined, and their effects on the other gait cycle parameters are to be studied.

The increase in the walking speed is 19%, and this has caused an increase in the BCoM vertical displacement of 8 mm. To reduce this extra deformation, different values for foot stiffness and ankle joint inclination angle are tried. The results show that an inclination angle of  $-3$  degrees or a change in the stiffness of the sole of 20% is necessary to reduce the 8 mm extra displacement in the system centre of mass. Figure 6.21 shows the BCoM displacement for four cases: The normal gait, the fast speed gait, the fast speed gait with modified ankle inclination, and the fast speed gait with increased sole stiffness.

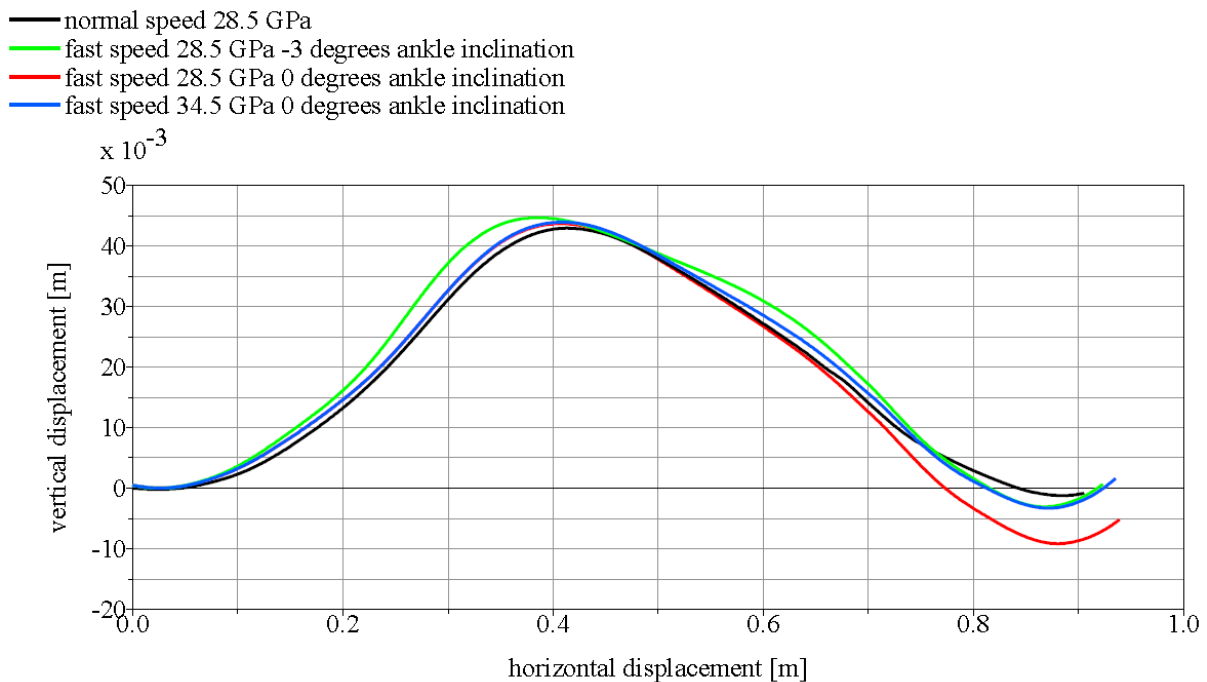


Figure 6.21: The simulated BCoM motion for the two walking speeds

Figure 6.22 represents the GRFs acting on the body before and after the changes in the foot properties. The GRF for the fast walking speed is higher than for the normal speed. The change in the stiffness has no effect on this force but the change in the inclination angle of the ankle has increased this force by 11% from 700 N to 772 N.



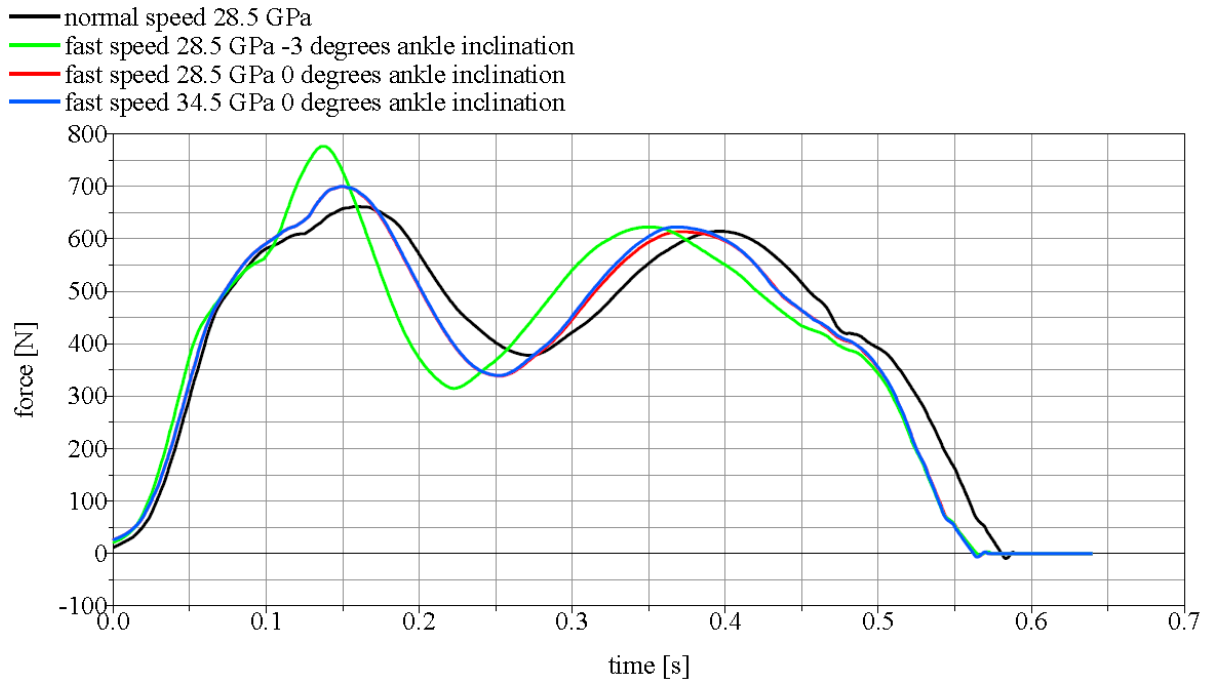


Figure 6.22: The simulated vertical GRFs acting on the prosthetic foot for two walking speeds

Changing the stiffness has changed the moment at the ankle joint very slightly but changing the inclination forced the foot to roll over the ground faster and reach the zero moment value at 0.14 s instead of 0.19 s as in the normal and fast speed without modification. The maximum torque values are similar for all cases with very small differences as it is shown in Figure 6.23.

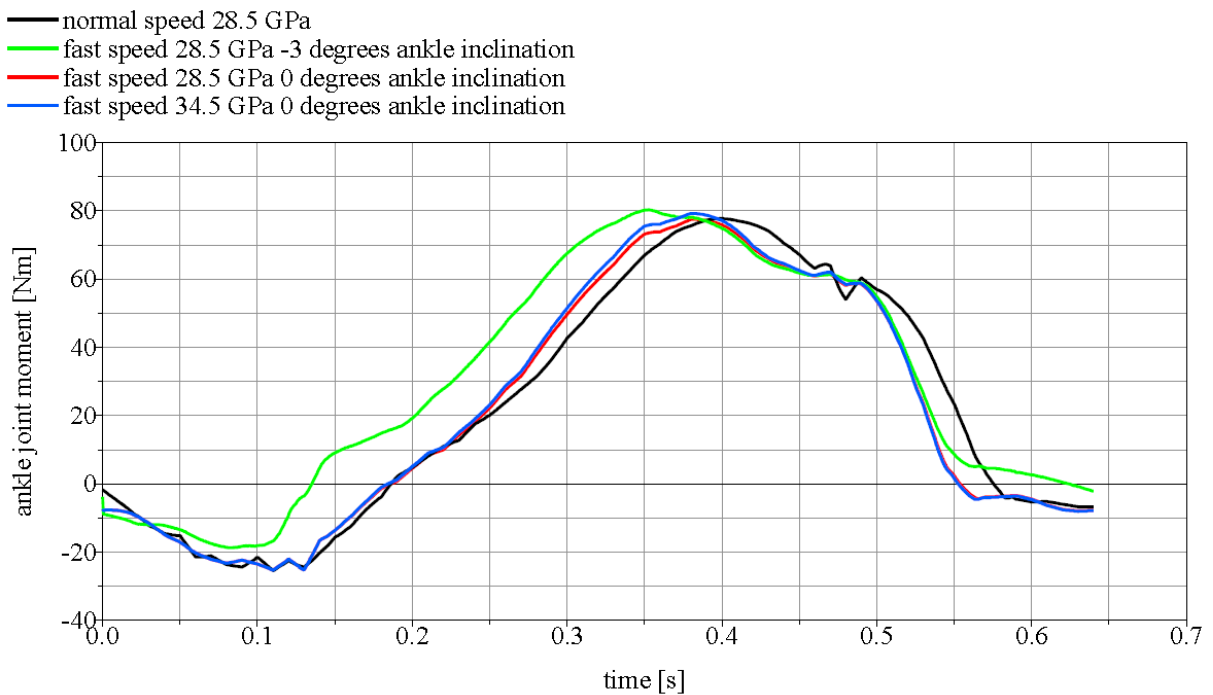


Figure 6.23: The simulated moment at the ankle of the prosthetic foot for two different walking speeds

Changing the stiffness value shows no significant changes in the hip joint rotations but changing the ankle joint inclination has shown a small change at the end of the stance period. This change was 6% of the total rotation. Since this change occurs as the prosthetic foot is leaving the ground (see Figure 6.24) it can be corrected with the rotation of the hip joint of the amputee.

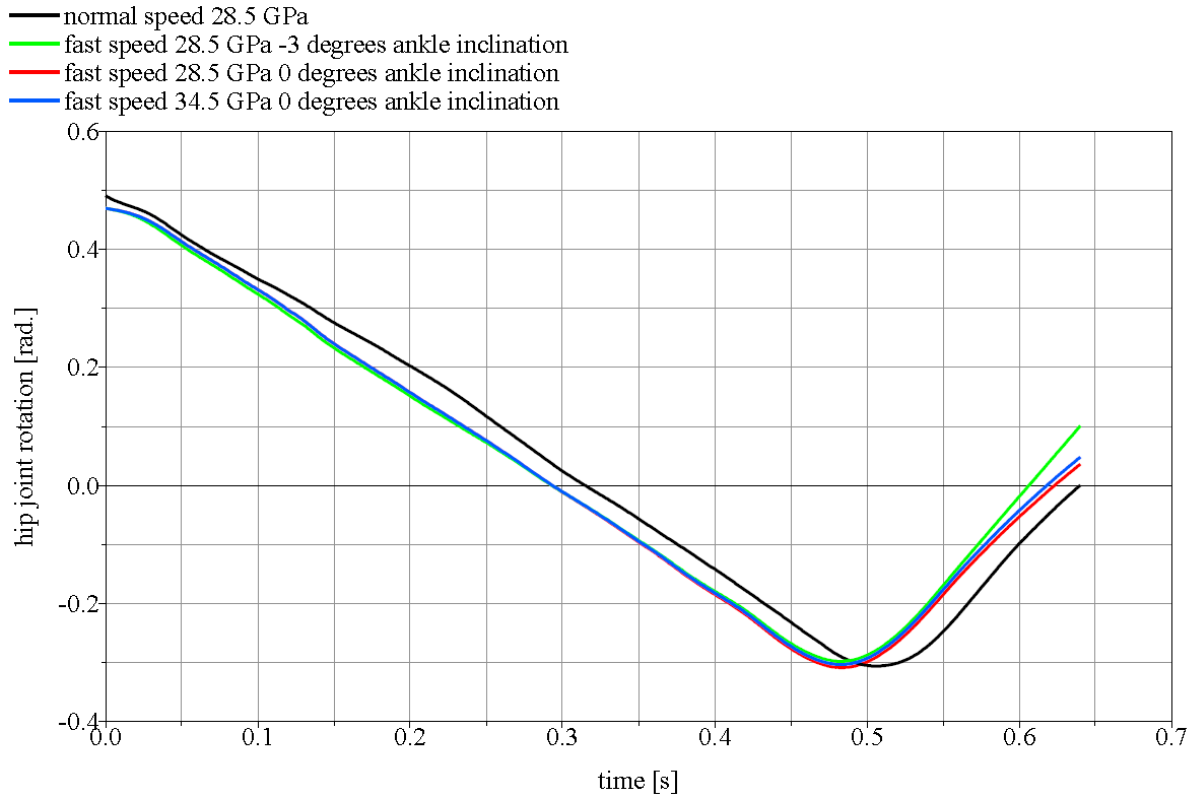


Figure 6.24: The simulated rotations of the thigh at the hip joint for the two walking speeds

## 7 Design of a Foot Sole with Changeable Stiffness

As it is shown in the previous section changing the stiffness of the foot sole has changed the motion of the BCoM and indicated an improvement in the gait. The purpose of this part of the work is to design a beam element with changeable stiffness to be used in an adaptive prosthetic foot's sole. The change in stiffness should be more than  $\pm 10\%$ . The design should take in consideration a lightweight system. Also a simple compact system with a minimum number of movable parts and minimum maintenance is a priority.

As a part of a project in the institute System Reliability and Machines Acoustic (SzM) three concepts were developed in the past [Carli 2006] to change the stiffness of a foot sole. One concept used the possibility of adjusting the static response of a plantar spring (here representing the foot sole) through piezoceramic patches. The concept was very compact and has led to very small changes in the form and weight of the foot sole but the changes in the stiffness were very much less than the  $\pm 10\%$  required. This shows that changing the stiffness using piezoceramic active layers is not an appropriate solution for systems that are already stiff unless new piezoceramic materials are developed that can cause higher changes in the stiffness and bear large deflections. The second concept utilized the effect of changing the cross sectional area of hollow beams in order to increase the moment of inertia of the cross section by increasing the pressure inside the hollow beams. The experimental results show changes in stiffness in order of 4%, which was better than the piezoceramic model but still far from the desired value of  $\pm 10\%$ . The third concept was based on controlling the deformation of two parallel plates by filling the space between the two plates with hydraulic fluid and increasing the stiffness by increasing the fluid pressure, which causes limitations on the inward displacement of the upper plate and respectively increases the system stiffness. This concept achieves a change of 12% in the numerical model but the prototype's results show much lower changes in the stiffness. For more information see [Carli 2006].

Since the models are designed to be used as replacements for human limbs (where the available external energy sources are limited) attention is given to model a lightweight system with minimum energy consumption. A lightweight design is very important since loading the body with extra masses leads to an increase in the energy expenditure. This increase in the energy expenditure depends on the position of the additional weights. An additional weight of 20 kg on the trunk of a healthy male did not show a significant increase in energy consumption. On the other hand, an additional weight of just 2 kg on each foot has increased the oxygen intake by about 30% [Waters 1992]. This could be explained by the fact that the trunk acceleration/deceleration is much less than that of the two legs. Accordingly, greater effort is required to move with loads located at the end of the lower extremities, and reducing the weight of the artificial limbs is of clinical significance.

Attention is also given to design a system that could be used with the different commercially available foot prostheses without the need to make large changes in the size and shape of the original models.

In order to verify the validity of these models, it is very important to try them on amputees, since such systems are very much so depending on the user's needs and limitations, and a mathematical evaluation will stay just a step before the real subjective evaluations are done by the users.

According to the previously mentioned goals and according to the needs shown, it is attended in this work to design a new model for the human foot sole, which could change its load-deformation form in order to improve the whole motion of the body. Two concepts are developed and studied theoretically, then two samples are manufactured and proved experimentally. The first concept utilizes the ability of changing the stiffness of beams through

changing their active cross sectional area. It consists of a hollow rectangular beam, and a perforated rectangular beam that slides through the first one. The second model utilizes the ability of increasing the stiffness of a system by increasing the effective load bearing elements in it gradually, and it consists of two beams connected together by screws.

## 7.1 Analytical Models of the Two Concepts

The suggested models are studied here analytically using the strength of materials equation without numerical simulations, since the analytical modelling can give a good approximation for the mechanical behaviour for the two suggested models taking in consideration the assumptions related to the models.

### 7.1.1 Sliding perforated plate

The stiffness of beams is a function of many parameters and one of them is their cross sectional area. In the first model the cross sectional area is to be changed in order to increase or decrease the stiffness of the effective parts of the beam.

This model consists of two beams; one is a hollow rectangular beam. This beam is slotted at many places with constant distance between the slots at one of its surfaces in order to reduce the stiffness of the beam and develop regions with a low moment of inertia. The second beam is also rectangular and matches the hollow area of the first beam. The surface of this beam is perforated in a manner that develops a number of cross sections with different areas and accordingly different moments of inertia (see Figure 7.1).

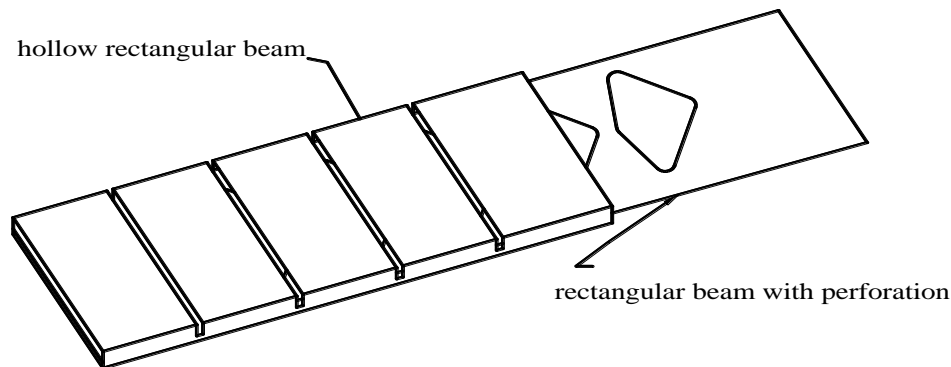


Figure 7.1: The first model consisting of two beams one sliding into the other

The idea in this model is to draw the perforated beam through the hollow beam, and since the hollow beam has slotted regions with low moment of inertia it is expected that these regions will change their moment of inertia and accordingly their stiffness as a function of the change in the area. Note that the other parts of the hollow beam are stiffer and assumed to have a smaller participation to the whole deflection of the beams.

To study the results of such changes in the moment of inertia, the system is divided into two sections. The first section represents the slotted region. A cross section of this part is shown in Figure 7.2, and a top view of the perforated beam is shown in Figure 7.1 and in the appendix. This perforation is suggested and used for the calculations since it is simple and achieves the goal of the design, although it could be also further optimized.

The moment of inertia  $I$  for this part is

$$I_y = \frac{bh^3}{12} + \frac{b_1h_1^3}{12}. \quad (7.1)$$

Note that the equivalent stiffness for small deflections is directly proportional to the moment of inertia

$$\frac{F}{w} = \frac{3EI_y}{\Delta^3}, \quad (7.2)$$

where  $\Delta$  is the slot length.

The maximum value of the moment of inertia is reached when  $b=b_1$ ,

$$I_y = \frac{b(h^3 + h_1^3)}{12}. \quad (7.3)$$

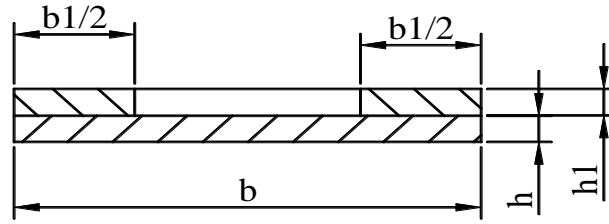


Figure 7.2: A cross section of the beam at the slotted region

Assuming a design with  $b_1$  equal 25% of  $b$  then the minimum value of  $I$  is

$$I_y = \frac{b\left(h^3 + \frac{h_1^3}{4}\right)}{12}. \quad (7.4)$$

The total change in the inertia in this section of the beam is a function of  $h$  and  $h_1$ . In the case  $h=h_1$  a change in  $I$  within a range of up to 37.5% of the maximum value is possible. Note: This change is just for the region  $\Delta$  and not for the whole structure.

For the second region where the cross section consists of the hollow rectangular beam and a part of the perforated beam, the moment of inertia is:

$$I_y = \frac{BH^3 - bh_1^3}{12} + \frac{b_2h_1^3}{12}. \quad (7.5)$$

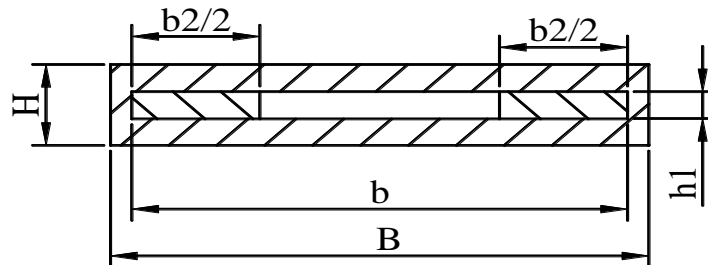


Figure 7.3: A cross section in the beam at the stiff region

Just in order to have a rough idea about the participation of the internal beam to the total moment of inertia the following simplifications are considered.

The average value of  $b_2$  along  $l_1$  is  $2/3b$ ,  $h=h_1$ ,  $H=3h$ , and  $B=b$  then the equation simplifies to the form

$$I_y = \frac{26bh^3}{12} + \frac{2/3bh^3}{12}. \quad (7.6)$$

The internal beam participates just by 2.6% of the total moment of inertia along D, where D is the distance between the two slots.

Now the total deflection of the beam is to be calculated. Since the beam is to be used as a foot sole, the system represents a beam fixed at one end and free at the other (a simple cantilever beam). Here a force  $F$  is assumed to be acting at the end of the beam in upward direction, and from strength of materials equations, the second derivative of the deflection is described through the equation

$$w''(x) = \frac{-M_y(x)}{EI_y(x)}. \quad (7.7)$$

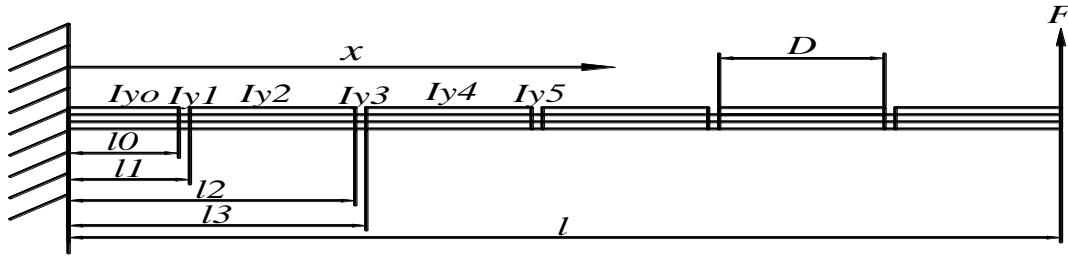


Figure 7.4: The model as a simple cantilever beam with the force acting upward

Then in this case  $M_y(x) = F(l-x)$  and by integration

$$w'(x) = \int_0^x \frac{-F \cdot (l-x)}{EI_y(x)} dx, \quad (7.8)$$

$$w'(x) = \int_0^{l_0} \frac{-F \cdot (l-x)}{EI_{y_0}} dx + \int_{l_0}^{l_1} \frac{-F \cdot (l-x)}{EI_{y_1}} dx + \int_{l_1}^{l_2} \frac{-F \cdot (l-x)}{EI_{y_2}} dx + \dots + \int_{l_N}^x \frac{-F \cdot (l-x)}{EI_y(x)} dx, \quad (7.9)$$

$$w'(x) = \frac{-F}{E} \left( \left[ \frac{lx - x^2/2}{I_{y_0}} \right]_0^{l_0} + \left[ \frac{lx - x^2/2}{I_{y_1}} \right]_{l_0}^{l_1} + \left[ \frac{lx - x^2/2}{I_{y_2}} \right]_{l_1}^{l_2} + \dots + \left[ \frac{lx - x^2/2}{I_{y_x}} \right]_{l_N}^x + C_1 \right),$$

where  $N$  is the number of full segments  $-1$  and  $C_1=0$  since  $w'(0)=0$ .

$$w'(x) = \frac{-F}{E} \left[ \frac{l_0 - l_0^2/2}{I_{y_0}} + \sum_{n=1}^N \left( \frac{l_n(2l - l_n) - l_{n-1}(2l - l_{n-1})}{2I_{y_n}} \right) + \frac{lx - x^2/2}{I_{y_x}} - \frac{l_N - l_N^2/2}{I_{y_x}} \right], \quad (7.10)$$

$$w(x) = \frac{-F}{E} \left[ \left( \frac{l_0 - l_0^2/2}{I_{y_0}} + \sum_{n=1}^N \left( \frac{l_n(2l - l_n) - l_{n-1}(2l - l_{n-1})}{2I_{y_n}} \right) - \frac{l_N - l_N^2/2}{I_{y_{N+1}}} \right) x + \frac{lx^2}{2I_{y_{N+1}}} - \frac{x^3}{6I_{y_{N+1}}} - C_2 \right], \quad (7.11)$$

since  $w(0)=0$  then  $C_2=0$ .

Through these equations it is possible to calculate the relation between the force and the deformation of the beam at different positions of the sliding beam.

### 7.1.2 Two screwed beams

For this part two variants are suggested:

#### a. Simply screwed beams

This system consists of two beams as shown in Figure 7.5. They are connected together using screws. The idea of this model is that two beams screwed together with zero clearance between them have a different stiffness compared with two beams having a clearance between them, such that controlling the clearance between the two beams leads to different force deflection behaviour.

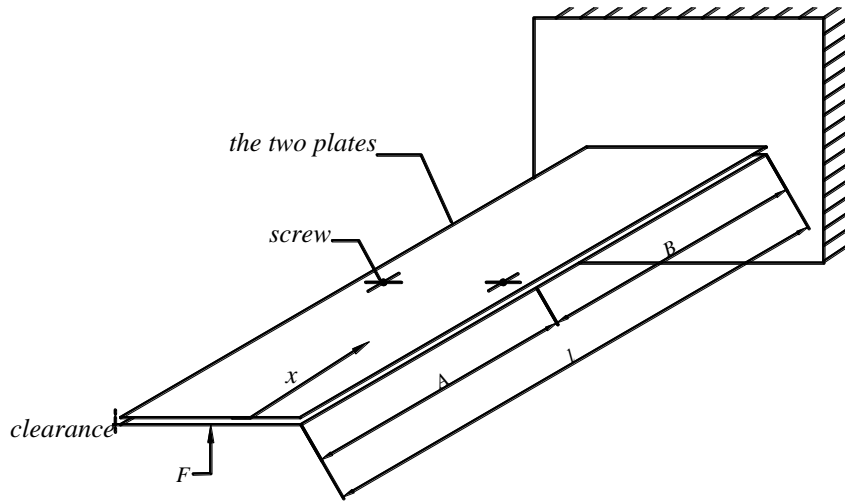


Figure 7.5: The model consisting of two beams connected together with screws

Note that the force will be acting on the lower beam and then transmitted to the upper one. Since the lower beam represents the main part of the foot sole and will be fixed to the ankle joint, it is considered as a beam fixed at one end and free at the other like a simple cantilever beam. The second beam will be used for increasing the stiffness of the system. Since the forces acting on this beam come from the contact points with the first beam then it is considered as a simply supported beam with force acting at some point in the middle. To derive the deformation equations of the system it is noted that the deformation of the lower beam and upper beam at the contact points should have the same values, and then the problem here is a statically undetermined structure.

The force acting on the system is  $F$ , and this force has two parts: one supported by the lower beam  $F_1$  and one supported by the upper beam  $F_2$  where  $F = F_1 + F_2$ . The acting force in the middle due to the screws is symbolized with  $F_m$ .

The force  $F$  will act on the lower beam, and as long as the upper beam is not deflected the deformation of the system is similar to that of the lower beam and will follow the equation (7.12), which is for a simple cantilever beam

$$w_1(x) = \frac{Fl^3}{6E_1I_{1y}} \left[ 2 - \frac{3x}{l} + \left( \frac{x}{l} \right)^3 \right]. \quad (7.12)$$

Note: This equation assumes a constant cross sectional area of the beam along its length, and accordingly a constant moment of inertia.

At  $x=A$

$$w_1(A) = \frac{Fl^3}{6E_1I_{1y}} \left[ 2 - \frac{3A}{l} + \left( \frac{A}{l} \right)^3 \right]. \quad (7.13)$$

At  $x=0$

$$w_1(0) = \frac{Fl^3}{3E_1I_{1y}}. \quad (7.14)$$

The deformation of the second beam depends on the clearance between the two plates. As long as the clearance between the two beams is equal or larger than  $\Delta$  (Figure 7.6) then no forces act on the upper beam, and the lower beam takes the whole load and deforms as previously mentioned. The clearance between the two beams is given the symbol  $\delta$ .

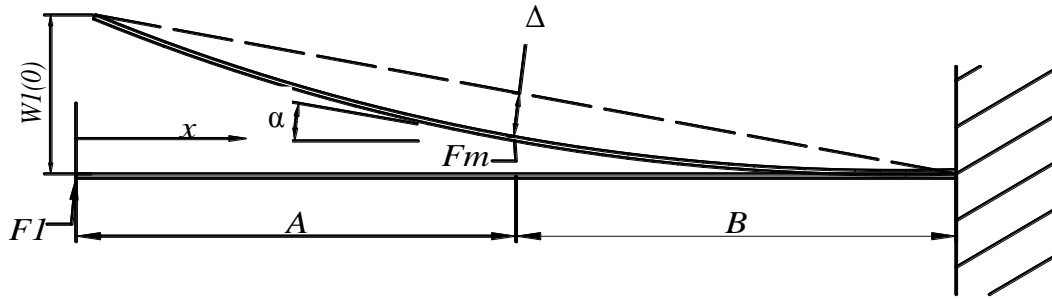


Figure 7.6: The deformation of the first lower beam (deforming as a cantilever beam free at one end)

When the upper beam deflects then the two beams develop together a statically undetermined structure and their deformation will follow the following equations.

For the lower beam two forces are acting on it ( $F_1$  and  $F_m$ ) and its deformation follows,

at  $x=A$

$$w_1(A) = \frac{(F_1 + F_m)B^3}{3E_1I_{1y}} + \frac{F_1AB^3}{2E_1I_{1y}}. \quad (7.15)$$

At  $x=0$

$$w_1(0) = w_1(A) + \frac{F_1A^3}{3E_1I_{1y}} + A\sin(\alpha) \quad (7.16)$$

and

$$\alpha = \frac{F_1AB}{E_1I_{1y}} + \frac{(F_1 + F_m)B^2}{2E_1I_{1y}} \quad (7.17)$$

Since the deflection is small  $\alpha = \sin(\alpha)$  can be used with an error less than 1% for  $\alpha < 14^\circ$ .

The deflection of the lower beam is:

$$w_1(0) = w_1(A) + \frac{F_mAB^2}{2E_1I_{1y}} + \frac{F_1A(A^2/3 + AB + B^2/2)}{E_1I_{1y}}. \quad (7.18)$$



From Figure 7.6

$$\frac{w_1(0)}{l} = \frac{w_1(A) + \Delta}{B} \quad (7.19)$$

$$F_1 = F - F_2 = F - \frac{F_m B}{l} \quad (7.20)$$

And by substituting the values of  $w_1(0)$  and  $w_1(a)$  in (7.19), and replacing  $F_1$  value with (7.20) then

$$\Delta = C_1 F + C_2 F_m, \quad (7.21)$$

where,

$$C_1 = \frac{AB}{E_1 I_{1y} l} \left[ \frac{A^2}{3} + \frac{AB}{2} + \frac{B^2}{6} \right], \quad (7.22)$$

and

$$C_2 = \left[ \frac{AB^3}{6E_1 I_{1y} l} - \frac{C_1 B}{l} \right]. \quad (7.23)$$

For the second upper beam, which represents a simply supported beam (see Figure 7.7), the deformation will follow the equation

$$w_2(x) = \frac{F_m AB^2}{6E_2 I_{2y}} \left[ \left( 1 + \frac{l}{B} \right) \frac{x^3}{l} - \frac{x^3}{ABl} \right] \quad \text{for } 0 \leq x \leq A, \quad (7.24)$$

and at  $x=A$

$$w_2(A) = \frac{F_m AB^2}{6E_2 I_{2y}} \left[ \left( 1 + \frac{l}{B} \right) \frac{A}{l} - \frac{A^2}{Bl} \right]. \quad (7.25)$$

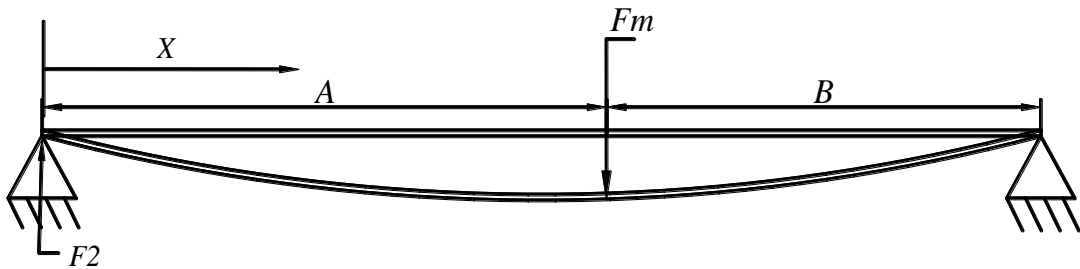


Figure 7.7: A simply supported beam representing the deformation of the upper beam

Then

$$w_2(A) = \frac{F_m A^2 B^2}{3E_2 I_{2y} l} = F_m C_3, \quad (7.26)$$

where

$$C_3 = \frac{A^2 B^2}{3E_2 I_{2y} l}. \quad (7.27)$$

Since the two beams are connected at some point in the middle at  $x=A$ , then the force acting at that point as a function of  $F_2$  will be

$$F_m = \frac{F_2 l}{B}. \quad (7.28)$$

The deflection in the upper beam is depending on the lower beam deflection and the clearance between the two beams and is described by

$$w_2(A) = \Delta - \delta. \quad (7.29)$$

Then from the equations (7.21), (7.26), and (7.29), the force  $F_m$  is found as a function of the total force

$$F_m = (C_1 F - \delta) / (C_3 - C_2). \quad (7.30)$$

The total deflection of the beam is then

$$w_1(0) = w_1(A) + \frac{F_m A B^2}{2E_1 I_{1y}} + \frac{(F - F_m B / l) A (A^2/3 + AB + B^2/2)}{E_1 I_{1y}} \quad \text{if } \delta < \Delta \quad (7.31)$$

$$w(0) = w_1(0) = \frac{Fl^3}{3E_1 I_{1y}} \quad \text{if } \delta > \Delta \quad (7.32)$$

## b. Screwed with preload

In this case a spring element is introduced at the screws in order to press the two plates together reducing their motion. The equations of deflection are the same as in the previous section with modifications for the newly introduced spring element Figure 7.8. One spring at each screw is used but in the equations of deflection they are represented as one spring since the system is symmetric. The deflection in the upper beam depends on the lower beam deflection and the clearance between the two beams. It is described by

$$w_2(A) = F_m C_3 = \Delta - \left( \frac{F_m - F_{\text{Preload}}}{k_s} \right) \quad (7.33)$$

Where  $F_{\text{Preload}}$  is the pre-load acting on the spring element in neutral position (no external loads or deflections) and  $k_s$  is the spring constant.

From the equations (7.21) and (7.33)

$$F_m = \frac{C_1 F + F_{\text{Preload}} / k_s}{C_3 + 1/k_s - C_2}. \quad (7.34)$$

For the deformation two equations apply:

When  $F_m$  is less than  $F_{\text{Preload}}$  then equation (7.31) applies with  $F_m$  as in (7.30)

When  $F_m$  is larger than  $F_{\text{Preload}}$  then equation (7.31) applies with  $F_m$  as in (7.34).

The deflection is a function of many parameters. Two of them are to be studied here; the changes in the preload of the springs and the stiffness of the spring elements.

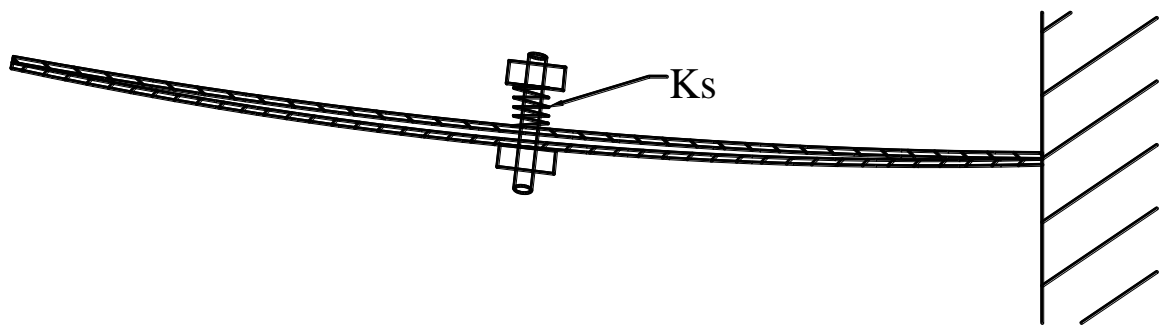


Figure 7.8: The two beams with spring element fixed at the screws

## 7.2 The Fabrication of the Prototype

Lightweight elements are a priority in the design of prostheses. Therefore in this work composite materials are selected to be used, which are also the material of many commercially available artificial limbs. Continuous fibre composites showed to be the most suitable materials because of their light weight, high flexibility and durability. Nevertheless it has a major problem of delamination, or separation of the lamina, since the interlaminar strength is matrix (binder)-dominated [Gibson 1994].

As a result of financial limitations the prototypes are produced with the available standard materials found in the market and are softer than the actual prosthetic foot soles, but satisfy the conditions to evaluate the validity of the two models as beam elements with changeable stiffness. For producing the first model consisting of a hollow beam and an internal perforated beam sliding through it, three plates of carbon fibre composites are brought together, two of them are 1 mm thick and the third is 2 mm thick. The two 1 mm thick plates have a mirror finish surface on one side and a rough surface on the other. The 2 mm plate has a mirror finish on both sides. The three beams are brought together with the mirror finish surfaces facing each other and the rough surfaces facing out (this sequence is followed to reduce the friction between the sliding beam and the hollow beam during the use and activation). Then a tissue (reinforcing fibres) with matrix (binder) is wound all over the assembly up to one millimetre from each side. The resulted element is then cut at the ends and the internal beam is pulled out.

The internal beam is perforated according the dimensions shown in appendix A resulting in a beam with a different cross sectional area along its longitudinal axis. The external beam is grooved at one of its sides with constant distance between the slots, to develop two regions with high and low stiffness values. The external dimensions of the beams were selected to suit the size of a prosthetic foot; they were found to be 180 mm x 55 mm.

Some notes on the fabrication process:

- The three plates are pressed together with a load to insure the minimum clearance between them.
- Since it is difficult to bend the carbon fibres at small corners, a glass fibre tissue is used for winding, and there were 8 layers for each side building up a 1 mm thick layer of glass fibre plate glued firmly to the 1 mm carbon fibre plate, and the sides have an acute angle insuring a minimum clearance.

For producing the second model consisting of two beams connected together with screws, two plates are simply cut with dimensions suiting the human foot. One of the plates is cut with the dimension 180 mm x 60 mm x 1.8 mm and the other 240 mm x 60 mm x 2 mm. The second is longer to be used in fixing the system at the test stand and represents the part to be fixed at the foot ankle in the prosthesis. Also by this model the two plates have mirror finish surfaces

reducing the friction during the use, and are drilled at the middle for the connecting screws. For details see Appendix A.

### **7.3 The Analytical and Experimental Results**

The previously derived equations are used in strength of materials for homogeneous and isotropic material's properties, and since here composite materials are selected for the system the following assumptions are to be considered for laminated beams such that the equations stay valid for this work purpose [Gibson 1994]:

- 1-Plane sections that are initially normal to the longitudinal axis of the beam remain plane and normal during flexure.
- 2-The beam has both geometric and material property symmetry about the neutral surface.
- 3-Each ply is linearly elastic with no shear coupling.
- 4-The plies are perfectly bonded together, so that no slip occurs at ply interfaces.
- 5-The only stress components present are the normal stress along the longitudinal axis and the shear stress parallel to this axis.
- 6-In the previous equations the effective flexure modulus of the beam (which depends on the ply stacking sequence and moduli) is to be used instead of the Young's modulus. In case that the properties do not change through the thickness of the beam, then the flexural modulus is the same as the Young's modulus.

#### ***7.3.1 Results of the sliding perforated plate concept***

By substituting the dimensions of the beam in equation (7.11) and assuming that the modulus of elasticity is constant for the whole system the following results were obtained for the deformation of the beam at the two extreme positions of the internal beam (0 mm and 21 mm) from the edge (the expected highest stiffness and the expected lowest stiffness position).

These deformations are function of:

1. The applied force at the end of the beam,
2. The modulus of elasticity and
3. The position of the internal beam.

Instead of substituting a value for the modulus of elasticity in the equations of deformation, the results of the equations are shown in Figure 7.9 with the displacement as a function of the elasticity modulus.

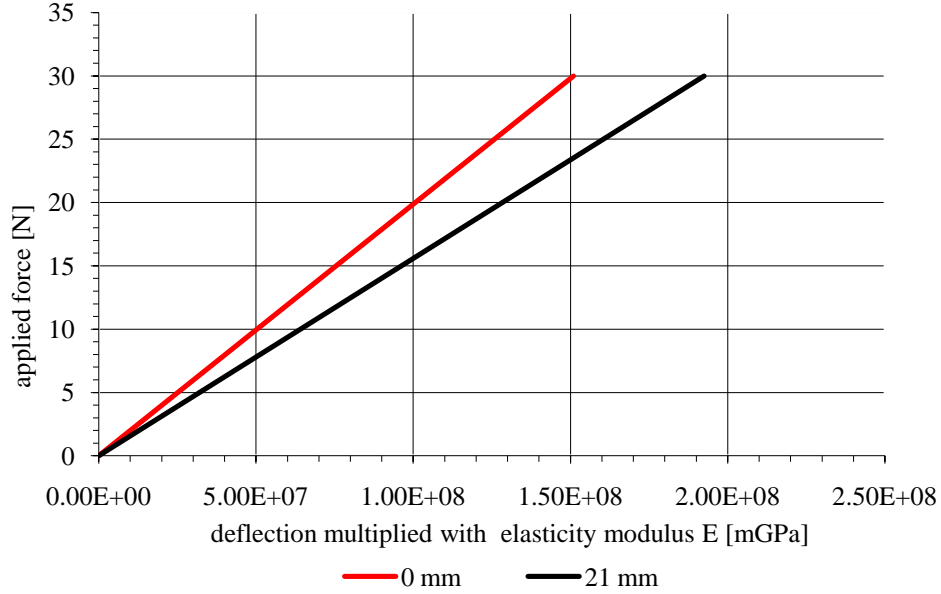


Figure 7.9: The results of the analytical model describing the system with one beam sliding through a hollow beam (0 and 21 mm are the sliding distances)

From Figure 7.9 the change in the stiffness is clear, and analytically it was found to be  $\pm 12\%$  of the average stiffness. This value is larger than the required change of  $\pm 10\%$ . This indicates that we can go further in the design and test the prototype experimentally.

An experimental test is performed on the prototype in order to verify the results from the mathematical model results. The dimensions of this prototype are all shown in the appendix. The beam was fixed as a cantilever beam at one end at a distance 180 mm from the edge. The force was applied at a distance 20 mm from the free edge causing the deflection of the beam. The test was repeated four times. Each time the displacement of the internal plate was changed. Since the beam cross sectional area changes along 21 mm of its length, four positions were selected 0 mm, 7 mm, 14 mm, and 21 mm, such that the position 0 mm should represent theoretically the stiffer position and 21 mm the softer position.

Since the prototype length was longer than the desired 180 mm which represents an average human foot length, the rest of the beam element was used to fix the beam on the testing machine. The results are shown in Figure 7.10. The stiffness of the beam has changed by the changes in the position of the internal perforated beam. These changes could be measured through the changes in the gradient of the lines. The line for 0 mm position has a slope 1.58 N/mm and that for 21 mm position has a slope 1.33 N/mm and this is equivalent to a change of  $\pm 8.6\%$ .

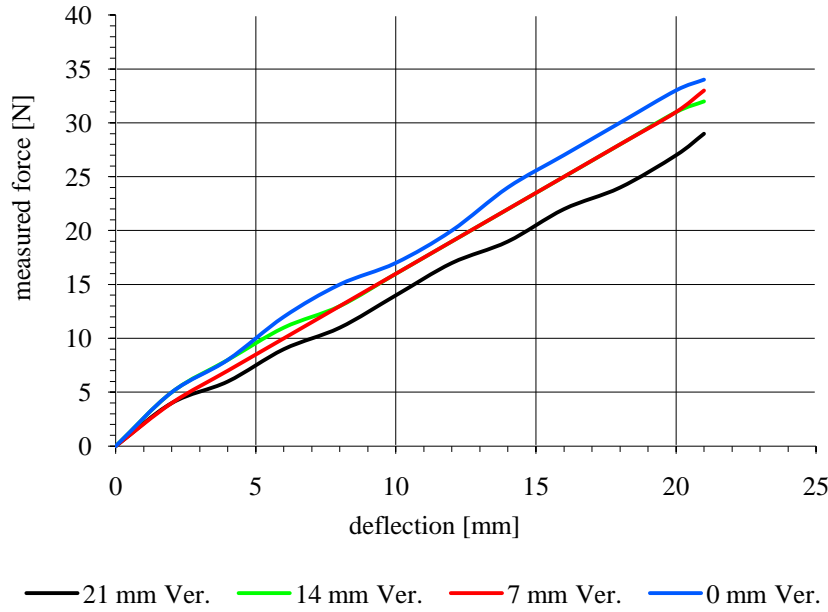


Figure 7.10: Experimental results of the model with one beam sliding through a hollow beam

A comparison of this result with the theoretical result, which was  $\pm 12\%$ , gives a good indication of the validity of this prototype in designing an adaptive foot's sole. Also it should be taken in consideration that the system has an optimization potential through changing the dimension of the elements used in the model, especially the thickness of the beams (both the hollow beam and the sliding beam), and the perforation of the sliding beam.

Also during the experimental measurements the results of the beam deflection shows a large difference between loading and unloading as seen in Figure 7.11. This change is considered to be due to two main reasons. The first is the high friction in the system between the two beams. The hollow beam is manufactured under pressure to insure the minimum clearance and air gaps between the two beams (that was the concept requirements). However this leads to a high friction reducing the efficiency of the system. The second reason depends on the measuring technique used. Since the forces in this model are too small, a piezoceramic force measuring sensor was used externally and not integrated in the test stand. This leads to loss in the charge, and therefore small changes in the measured force over long periods.

In the Figure 7.10 it is clear that the two positions 7 mm and 14 mm have values between the two extremities, which verifies the validity of this concept, but in both cases there is almost the same slope, which is referred mainly to the high friction in the whole system.

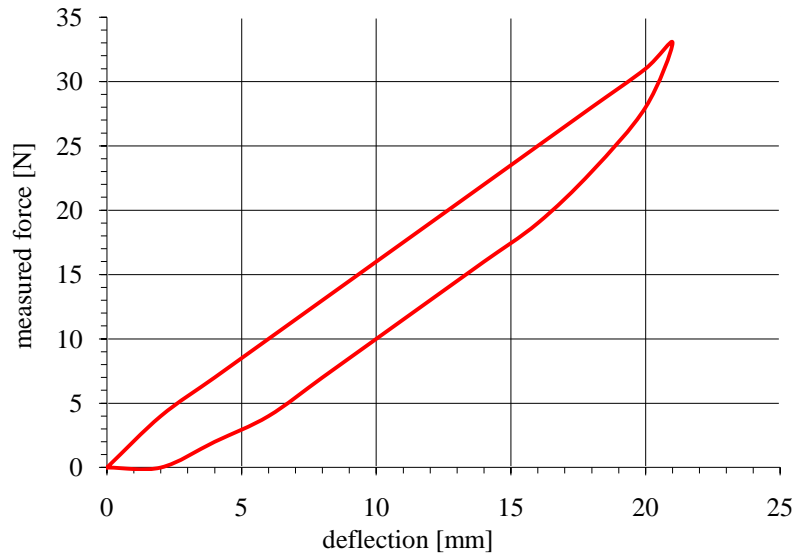


Figure 7.11: The difference in the measured force between loading and unloading of the system measured for the beam at the position of 7 mm

### 7.3.2 Results of the two screwed beams concept

As a result of the analytical analysis of the second concept three variables are to be evaluated here depending on the equations previously derived. Firstly substituting the dimensions of the beams in equations (7.31) and (7.32) by evaluating the system at three different clearances between the two beams (0 mm, 0.65 mm, and very large clearance (just one beam is active)). For the evaluation process an average value of 40 GPa effective modulus of elasticity is used for the carbon fibre reinforced material.

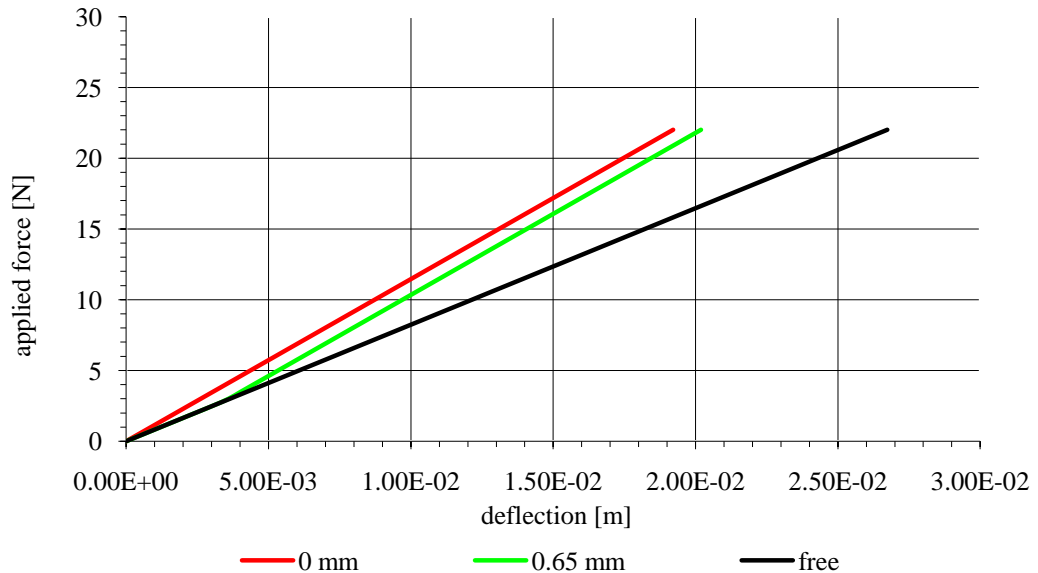


Figure 7.12: The results of the analytical model describing the two beams screwed together with different clearance values between them

From Figure 7.12 the change in the stiffness is clear. The maximum change is  $\pm 16.4\%$  of the average stiffness. This value is larger than the desired change of  $\pm 10\%$ . That indicates that this configuration has brought a large change with a very simple design and with minimum

activation and control energy. Nevertheless the figure shows that the changes in the stiffness occurs in steps form but this should not be necessarily a problem since the goal of the work is changing the stiffness to keep symmetry in the human walk with prosthesis, and reducing the changes in BCoM motion at different loads.

The second modification for this concept is to use spring elements with the screws that keep the two plates in contact and apply load as they deform. The spring elements are preloaded at different levels. This concept is also calculated from the equations of deformation, and the results are shown in Figure 7.13. From this figure and the results it is clear that the stiffness changes here are also a function of the preload, and in case of spring element with 1000 N/m stiffness, the maximum change in stiffness is found to be  $\pm 14.4\%$ . The behaviour of the beam element shows a stepwise change in stiffness, starting with a high stiffness and going down to a lower stiffness.

It is difficult to evaluate such a system just objectively, as a subjective evaluation done by an amputee may reveal a better evaluation of the preferred system. Nevertheless it is suggested here in this work to consider the model without spring elements for further experimentations.

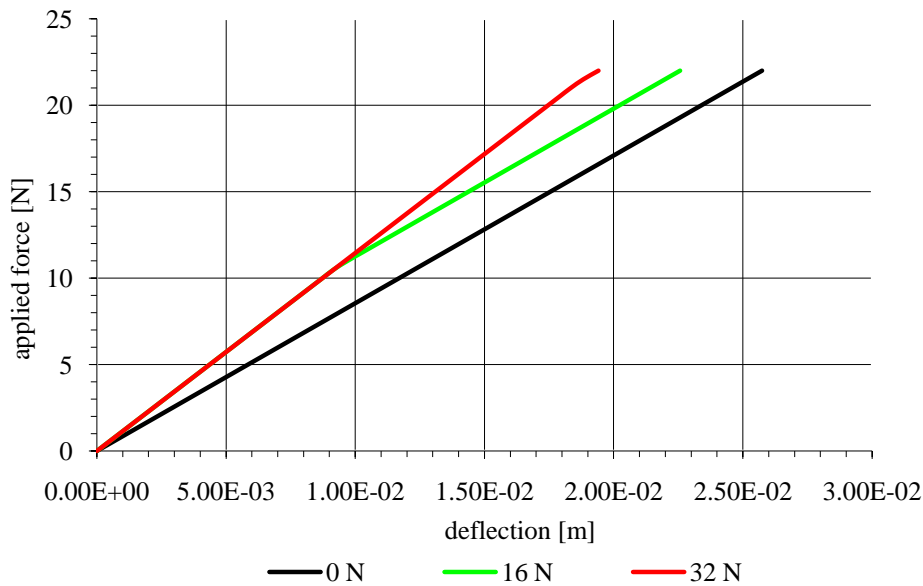


Figure 7.13: Analytical force deflection relation result of the model describing the two beams screwed together with different spring preloads

The third modification for this model is to use a spring element with different stiffness values at the two screws. From the Figure 7.14 it can be determined that a change in the stiffness of the spring from 1000 N/m to 10000 N/m a maximum change in the stiffness of the system is just  $\pm 7.4\%$ . These results show a continuous and smooth change in the system stiffness however to achieve this a large change in the springs stiffness is necessary, which is out the scope of this work. This system will be just analytically verified. The potential advantages of this system are that it shows that the total deflection of the beams is controlled through two points where the springs are fastened. As a result when spring elements are developed with the ability to change their stiffness in this range, then they are to be fixed just at these two points.



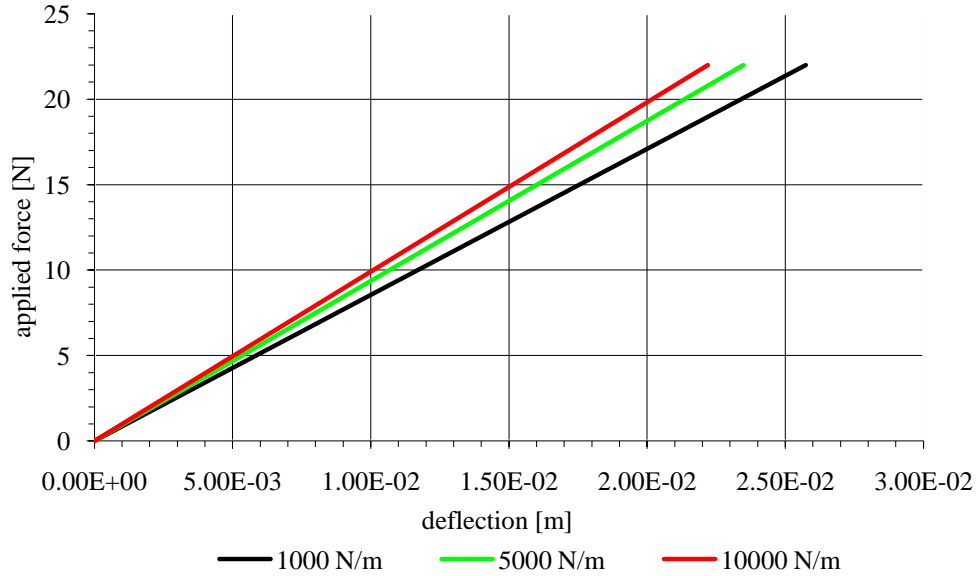


Figure 7.14: The results of the analytical model describing the two beams screwed together with springs with different spring constants at the screws

An experimental test is performed on the prototype in order to verify the analytical model results. The dimensions of this prototype are all shown in the appendix. The beam was fixed as a cantilever beam at one end at a distance 180 mm from the edge. The force was applied at 20 mm from the free edge causing a deflection in the beam. The test was repeated three times. Each time the clearance values between the two beams were changed by adjusting the screws. The three values for the clearance were 0 mm, 0.65 mm, and free (no contact occur, such that just one beam is loaded). The 0 mm clearance should represent the highest stiffness and the unscrewed should represent the lowest stiffness value.

The stiffness of the beam has changed by the changes in the clearance between the two plates, the lines for 0 mm clearance and for free represent the two extremities (see figure 7.15). These changes could be measured through the changes in the slope of the lines. The line for 0 mm clearance has a slope 1.984 N/mm and that for very large clearance (screws unscrewed) has a slope 1.367 N/mm and this is equivalent to a change of  $\pm 18.4\%$ .

The comparison of this result with the theoretical result ( $\pm 16.4\%$ ) shows that this concept is also valid for designing an adaptive foot's sole. As in the previous cases the system here has the potential to be optimized through changing the dimensions of the elements, especially the thickness of the beams (changing the upper beam thickness), and the material of the upper or lower beam. From the Figure 7.15 it is clear that the system with 0.65 mm clearance has two major slopes, starting with the smaller stiffness and then moving to the higher, which is the same behaviour as in the analytical results but here the curve is more smooth in its change.

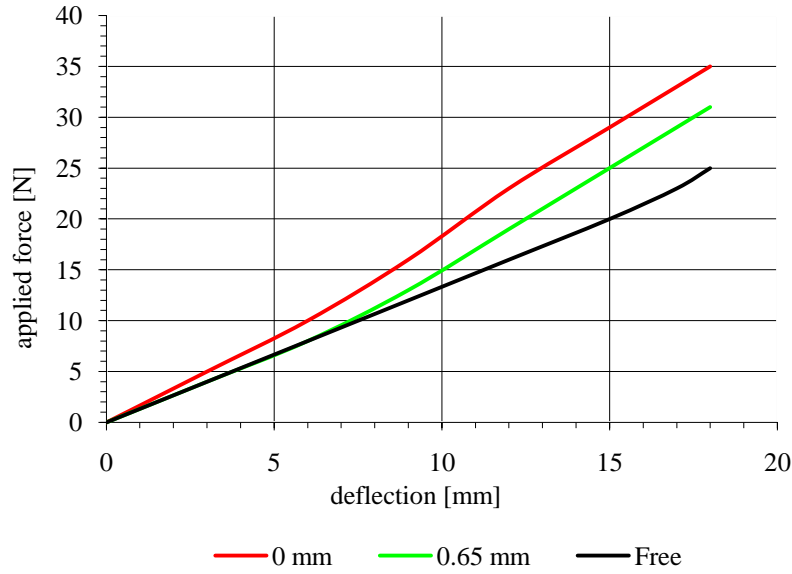


Figure 7.15: Experimental Results of the model with two beams screwed together with different clearance in between

During the experimental measurements of the beam deflection a difference between loading and unloading was noted as shown in Figure 7.16. This change is considered to be due to the measuring technique used and the friction in the assembly.

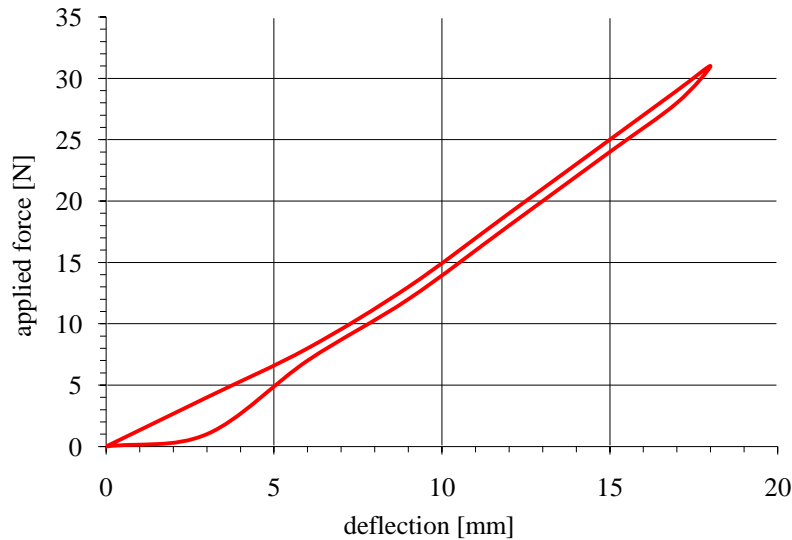


Figure 7.16: The difference in the measured force between loading and unloading of the system measured for the beams with 0.65 mm clearance

#### 7.4 An Operating System for the Adaptive Sole

In the previous sections two concepts were developed for a foot's sole that can change its stiffness. To integrate these suggested foot's soles in the real artificial limb an operating system is required. In this section a rough description of such a system and its operation is shown. This system should consist of the following components: a sensor array, a control unit, an actuator and an energy source. With these elements the whole system could be controlled and activated. The sole operating system should be compact, light and integrated in the foot. The sensor has the function to determine the foot condition and the gait boundary conditions (change in

walking speed, surface inclination, and etc.) this information are feed into a control unit that processes the data and send an appropriate signal to the actuator. A feedback signal for the control unit is taken from the sole. The actuator has the function of driving the sole system (for example: pulling the internal beam, or screwing the screws in the two screwed beams system). Since during the swing period of the gait cycle the foot sole is not loaded, then it will be convenient to drive its element at this period. The swing phase takes 0.38 s if the change in the properties is very large then it could be done gradually during more than one step. The actuator can have many forms just like an electric motor or a hydraulic system. A sample configuration of the system is displayed in Figure 7.17.

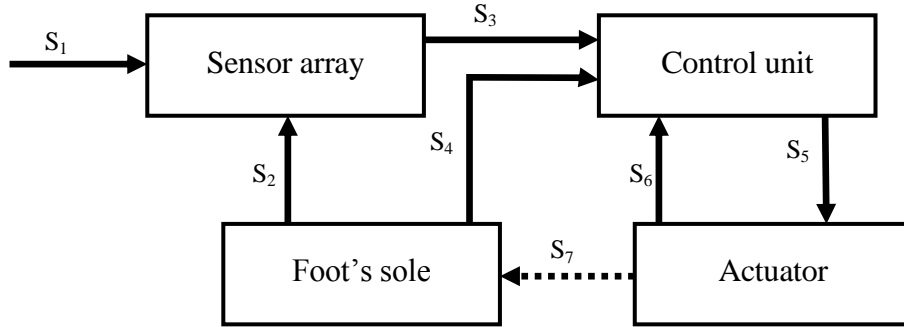


Figure 7.17: Configuration of an adaptive foot system

Signal  $S_1$  and  $S_2$  represent the boundary conditions, and the state of the foot's sole, respectively.  $S_3$  represents the resultant signal of the foot condition and boundary condition, which is processed in the control unit with the signal  $S_4$  (foot's sole active element state (sliding beam position or two screwed beams clearance) and  $S_6$  (actuator state) to send the signal  $S_5$  to the actuator which in turn drives the adaptive foot's sole (changes the clearance between the screwed beams or the sliding beam position).

Energy is required to operate the system shown in the Figure 7.17. A rechargeable battery can be used to provide the system with energy but it has the disadvantage of the high weight and the need to recharge it regularly. A possible solution to this problem can be reached by utilizing the energy available from the motion of the foot and the deflection of the foot sole in driving the actuator, which is the largest energy consumer in the system, and using smaller battery for providing the sensor array and the control unit with the required energy. This could be done for example by storing a part of the energy of walking during stance phase in spring elements (or any other proper form) and utilize this stored energy later in driving the actuator. The design and development of these systems are out of the scope of this work and could be realized in future works.

## 7.5 Comments

From the experimental results of these two models, the goal of the work is achieved to develop a system that changes its stiffness with a minimum value of  $\pm 10\%$ . In the first model the changes were  $\pm 8.6\%$  and in the second  $\pm 18.4\%$ . Also there are still the possibilities to improve the systems and optimize them according to the needs of the prostheses designs, for example:

- In the sliding beam model the number of slots can be reduced, such that the change in stiffness could be better controlled, and the manufacturing of the elements will be much easier, since the effect of the clearance inaccuracy, the high friction and high force required in positioning the internal beam could all be reduced.

- In the screwed beams model, the thickness of the second beam could be increased leading to a larger change in the stiffness within a very small clearance change. Also here the selection of a new material for the upper beam can give a similar improvement benefit.
- In the screwed beams model, the size of the upper plate and its thickness could also be modified leading to a smoother change in the stiffness of the whole system.

During the production of the two systems, there were no special difficulties to be mentioned, but in the first model it was very important to keep the clearance between the layers as small as possible avoiding large gaps, which will affect the functionality of the system. Since the deformation of the composite material beams used as foot sole are relatively large, a study of the inter-laminar fracture is necessary to evaluate the life time of the system.

During pulling the perforated beam through the hollow one, a large force was required to overcome the friction and wall pressure, which means that the system controlling in future as a prosthesis foot will need a large energy and force, which was recommended to be avoided at the beginning of the work.

In the second model consisting of two beams screwed together, the system shows a nonlinear deformation, and here it is possible to use the system as a nonlinear spring element such that the deformation rate will be less as the force acting on it is increased, and this leads to the use of the sole at a wide range of loads with a minimum change in the deflections of the foot and in the motion of the BCoM.

In order to have a better evaluation of the system's validity it is very important to try it out on an amputee, since the evaluations of prostheses have their subjective and objective sides that both need to be tested. Before that, the designs of the foot sole are to be modified according to the size and force requirements of an original model, since, in this work, the materials and designs were limited with the commercially available composites plate to reduce the costs, and the goal of the work was to study the functionality of the two models as a first step before the work can be further developed.

In the second model consisting of two screwed beams, the energy required to drive the system is very low, and the potential of developing a system to supply it with energy from the human motion is very high, and may be done through piezoceramic elements. Here it will be recommended to design a local energy harvesting system for it. The system can be a part of the foot sole itself, such that the foot sole generate the energy that it needs during walking and supplies it directly to the control system.

## 8 Discussion and Conclusions

In this work the human gait of an above knee amputee is modelled and some properties of the foot are studied. The numerical model was able to simulate the stance phase of human walking successfully using an elastic foot, which makes it a potential design and evaluation tool for prosthetic limbs before manufacturing the costly prototypes. The results of simulation show that the changes in the inclination angle of the ankle joint have lead to the largest changes in the kinetic and kinematic properties of the gait followed by the stiffness of the foot sole. Changing the ankle joint angle also has increased the step size during walking on inclined surfaces which makes it an adaptive property that may reduce the energy consumption needs of amputees.

During the simulation a trial was done to simulate the human gait of an amputee with the foot C-Walk using data from an amputee who had used a different artificial limb namely Flex-Walk but the results of this trial varied largely from the expected results. It was not possible to use this model for studying the adaptive properties of the prosthetic foot. From this trial it could be concluded that the data used as inputs to the model depend on the individual amputees and any changes in the model require a new set of data to be given as inputs for the system. This coincides with the fact that the use of prosthetic limbs is a learning process. Prostheses are used from amputees who still have active muscles and can adapt partially to the changes in the prostheses in order to take most of the advantages of the artificial foot.

The results expected by the simulation model reflect the tendencies of changes in the gait due to the changes in the limb properties, but do not give the exact quantity of these changes since the prosthetic limbs are used by amputees who still have active muscles. Changes in the foot or whole limb properties will be recognized from the user and the user will adapt his remaining muscles to suit the new situation as best as possible. One of the benefits of using simulation in studying the human gait was the fact that numerical simulation and modelling have the capability to change just one parameter and keep the others fixed. This capability makes it possible to study many parameters in order to evaluate their participation to the whole human gait. Experimentally it is not possible to change just one parameter and keep the others fixed since subjects in reality may adapt their gait pattern and mask any changes due changes in a single parameter.

The differences in the input data, system description, and initial conditions have a significant effect on the ability of the numerical model to predict the original gait patterns. This indicates that the difference in the results from this model compared with the originally measured data can have many sources and not only the assumptions used throughout the modelling of the different elements.

Despite that the study of gait and the measuring techniques have largely developed in the recent years, it is still difficult in many situations to study the forces acting on the body and on the artificial limbs without influencing their function. However the numerical model makes it possible to measure these forces at different locations in the system (for example the local forces acting along the foot sole).

New concepts for an adaptive sole with changeable stiffness were developed and verified experimentally. The variance in the stiffness was sufficient for an adequate influence on the gait speed. From the experimental results of the two models, the goal of the work has been achieved to develop a system that changes its stiffness. In the first model the changes are  $\pm 8.6\%$  and in the second  $\pm 18.4\%$  also there is still the possibility to improve these systems and optimize them according to the needs of the prostheses designs. The two concepts have the benefit of light weight and simplicity. Also a system for operating the adaptive foot is suggested and requires further realization.

## 9 Future Work

Since the numerical modelling of the human gait for amputees shows clear and reasonable results it is suggested to develop it further into a three-dimensional model. Then as it was shown in the study the use of a two dimensional model has caused some deviations from reality due to the absence of three of the gait determinant, and this could be largely improved by further developing the model into three dimensions. Also such improvements make it possible to utilize the model in studying other properties that are still not considered in the design of prosthesis (for example ankle joint inclination in anterior/posterior directions).

Utilization of the model in the calculation of the energy cost of human ambulation could be an additional important improvement that will help in optimizing the design of elastic prosthetic feet. Also the elastic elements integrated in the numerical model make the model a possible tool in studying the energy harvesting potential from the amputees' locomotion and using this energy to supply the operating system of the adaptive prostheses. Then such a tool can determine the effect of taking a part of the gait energy on the gait parameters, and can be utilized in determining the best location of energy harvesting systems.

Optimizing the new sole designs and trying them experimentally on amputees to get more accurate results about the efficiency and subjective influence of these changes, also design of an operating and control systems for the new adaptive sole concepts.

Since the rotation of the ankle joint has caused large changes in the kinematic and kinetic gait parameters especially walking on inclined surfaces, it will be very valuable to design an adaptive rotatable ankle joint.

In order to verify the validity of these changes and models and to evaluate their usefulness, it is very important to try them on amputees, because such changes are much depending on the users' needs and limitations. A numerical evaluation will stay just a step before the real subjective evaluations is done by the user under different gait patterns.

## References

- [Adams 2008] Mechanical Dynamics, Inc.: Documentation of the Program: Theory of Flexible Bodies. Mechanical Dynamics Inc., 2008.
- [Ansys 2007] ANSYS, Inc.: Documentation for ANSYS ICEM CFD/AI\*Environment 11.0. ANSYS, Inc., Dokumentation zum Programm, 2007.
- [AnyBody 2009] AnyBody Technology A/S: The AnyBody Modeling System: AnyScript Reference Manual, version 4.0.0, AnyBody Technology A/S, April 2009.
- [Bogey 2005] Bogey, R. A.; Perry, J.; Gitter, A.J.: An EMG-to-Force Processing Approach for Determining Ankle Muscle Forces During Normal Human Gait, IEEE Transactions on Neural Systems and Rehabilitation Engineering, Vol. 13, No. 3, pp. 302-310, 2005.
- [Carli 2006] Carli, V.: Design of an Active Foot for a Smart Prosthetic Leg, Dissertation, Technische Universität Darmstadt, Darmstadt, Dezember 2006.
- [Chi 2005] Chi, K.; Schmitt, D.: Mechanical Energy and Effective Foot Mass During Impact Loading of Walking and Running, Journal of Biomechanics, Vol. 38, pp. 1387-1395, 2005.
- [Craig 1968] Craig, R.; Bampton, M.: Coupling of Substructures for Dynamic Analyses. AIAA Journal, Vol. 6, No. 7, July 1968.
- [Croce 2001] Croce, U. D.; Riley, P. O.; Lelas, J. L.; Kerrigan, D. C.: A refined view of the determinants of gait, Journal of Gait and Posture, Vol. 14, pp. 79-84, 2001.
- [Crowe 1995] Crowe, A.; Schiereck, P.; de Boer, R. W.; Keesen, W.: Characterization of Human Gait by Means of Body Center of Mass Oscillations Derived from Ground Reaction Forces, IEEE Transactions on Biomedical Engineering, Vol. 42, No.3, pp. 293-303, 1995.
- [Dietl 1998] Dietl, H.; Kaitan, R.; Pawlik, R.; Ferrara, P.: C-Leg – Ein neues System zur Versorgung von Oberschenkelamputationen. Orthopädie Technik, Dortmund, edition 3/98, 1998.
- [Fischer 2009] Fischer, F.: Behandlung des PAINLEVÉschen Paradoxen in der modernen Mehrkörperdynamik, Dissertation, Technische Universität Darmstadt, Darmstadt, September 2009.
- [Fleck 1994] Fleck, J.T.; Butler, F.E.; Vogel, S.L.: An Improved Three Dimensional Computer Simulation of Motor Vehicle Crash Victims. Technical Report ZQ-5180-L-1, Calspan Corporation, Buffalo, NY, 1994.
- [Gard 2001] Gard, S. A.; Childress, D. S.: What Determines the Vertical Displacement of the Body During Normal Walking. Journal of Prosthetics and Orthotics, Vol. 13, No. 3, pp. 64-67, 2001.
- [Gard 2004] Gard, S. A.; Miff, S. C.; Kuo, A. D.: Comparison of kinematic and kinetic methods for computing the vertical motion of the body centre of mass during walking. Human Movement Science, Vol. 22, pp. 597-610, 2004.

- [Gerritsen 1995] Gerritsen, K. G. M.; van den Bogert, A. J.; Nigg, B. M.: Direct Dynamics Simulation of the Impact Phase in Heel-Toe Running, *Journal of Biomechanics*, Vol. 28, No. 6, pp. 661-668, 1995.
- [Ghiringhelli 2000] Ghiringhelli, G.; Masarati, P.; Mantegazza, P.: Multibody Implementation of Finite Volume C° Beams. *AIAA Journal*, Vol. 38, No. 1, January 2000.
- [Gibson 1994] Gibson, R. F.: *Principles of Composite Material Mechanics*. McGraw-Hill, 1th Edition, 1994.
- [Gilchrist 1996] Gelchrist L. A.; Winter, D. A.: A Two-Part Viscoelastic Foot Model for use in Gait Simulation, *Journal of Biomechanics*, Vol. 29, No. 6, pp. 795-798, 1996.
- [Gilchrist 1997] Gilchrist L. A.; Winter, D. A.: A Multisegment Computer Simulation of Normal Human Gait, *IEEE Transactions on Rehabilitation Engineering*, Vol. 5, No. 4, pp. 290-299, 1997.
- [Gordon 2009] Gordon, K. E.; Ferris, D. P.; Kuo, A. D.: Metabolic and Mechanical Energy Costs of reducing Vertical Centre of Mass Movement During Gait, *Arch Phys Med Rehabil*, Vol. 90, pp. 136-144, 2009.
- [Götz-Neumann 2006] Götz-Neumann, K.: *Gehen Verstehen*. Georg Thieme Verlag, Stuttgart, 2. Auflage 2006.
- [Hagedorn 1995] Hagedorn, P.: *Technische Mechanik, Band 2: Festigkeitlehre*, Verlag Harri Deutsch, 1995.
- [Hamilton 1997] Hamilton, N.; Luttgens, K.: *Kinesiology (Scientific Basis of Human Motion)*. McGraw-Hill, Ninth edition, 1997.
- [Hansen 2004] Hansen, A. H.; Childress, D. S.; Miff, S. C.: Roll-over characteristic of human walking on inclined surfaces, *Human Movement Science*, Vol. 23, pp. 807-821, 2004.
- [Huston 1976] Huston, R.; Hessel, R.; Winget, J.W.: Dynamics of Crash Victims – A Finite Segment Model. *AIAA Journal*, Vol. 14, No. 2, pp. 173-178, 1976.
- [Huston 1990] Huston, R.: *Multibody Dynamics*. Butterworth-Heinemann, Stoneham, 1990.
- [Inman 1981] Inman, V.; Ralston, H.J.; Todd, F.: *Human Walking* . Baltimore: Williams and Wilkins, 1981.
- [Intec 2005] INTEC GmbH (Ingenieurgesellschaft für neue Technologien): *An Overview of how to use SIMPACK, Dokumentation zum Programm*, 2005.
- [Jang 2001] Jang, T.S.; Lee, J.J.; Lee, D.H.; Yoon, Y.S.: Systematic Methodology for the Design of a Flexible Keel for Energy-Storing Prosthetic Feet, *Medical and Biological Engineering and Computing*, Vol. 39, pp. 56-64, 2001.
- [Jo 2007] Jo, S.; Massaquoi, S. G.: A Model of Cerebrocerebello-Spinomuscular Interaction in the Sagittal Control of the Human Walking, *Biological Cybernetics*, Vol. 96, pp. 279-307, 2007.



- [Kastner 1999] Kastner, J.; Nimmervoll, R.; Wagner, P.: „Was kann das C-Leg?“ – Ganganalytischer Vergleich von C-Leg, 3R45 und 3R80, Med. Orthopädie Technik, Stuttgart, 119, S. 131-137, 1999.
- [Kwan 2007] Kwan, M.; Hubbard, M.: Optimal Foot Shape for a Passive Dynamic Biped, Journal of Theoretical Biology, Vol. 248, pp. 331-339, 2007.
- [Leardini 2002] Leardini, A.; Moschella, D.: Dynamic Simulation of the Natural and Replaced Human Ankle Joint, Medical and Biological Engineering and Computing, Vol. 40, pp. 193-199, 2002.
- [Leardini 2007] Leardini, A.; Benetti, M.G.; Berti, L.; Bettinelli, D.; Natio, R.; Giannini, S.: Rear-Foot, Mid-Foot and Fore-Foot Motion during the Stance Phase of Gait, Gait and Posture, Vol. 25, pp. 453-462, 2007.
- [Mak 2003] Mak, A. F.-T.; Zhang, M.; Leung, A. K.-L.: Artificial Limbs. In: Comprehensive Structural Integrity. Vol. 9, Bioengineering. Milne, Ian; Ritchie, R.; Karihaloo, B.L., eds. Elsevier, pp. 329-363, 2003.
- [Marks 1905] Marks, A. A.: Manual of artificial limbs. New York: A.A. Marks Inc., pp. 17-20, 1905.
- [Marks 2001] Marks, L.; Michael, J.: Clinical review: Artificial limbs, British Medical Journal Vol. 323 pp. 732-735, 29 September 2001.
- [Murali 2001] Murali, L.: Advances in Lower Extremity Prosthetics, Indian Journal of Physical Medicine and Rehabilitation, Vol. 12, pp. 35-38, April 2001.
- [Müller 1999] Müller, O.; Häußler, P.; Lux, R.; Ilzhöfer, B.; Albers, A.: Automated Coupling of MDI/ADAMS and MSC.CONSTRUCT for the Topology and Shape Optimization of Flexible Mechanical Systems, International ADAMS User's Conference, Berlin, November 17-19 1999.
- [Noble 2006] Noble, J. W.; Prentice, S. D.: Adaptation to unilateral change in lower limb mechanical properties during human walking, Exp Brain Res, Vol. 169, pp. 482-495, 2006.
- [Nupoc 2005] Northwestern University, Prosthetics-Orthotics Centre: Prosthetic History, Online in WWW under URL: <http://www.nupoc.northwestern.edu/prosHistory.shtml> (accessed: 01.02.2005).
- [Onyshko 1980] Onyshko, S.; Winter, D. A.: A Mathematical Model for the Dynamic of the human Locomotion, Journal of Biomechanics, Vol. 13, pp. 361-368, 1980.
- [Ottobock 2009a] Otto Bock: C-Walk 1C40 – Energie und Komfort, Online in WWW under URL: [http://www.ottobock.se/cps/rde/xbcr/ob\\_se\\_sv/im\\_646a154\\_gb\\_c\\_walk\\_1c40.pdf](http://www.ottobock.se/cps/rde/xbcr/ob_se_sv/im_646a154_gb_c_walk_1c40.pdf) (accessed: 02.07.2009).
- [Ottobock 2009b] Otto Bock: Date, facts and figures about the C-Leg Product Line, Online in WWW under URL: [http://www.ottobock.com/cps/rde/xchg/ob\\_com\\_en/hs.xsl/7098.html](http://www.ottobock.com/cps/rde/xchg/ob_com_en/hs.xsl/7098.html) (accessed: 14.08.2009).

- [Össur 2009] Össur: Flex-Foot Vari-Flex, Online in WWW under URL: <http://www.ossur.de/pages/7068> (accessed: 01.07.2009).
- [Pandy 1988] Pandy, M. G.; Berme, N.: Synthesis of Human Walking: A Planar Model for Single Support, *Journal of Biomechanics*, Vol. 21, No. 12, pp. 1053-1060, 1988.
- [Perry 1992] Perry, J.: *Gait Analysis (Normal and Pathological Function)*. SLACK Incorporated, Thorofare, NJ, 1992.
- [Pflanz 2001] Pflanz, B.: Entwicklung von Simulationsmodellen zur konstruktiven Optimierung von Stoßdämpfersystemen an Beinprothesen. Hausarbeit im Rahmen der Ersten Staatsprüfung für das Lehramt an Gymnasien. Göttingen, Germany, 2001.
- [Raynor 2002] Raynor, A. J.; Yi, C. J.; Abernethy, B.; Jong, Q. J.: Are Transitions in Human Gait Determined by Mechanical, Kinetic or Energetic Factors? *Human Movement Science*, Vol. 21, pp. 785-805, 2002.
- [Ren 2007] Ren, L.; Jones, R. K.; Howard, D.: Predictive Modelling of Human Walking over a Complete Gait Cycle, *Journal of Biomechanics*, Vol. 40, pp. 1567-1574, 2007.
- [Sasaki 2006] Sasaki, K.; Neptune, R.: Muscle Mechanical work and elastic energy utilization during walking and running near the preferred gait transition speed, *Journal of Gait and Posture*, Vol. 23, pp. 383-390, 2006.
- [Saunders 1953] Saunders, J.B.D.M.; Inman, V.T.; Eberhardt, H.D.: The Major determinants in normal and pathological gait. *The Journal of Bone and Joint Surgery* 35-A, No. 3, pp. 543-558, 1953.
- [Schnell 1989] Schnell; Gross; Hauger: *Technische Mechanik, Band 2: Elastostatik*, Springer-Verlag, Zweite Auflage, 1989.
- [Schutte 2006] Schutte, L.M.; Narayanan, U.; Stout, J.L.; Selber, P.; Gage, J.R.; Schwartz, M.H.: An index for quantifying deviations from normal gait, *Journal of Gait and Posture*, Vol. 11, pp. 25-31, 2000.
- [Scott 1993] Scott, S. H.; Winter, D. A.: Biomechanical Model of the Human Foot: Kinematics and Kinetics During the Stance Phase of Walking, *Journal of Biomechanics*, Vol. 26, No. 9, pp. 1091-1104, 1993.
- [Shabana 1997] Shabana, A.A.: Flexible Multibody Dynamics: Review of Past and Recent Developments. *Multibody System Dynamics*, Vol. 1, pp. 189-222, 1997.
- [Silva 2002] Silva, M.P.T.; Ambrosio, J.A.C.: Kinematic Data Consistency in the Inverse Dynamic Analysis of Biomechanical Systems, *Multibody System Dynamics*, Vol. 8, pp. 219-239, 2002.
- [Usherwood 2003] Usherwood, J. R.; Bertram, J. E. A.: Gait transition cost in humans, *Journal of Applied Physiology*, Vol. 90, pp. 647-650, 2003.
- [Wallrapp 1999] Wallrapp, O.; Schwertassek, R.: *Dynamik flexibler Mehrkörpersysteme*. Vieweg & Sohn Verlagsgesellschaft mbH, Braunschweig/ Wiesbaden, 1999.

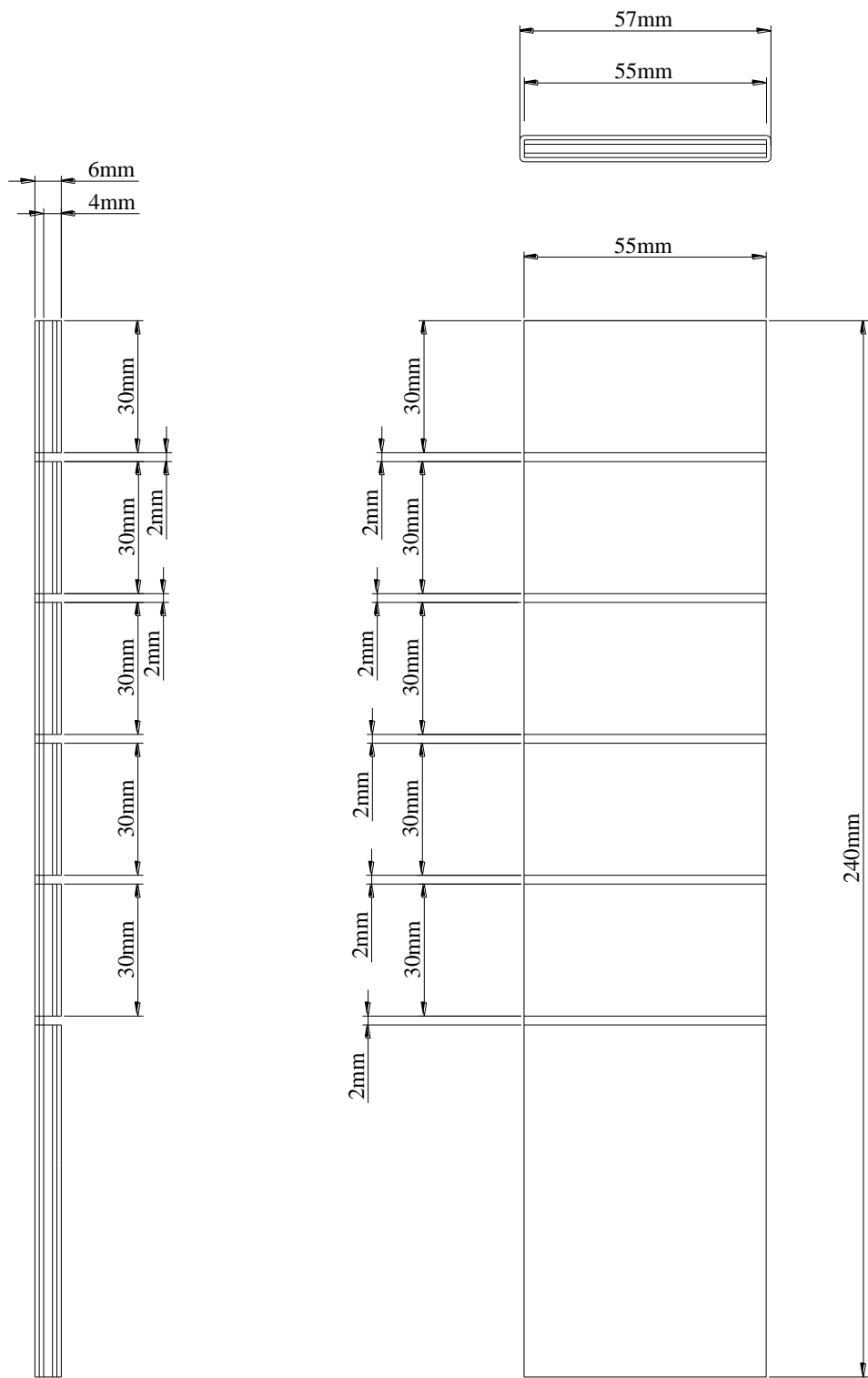
- [Wang 2003] Wang, W.J.; Crompton, R.H.; Li, Y.; Gunther, M.M.: Energy Transformation During Erect and 'Bent-hip, Bent-knee' Walking by Humans with Implications for the Evolution of Bipedalism, *Journal of Human Evolution*, Vol. 44, pp. 563-579, 2003.
- [Waters 1992] Waters, R. L.: *Atlas of Limb Prosthetics: Surgical, Prosthetic, and Rehabilitation Principles*. Chapter 15: The Energy Expenditure of Amputee Gait. Rosemont, IL, American Academy of Orthopedic Surgeons, edition 2, 1992, reprinted 2002.
- [Wetz 2005] Wetz, H. H.; Hakkemeyer, U.; Wühr, J.; Drerup, B.: Einfluss des C-Leg-Kniegelenk-Passteiles der Fa. Otto Bock auf die Versorgungsqualität Oberschenkelamputierter, *Orthopäde Technik*, Dortmund, Edition 34, S. 298-319, 2005.
- [Weule 2003] Weule, H.; Fleischer, J.; Neithardt, W.; Emmrich, D.; Just, D.: Structural Optimization of Machine Tools including the static and Dynamic Workspace Behaviour. The 36<sup>th</sup> CIRP-International Seminar on Manufacturing Systems, Saarbrücken, Germany, 03-05 June 2003.
- [Wilson 1992] Wilson, B.: *Atlas of Limb Prosthetics: Surgical, Prosthetic, and Rehabilitation Principles*. Chapter 1: History of Amputation Surgery and Prosthetics. Rosemont, IL, American Academy of Orthopedic Surgeons, edition 2, 1992, reprinted 2002.
- [Wojtyra 2000] Wojtyra, M.: Dynamical Analysis of Human Walking. Technical paper, 15th European ADAMS Users' Conference, November 2000.
- [Wölfel 1998] Wölfel, H.P.; Buck, B.; Pankoke, S.: Dynamic FE Model of Sitting Man Adjustable to Body Height, Body Mass and Posture Used for Calculating Internal Forces in the Lumbar Vertebral Disks, *Journal of Sound and Vibration*, Vol. 215, pp. 827-839, 1998.
- [Wylie 1995] Wylie, C. R.; Barrett, L. C.: *Advanced Engineering Mathematic McGraw-Hill*, 6th Edition, 1995.
- [Zahedi 2004] Zahedi, S.: *Atlas of Amputations and Limb Deficiencies: Surgical, Prosthetic and Rehabilitation Principles*. Chapter 52: Lower Limb Prosthetic Research In the 21st century. Smith DG, Michael JW, Bowker JH, eds. Rosemont, IL, American Academy of Orthopaedic Surgeons, edition 3, 2004.
- [Zahedi 2005] Zahedi, S.; Sykes, A.; Lang, S.; Cullington, I.: Adaptive prosthesis – a new concept in prosthetic knee control, *Robotica*, vol. 23, pp. 337-344, 2005.

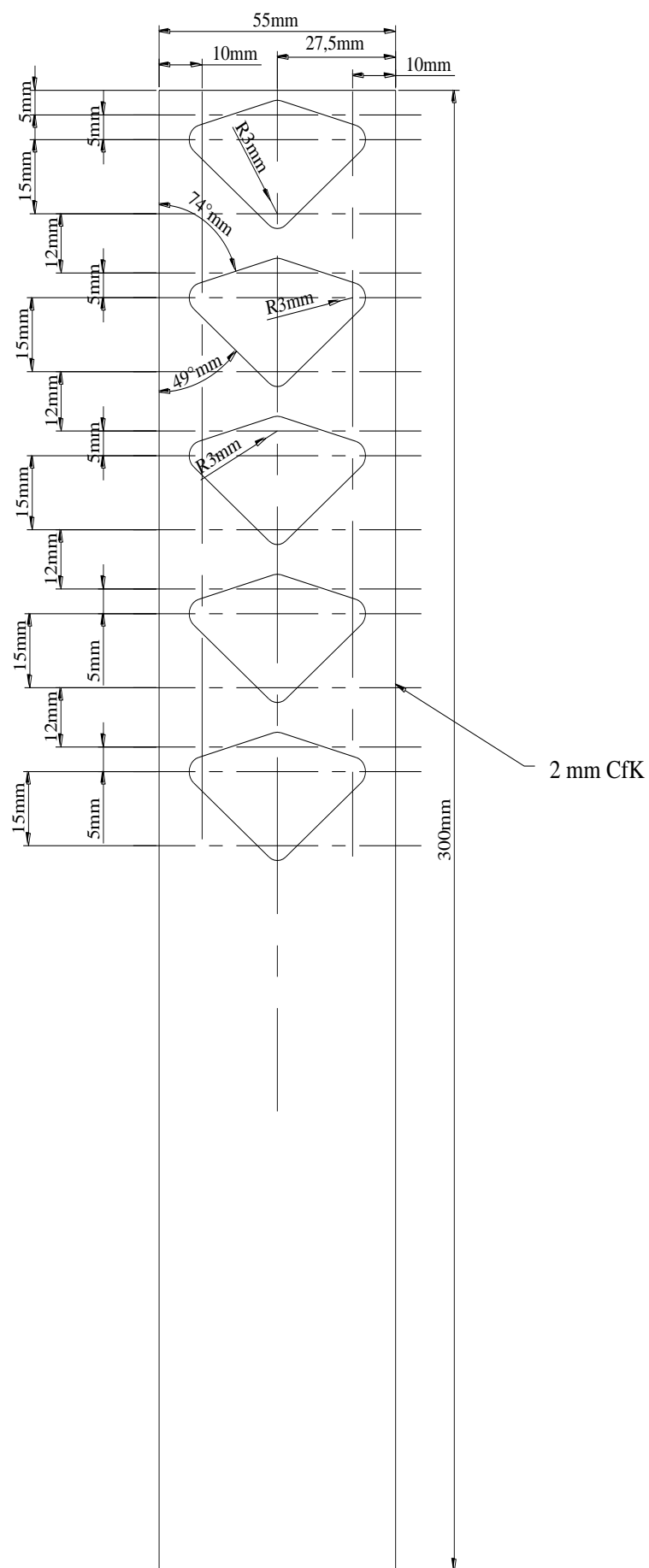


**Appendix**

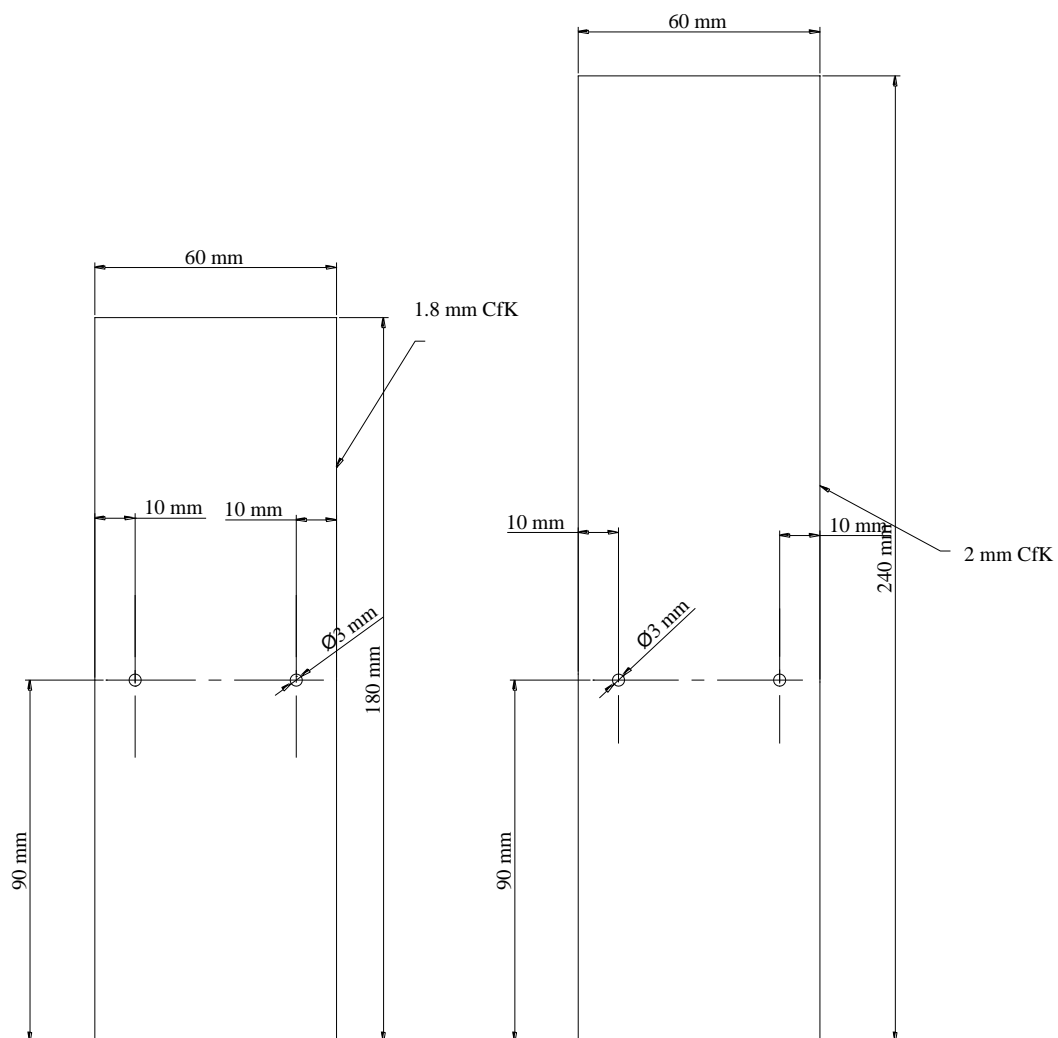
The drawings of the prototypes with all dimensions:

**A.1 The Sliding Perforated Plate**





## A.2 The Two Screwed Beams:



## **Resume of the Author**

### **Personal Information**

Name: Nasim George Alnu'man  
Date of birth: June 04, 1978  
Place of birth: Amman, Jordan  
Nationality / Citizenship: Jordanian  
Marital status: Single  
Email-address: nasim\_numan@yahoo.com

### **School Education:**

9/1984 – 6/1996 National Patriarchal College in Amman, Jordan  
General Secondary Education Certificate Examination 1996 –  
Scientific Stream, Percentage Average: 94.8%

### **University Education:**

9/1996 – 2/2001 B. Sc. Degree in Mechanical Engineering, University of Jordan,  
Amman, Jordan  
Graduate Average: 3.38/4.0, Rating: Very Good  
Graduation Project: Force-Motion Programming for Spring  
Loaded Mechanisms  
Training in Royal Jordanian Airline (Including Departments of  
Service engineering, Ground Support, Engine overhaul, and  
Components shops)  
9/2001 – 2/2004 M. Sc. Degree in Mechanical Engineering, University of Jordan,  
Amman, Jordan  
Graduate Average: 3.32/4.0 Rating: Very Good.  
Thesis: Thermal Contact Conductance of Elastically Deforming  
Flat Rough Surfaces Using Fractal Geometry  
1/2006 – 5/2010 Ph. D. Student at the Department of System Reliability and  
Machine Acoustics, Technische Universität Darmstadt, Germany

### **Work Experience**

10/2001 – 7/2002 Q.A. Engineering Company, Amman, Jordan  
Design and Manufacturing Engineer: Designing and  
manufacturing of steel structures and machines  
8/2002 – 5/2004 Light Industry Company, Amman, Jordan  
Production and Maintenance Engineer: Manufacturing of cars'  
radiators using copper and copper's alloys  
6/2004 – 6/2005 Getzner Werkstoffe, Amman, Jordan  
Technical Engineer: Noise and Vibration Isolation. Vibration  
Isolation of machinery using polyurethane Materials. Structure  
and Air born sound isolation

### **Languages**

Arabic Fluent  
English very good  
German very good